DELETERIOUS EXPANSION OF CEMENT PASTE AND CONCRETE

by

John A. Wells

A Thesis
presented to the University of Manitoba
in partial fulfillment of
the requirements for the degree of
Master of Science
in the Department of Civil Engineering

Winnipeg, Manitoba
April, 1990

ISBN 0-315-63217-8

DELETERIOUS EXPANSION OF CEMENT PASTE AND CONCRETE

BY

JOHN A WELLS

A thesis submitted to the Faculty of Graduate Studies of
the University of Manitoba in partial fulfillment of the requirements
of the degree of

MASTER OF SCIENCE

ABSTRACT

Degradation in concrete arises through many mechanisms which are either physical or chemical in nature. In this study, two forms of chemical attack are evaluated, late formation of ettringite and alkali-aggregate reaction (AAR).

The experimental program is designed to develop and evaluate test methods for expansion due to late formation of ettringite and AAR in concrete. Five cements and seven aggregates from various regions of Canada are utilized to fabricate cement paste and concrete specimens. Reactivity is gauged by specimen expansion. Scanning electron microscopy coupled with energy-dispersive x-ray analysis is utilized in the identification of reaction products.

The test results show that cement paste specimens made with cements produced in different regions of Canada exhibit significant differences in expansion when pretreated by subjecting them to wet-dry cycles. The reason for this expansion is late formation of ettringite in the hardened paste. Concrete specimens made with reactive aggregates and stored in 1 M NaOH solution at 80 C expand significantly. Different morphologies of alkali-aggregate reaction product are observed in the test specimens.

The procedures utilized in this study are proposed as test methods to evaluate cements and aggregates for their potential to cause expansion and cracking of concrete.

ACKNOWLEDGEMENTS

The author wishes to express his sincere thanks to Dr. Emmanuel Attiogbe for the excellent guidance, advice, encouragement and thoroughness with which he handled the entire research program, and to Dr. Sami Rizkalla for his technical input and advice.

The assistance given by Messrs. Ed Lemke, Brian Turnbull, Marty Green and Jeff Ramsay during the experimental work is greatly appreciated.

The author is grateful for the technical and financial assistance provide by Canadian National Railways and the Transport Institute of the University of Manitoba.

Finally, the author is indebted to his fiancee Tamara, for her never ending support, encouragement and most of all, for her patience throughout his studies. It is to her that this thesis is dedicated.

TABLE OF CONTENTS

LIST OF TABLES

LIST OF FIGURES

1. INTRODUCTION

1.1 GENERAL

Concrete durability considerations are playing an increasing role in design, due to the rapid deterioration of many concrete structures in service. Concrete deterioration may be caused by either physical or chemical means. Deterioration due to the freezing and thawing action of water in concrete is an example of physical attack, while deterioration due to reactions between alkalis in cement and certain types of aggregate is an example of chemical attack.

There is a form of concrete deterioration caused by the late formation of ettringite (7). Ettringite is one of the hydration products of portland cement. Its formation during the early hydration of cement is beneficial because it prevents the flash set of concrete (9,17). If it forms in the hardened concrete, the accompanying volume expansion can lead to cracking. Precast concrete units that have been heat treated during production are known to show deterioration due to late formation of ettringite in those components that have been subjected to frequent drying and moisture saturation (7). This deterioration is in the form of map cracking and loss of bond between the cement paste and coarse aggregate. The degree of degradation appears to be directly related to the composition of the cement (7). A rapid test method needs to be developed to determine if a given cement is likely to render concrete susceptible to deterioration due to late formation of ettringite.

Alkali-aggregate reaction (AAR) refers to reaction between minerals in certain rock types and soluble alkalis in the concrete (9). The alkalis are derived from the cement but

can also be introduced into the concrete from external sources. There are three types of alkali-aggregate reaction (2). These are:

(1) Alkali-silica reaction (ASR)

(2) Slow/late-expanding alkali-silicate/silica reaction;and

(3) Alkali-carbonate reaction (ACR)

All three types are encountered in Canada. Three factors which control the reaction mechanism are the amount of reactive minerals in the aggregate, the amount of available alkali, and the availability of moisture.

Alkali-aggregate reaction produces extensive map cracking in concrete, frequently accompanied by gel exuding from the cracks. In severe cases, the reaction can cause significant reductions in the engineering properties of concrete. Losses in compressive and flexural strengths can be as high as 40 and 75 percent, respectively (20).

The need for safe and economical concrete structures requires that the potential reactivity of an aggregate be determined prior to its use in concrete. The current CSA (2) and ASTM (1) tests for evaluating the potential reactivity of aggregates takes six to twelve months to give results. These tests do not always yield reliable results for all aggregates. A rapid, more reliable test is needed to better assess the potential reactivity of aggregates.

1.2 OBJECTIVE AND SCOPE

The purpose of this study is to develop test procedures for evaluating deleterious expansion and cracking of concrete due to (i) late formation of ettringite, and (ii) alkali-aggregate reaction.

Four CSA Type 30 and one CSA Type 10 cements produced in different regions of Canada are used in fabricating the test specimens. Coarse aggregates from seven different sources across Canada are used. ASTM standard sand is used in all the concrete mixes. The primary variables in the study are the duration of moist curing, the number of wet-dry cycles, the water-cement ratio, the storage medium for the test specimens, and the specimen size.

Length measurements of the test specimens are used to monitor the extent of expansion. At the conclusion of the length measurements, representative specimens are examined using a scanning electron microscope (SEM) equipped with an energy dispersive x-ray analyzer. Photomicrographs are obtained to show the nature of reaction products in the test specimens. The chemical composition of the reaction products are also obtained and used to describe their characteristics.

Test procedures are proposed to evaluate the potential expansion of concrete due to the two forms of chemical attack investigated in this study.

2. PREVIOUS STUDIES

2.1 GENERAL

Various studies have been undertaken to evaluate deleterious expansion and cracking in concrete due to late formation of ettringite and alkali-aggregate reaction (AAR). Literature pertaining to late formation of ettringite is relatively scarce. Alkali-aggregate reaction (AAR), on the other hand, is well documented.

A summary of relevant research pertaining to deleterious expansion and cracking in concrete due to late formation of ettringite and AAR is presented in this chapter. The two forms of chemical attack on concrete are separate entities and will be treated as such. However, deleterious expansion and cracking can be compounded due to the presence of both reaction mechanisms. That is, it is feasible for both reactions to occur in a concrete structure.

2.2 EXPANSION OF CONCRETE DUE TO LATE FORMATION OF ETTRINGITE

In recent years, precast units made of high strength concrete and having been heat treated during production have shown considerable reductions in structural integrity due to the formation of cracks and loss of bond between the cement paste and the coarse aggregate (7). Heinz and Ludwig (7) have shown this damage to be caused by the late formation of ettringite.

In their investigation of the mechanism of late formation of ettringite, Heinz and Ludwig (7) subjected mortar specimens to various treatments. In particular, the effects of

initial curing temperature, molar ratio of SO_3 to AL_2O_3, humidity of storage and water-cement ratio on expansion were examined.They found that initial curing temperatures above or equal to 75 C lead to expansion, cracking and decrease in strength. Temperatures below 75 C did not bring about any damaging reaction. Furthermore, the induced expansion and decrease in strength are related to the formation of a new phase in the cement matrix of the mortar. This new phase was found to be ettringite. Molar ratios of SO_3 to Al_20_3 below 0.55 and relative humidities below 95 % cause no expansion or strength loss. Water-cement ratio of 0.4 and increase in air void content with the use of air-entraining agent suppress the damage reaction.

Heinz and Ludwig explained the mechanism of late formation of ettringite by suggesting that when concrete is cured rapidly through heat treatment, increasing temperatures decrease the formation of calcium sulphoaluminate hydrate phases. Aluminate and sulphate ions get bound within the hydration products. During subsequent storage of the hardened concrete under water, these ions become available to form ettringite.

Tepponen and Eriksson (21) examined damage in concrete railway ties. During production, heat treatment was utilized for rapid curing of the ties. The heat treatment consisted of heating the units to 80 C for 2.5 to 4 hours, followed by cooling to 20 C. During their investigations, Tepponen and Eriksson examined specimens that had been sawed-off or cored from various areas of the ties. They evaluated the specimens based on the following: strength; petrographic examination, including scanning electron microscope (SEM) analysis; and x-ray diffraction.

Tepponen and Eriksson found that cements with a high SO_3/Al_2O_3 ratio tend to have larger quantities of crystallizing ettringite compared to cements with low SO_3/Al_2O_3

ratios. Microfissures produced by the heat treatment process facilitate moisture movements in the concrete. If enough moisture and reactive calcium sulphate is available within the matrix, future recrystallization of ettringite becomes possible. Reducing the aggregate grain size and the quantity of cement greatly reduces expansion and cracking. In support of Heinz and Ludwig (7), Tepponen and Eriksson also showed that by eliminating high temperature heat treatment, late formation of ettringite is greatly reduced.

Scott and Duggan (14) used a cyclic wetting and drying procedure to evaluate the potential expansion of concrete specimens due to a reaction between the aggregates and the cement alkalis. Large expansions were obtained for some specimens within six weeks. However, no evidence of reaction products was obtained in order to determine the cause of the expansion. In the present study, the test procedure developed by Scott and Duggan is modified and used to evaluate expansion of cement paste and concrete specimens. A scanning electron microscope equipped with an energy-dispersive x-ray analyzer is used to examine the nature of reaction products in the test specimens.

No standard test is currently available for evaluating the potential deleterious expansion of concrete due to late formation of ettringite. Such a test appears to be needed to protect against premature deterioration in concrete structures, particularly pre-cast units, that are subjected to alternating wet-dry cycles.

2.3 EXPANSION OF CONCRETE DUE TO ALKALI-AGGREGATE REACTION

Research by Stanton in the early 1940's diagnosed failures in concrete structures due to expansions caused by a chemical reaction between the alkalis contained in the cement paste and certain reactive forms of silica within the aggregate (9).

There are three types of AAR: Alkali-silica, alkali-carbonate and alkali-silicate reaction. Stanton determined that there exists several factors which control alkali-aggregate reaction: 1) nature and amount of reactive silica, 2) particle size of reactive material, 3) amount of available alkali, and 4) amount of available moisture.

Alkali-silica reactive aggregates tend to contain various forms of poorly crystalline reactive silica. Expansions for this type of reaction tend to occur early and are coupled with a high rate of expansion. Structures suffering from alkali-silica reaction usually exhibit cracking within 10 years of construction (2).

Alkali-silicate reaction is a much slower reaction compared to the alkali-silica reaction. Cracking can be delayed for as much as 20 years after construction. No correlation has been found between the expansion of test specimens and the amount of gel formed (12).

Expansion due to alkali-carbonate reaction occurs much faster than in the case of alkali-silica and alkali-silicate reactions. Structures undergoing alkali-carbonate reaction can exhibit significant map cracking within five years of construction (2). The culprit aggregate is usually coarse dolomitic limestones. The rocks are typically grey, very fine grained, dense and close in texture (12).

The integrity of structures undergoing AAR can be significantly reduced. In the case of alkali-silica reaction, losses in flexural strength can be as high as 50 percent for a corresponding expansion of 0.1 percent (20). However, losses in engineering properties do not occur at the same rate or in proportion to expansion. Therefore, as suggested by Swamy and Al-Asali (20), a rapid reliable test for potential aggregate reactivity and critical limits of deleterious expansion must be developed according to the type and use of a

concrete structure.

2.3.1 Standard Tests

There are four major tests listed in the ASTM standards (1) for evaluating potential alkali-aggregate reactivity. They are: 1) C 227 mortar bar method, 2) C 289 chemical method, 3) C 295 petrographic examination and 4) C 586 rock cylinder method (alkali-carbonate reaction only).

ASTM C 227 mortar bar test is used extensively in the determination of potentially reactive cement-aggregate combinations. The test recognizes both alkali-silica and alkali-silicate reactions. The test is not however recommended for the detection of the alkali-carbonate reaction because expansions in the mortar bars can be much less than expansions related to alkali-silica reaction.

The ASTM chemical method, C 289, measures the amount of reaction between 1 N NaOH solution and crushed aggregate over 24 hours at 80 C. The amount of dissolved silica is estimated plus the reduction in the original hydroxide ion concentration due to the reaction of alkali with the aggregate. A standard curve is then produced relating the amount of dissolved silica and alkalinity reduction. Three regions are delineated on the curve to represent inert aggregates, potentially deleterious and deleterious aggregates.

Petrographic examination, ASTM C 295, is used to identify potentially alkali-silica reactive and alkali-carbonate reactive constituents of the aggregate. Further tests can then be performed to evaluate the potential reactivity of the cement-aggregate combination.

The rock cylinder test, ASTM C 586, determines the expansive characteristics of carbonate rocks while immersed in a solution of sodium hydroxide at room temperature.

The test specimen is in the form of a right circular cylinder with conical ends and an overall length of about 35 mm and a diameter of about 9 mm. Changes in cylinder length are measured at various intervals, for a period up to 1 year.

ASTM chemical method (C 289), petrographic examination (C 295), and the rock cylinder method (C 586) are useful primarily as screening tests rather than tests for specification enforcement. Data obtained from these tests supplement data from field service records and other laboratory tests for alkali-aggregate reaction.

The CSA standard (2) utilizes concrete prisms for the determination of potential alkali-aggregate reactions. The procedure, A23.2-14A, is recommended for identifying the slow/late alkali-silicate and the alkali-carbonate reactions.

Both the ASTM and CSA standards utilize prisms with dimensions in the range 75x75x300 mm to 120x120x450 mm. A minimum of two specimens are recommended for each cement-aggregate combination. The specimens are cast, moist cured for 24 hours, demolded, measured and then inserted into a storage container in which the temperature is 38 C and 100 % humidity. Measurements of the prisms are taken at fixed intervals over one year. The limits of expansion for the ASTM C 227 test are 0.05 % at 3 months and 0.1 % at 6 months. The CSA concrete prism test specifies expansion limits of 0.01 % at 3 months and 0.025 % at 1 year for the alkali silicate reaction, and 0.04 % at 1 year for the alkali-carbonate reaction. Any recorded expansion greater than these values suggests that the aggregate is potentially reactive.

2.3.2 Recent Developments

To facilitate the evaluation of AAR, a single rapid and reliable test is required for all three reaction types. It would be desirable to use such a test to evaluate the condition of existing concrete structures. The following summarizes some of the recent work pertaining to the development of rapid test methods for AAR.

A recently proposed test which has received widespread attention is that of Oberholster and Davies (10). Their test involves the preparation of three mortar prisms prepared according to ASTM C 227 procedures. The prisms are stored in 1 N sodium hydroxide (NaOH) solution at 80 C. The prisms are then measured everyday over 14 days. The average expansion of the three prisms after 12 days is taken as the reference value for assessing potential alkali-reactivity.

Shayan et al. (15,16) utilized both mortar bar and concrete prisms in the evaluation of potential alkali-aggregate reactivity. The specimens were subjected to both the standard mortar bar test and the test proposed by Oberholster and Davies (10). With the mortar bar specimens in 1 N NaOH solution, significant expansions were obtained within two weeks for alkali-silica and alkali-silicate reactive aggregates. While carbonate reactive aggregates exhibited very little expansion with mortar bar specimens, significant expansions were obtained with concrete specimens. As such, concrete specimens appear to be more suitable than mortar specimens for testing the reactivity of carbonate aggregates when using the NaOH test. Shayan et al. found that alkali-silica and alkali-silicate reactive aggregates do not produce appreciable expansions, when concrete prisms are used.

Chatterji et al. (3) utilized both alkali-hydroxide and alkali salt solutions as storage media to determine which had the greatest effect on reaction rate. Chatterji et al. (3)

found that alkali salts do not depress expansion capacity like hydroxides and are preferable for use in an accelerated testing program. They explained that alkali salts take part in the alkali-silica reaction directly and not through their conversion to corresponding alkali hydroxides, as is believed by others (3). Chatterji et al. concluded that potassium ions penetrate the cement paste matrix faster than sodium ions and that a potassium containing cement will cause a more rapid alkali-silica expansion than a corresponding sodium containing cement. Thus, they suggested that it is preferable to utilize potassium chloride solution to increase the reaction rate (4). Oberholster and Davies (10), on the other hand, found that a high concentration of alkali-salt solution at 50 C did not significantly reduce the time required to obtain expansion results for quartz-bearing aggregates. They concluded that a 1 N NaOH solution at 80 C was the most effective storage medium in accelerating the alkali aggregate reaction.

The effects of temperature and alkali concentration were investigated by Oberholster and Davies (10), Chatterji et al. (3) and Swamy and Al-Asali (19). Oberholster and Davies determined that expansions were highest for specimens stored at 80 C in 1 N NaOH compared to specimens stored at 70 and 90 C. A 1 N NaOH solution produced greater expansions than concentrations of 0.5 N and 1.5 N. Chatterji et al. (3) concluded that for specimens in an alkali-salt solution, expansion decreased with a decrease in concentration of the storage solution. No expansion occurred when the alkali-chloride concentration was below 0.5 N.

Swamy and Al-Asali (19) reported that under moist conditions both the rate of reaction and final expansion occur much more rapidly at higher temperatures, and that expansions appear to stabilize much earlier. The alkali content of the cement and the cement content

of the concrete influence both the rate and magnitude of expansion. Results indicated that cement bound alkalinity above 3-4 kg/m^3 NaOH equivalent produces a dramatic increase in expansion. Swamy an Al-Asali also determined that when alkali from sources other than the cement is present,the resulting expansions are increased beyond those due to the cement alkalinity alone.

Hudec and Larbi (8) utilized concrete core specimens with a nominal diameter of 19 mm and a nominal length of 70 mm, in the accelerated test proposed by Oberholster and Davies (10). The alkali content of the concrete mixes was increased by addition of NaOH to the mix water. The cores were extracted from concrete blocks that had been cast and subsequently cured for 28 days. The specimens were immersed in a 1 N NaOH solution at 80 C. Length measurements of the cores were recorded every two days for 30 days. Cores containing reactive aggregates exhibited large expansions compared to those containing non-reactive aggregates. Significant results were obtained for all three types of alkali aggregate reactions.

Alkali-aggregate reaction products were studied by Davies and Oberholster (5), Shayan (16) and Chatterji et al. (3). This study is important in order to not only confirm the existence of reaction products but to show that the test procedures used only accelerate the reaction and do not modify the naturally occurring process. Davies and Oberholster (5) observed many changes in concrete pats that had been immersed in 1 N NaOH solution at 80 C. Gel was observed on the aggregate surfaces after only 48 hours of immersion. The gel continued to grow throughout the test duration. After 20 days, well-defined microscopic cracks were filled with a translucent gel. White reaction product was observed within the air voids and cracks in the pats. Through SEM examination with energy

dispersive x-ray analysis (EDAX), Oberholster and Davies observed massive and rosette-like gels in mortar and concrete prisms which had been immersed in 1 N NaOH solution at 80 C. By comparing the morphology and chemistry of reaction products formed in the accelerated test with those products formed in actual concrete structures, they concluded that the reaction mechanism is not altered by the test conditions, only accelerated. Shayan (16) conducted SEM with EDAX analysis on reacted aggregate specimens. It was determined that the gel contained high amounts of silica, calcium and traces of potassium. Micrographs of reaction products depicted rosettes of crystals similar to that observed by Oberholster and Davies (5).

Oberholster and Davies (10) proposed a critical limit of expansion for their test by comparing results obtained in their test with those obtained in the ASTM C 227 test. They proposed a limit of 0.11 % expansion at 12 days to be used in evaluating aggregates for alkali-silica and alkali-silicate reactivity. Hudec and Larbi (8) proposed limits of 0.17 % after 12 days and 0.33 % after 24 days for alkali-silica and alkali-silicate reactive aggregates. For alkali-carbonate reactive aggregates, they proposed a limit of 0.16 % after 24 days.

The test results obtained by Hudec and Larbi (8) show that the proposed test method by Oberholster and Davies (10) could be modified to become a rapid and consistent procedure for evaluating all three types of alkali-aggregate reaction, utilizing concrete specimens.

3. EXPERIMENTAL STUDY

3.1 GENERAL

The experimental program was designed to develop and evaluate test methods for expansion due to late formation of ettringite and alkali-aggregate reaction in concrete. The experimental work for the two forms of chemical attack are presented separately in Sections 3.3 and 3.4, respectively. The same cements and aggregates were used in fabricating test specimens for both forms of chemical attack.

The test specimens consisted of cores with nominal diameters of 25 mm (1 inch) and 57 mm (2-1/4 inch) and a length-to-diameter ratio of two. Length changes of the test specimens were measured and used to determine expansion due to each chemical attack. Following the length measurements, representative specimens were examined using a scanning electron microscope (SEM) equipped with an energy dispersive x-ray analyzer. Photomicrographs and chemical composition of the test specimen microstructure were obtained and used to determine the nature of reaction products.

3.2 MATERIALS

A total of five cements were utilized in the experimental study, four Type 30 and one Type 10 cements. The cements are designated by letters A to E. Three cements are from eastern Canada: Montreal (B), St. Marys (C) and St. Lawrence (E); one from central Canada, Winnipeg (D); and one from western Canada, Edmonton (A). Cement E is the Type 10 cement. The oxide compositions of the five cements are presented in Table 3.1.

Table 3.1 shows that of the five cements used, the eastern cements have higher alkali contents than their central and western counterparts. Cement C has the highest alkali content of 1.17 % while cement A has the lowest alkali content of 0.52 %.

A total of seven aggregates from active Canadian quarries were used in the experimental study. The aggregates are designated by numbers ranging from 1 to 7. The seven aggregates used were: Nelson (aggregate 1), Spratt (aggregate 2), Pittsburg (aggregate 3), Joliet (aggregate 4), Sudbury (aggregate 5), and two aggregates from Manitoba (aggregates 6 and 7). Aggregates 1 to 5 are from eastern Canada, and aggregates 6 and 7 are from quarries located not far from Winnipeg, Manitoba. Aggregate 1 is a known non-reactive aggregate whereas aggregates 2 and 4 are known alkali-silica reactive aggregates. Aggregates 3 and 5 are known to be alkali-carbonate and alkali-silicate reactive, respectively. Aggregates 6 and 7 have good service records and are not known to be reactive. These latter aggregates are similar but are obtained from different quarries.

Each aggregate was mechanically sieved. The gradation used passed through 1/2 inch sieve but was retained on No. 4 sieve. Thus the maximum aggregate size was 13 mm (1/2 inch). The aggregates were washed and oven dried prior to their use. Bulk specific gravity, unit weight, and absorption capacity were determined for aggregates 1 to 4 using ASTM procedures C 127-84, C 29-78 and C 127-84 respectively. The bulk specific gravities for these aggregates were 2.74, 2.69, 2.73 and 2.70, respectively. The unit weights for the four aggregates were 1941, 2008, 2005 and 2033 kg/m^3, respectively. The absorption capacities were 1.50, 0.85, 1.26 and 0.77 for the four aggregates, respectively.

ASTM standard silica sand was utilized in all concrete mixes. The bulk specific gravity of the sand was determined to be 2.66, the unit weight was 2124 kg/m^3 and the

absorption capacity was 0.83 %.

Ordinary tap water at room temperature was used in preparing all the cement paste and concrete mixes. The cement paste mixes are identified by the cement designations. The mix designations are shown in Table 3.2.

3.3 LATE FORMATION OF ETTRINGITE

3.3.1 Test Procedure

The general test procedure for evaluating expansion due to late formation of ettringite consisted of pretreating the test specimens, followed by storage in distilled water at a temperature of 23 C. Sodium chloride solution was also used as a storage medium for one set of tests, as described later in this section. Pretreatment of the test specimens consisted of alternate immersion in distilled water to attain saturation followed by oven drying to a constant weight. One, two and three cycles of wetting and drying were employed. An oven with a thermostat control was used. The oven temperature was maintained at 80 C and checked regularly using a digital thermocouple.

The test specimens consisted of cores with nominal diameters of 25 mm (1 inch) and 57 mm (2-1/4 inches) and a length-to-diameter ratio of two. The 57 mm diameter cores were used in only one set of tests. To determine the time required for drying of the 25 mm diameter core specimens, saturated concrete specimens were placed in the oven. Weight measurements were taken at selected time intervals until a constant weight was obtained. Conversely, to determine the time to saturation, oven dried specimens were immersed in distilled water and weighed at selected time intervals until a constant weight was obtained. A Mettler PJ 3000 balance with a sensitivity of 0.01 g was used in weighing

the specimens.

Weight gain and weight loss results are shown in Figures 3.1 and 3.2 respectively. The figures show that the time required to achieve saturation is about four hours, whereas at least three days are required to achieve complete drying of the specimens. The periods selected for saturation and drying were two and three days, respectively. Two days was selected for saturation to allow for any shrinkage recovery following the drying process. Thus, one wet-dry cycle consisted of placing saturated specimens in the oven at 80 C for three days, removing from oven and allowing to cool to room temperature for one hour and then immersing in distilled water for two days. This wet-dry cycle was found to be adequate also for the larger 57 mm diameter cores and for the cement paste specimens.

The initial length of the cores was measured following the final saturation process of the pretreatment cycle. During storage of the cores in distilled water, length changes of the cores were monitored. Five 25 mm diameter cores and three 57 mm diameter cores were used in each set of tests.

In assessing the damage reaction due to secondary ettringite formation, the effect of the following factors on test specimen expansion were evaluated: specimen drying, number of wet-dry cycles, water-cement ratio, curing duration, storage medium and specimen size.

Effect of specimen drying: In evaluating the effect of specimen drying, two sets of cement paste specimens which were stored in distilled water at 23 C were monitored for length change. One set of specimens was pretreated by subjecting it to a single wet-dry cycle whereas the second set was not dried but placed in a distilled water bath and heated to 80 C for 48 hours.

Effect of number of wet-dry cycles: To evaluate the effect of the number of wet-dry cycles, cement paste specimens were subjected to one and two wet-dry cycles. Length changes of the specimens were monitored when stored in distilled water at 23 C.

Effect of water-cement ratio: The effect of water-cement ratio (w/c) was investigated using cement paste specimens that were pretreated by subjecting them to one wet-dry cycle. Four values of w/c ratios were employed: 1, 0.7, 0.5 and 0.3. The specimens were stored in distilled water at room temperature and monitored for expansion.

Effect of curing duration: To evaluate the effect of curing duration, two groups of specimens were monitored for expansion. One group was moist cured for two days while the other was moist cured for seven days. The specimens were pretreated by subjecting them to a single wet-dry cycle.

Effect of storage medium The effect of storage medium was investigated by comparing the length change of specimens stored in distilled water to that of specimens stored in saturated sodium chloride solution. The specimens were pretreated by subjecting them to three wet-dry cycles. Both cement paste and concrete specimens were utilized. Cements A and B, and aggregates 1 and 2 were used in fabricating the specimens. Thus, two cement paste specimens and four concrete specimens were utilized.

Effect of specimen size: To evaluate the effect of specimen size on expansion, two different core sizes were utilized. The two core sizes employed had nominal diameters of 25 mm (1 inch) and 57 mm (2-1/4 inches), and a length-to-diameter ratio of two.

3.3.1.1 Test Specimens

Two specimen sizes, 75x75x380 mm prisms and 150 mm cubes, were prepared. Batching was performed at room temperature. Cement paste specimens were mechanically mixed in accordance with ASTM C 305-82 specifications. Sand and coarse aggregate for the concrete specimens were oven dried and allowed to cool prior to batching. During batching of the concrete, the cement and sand were first dry-mixed manually. The coarse aggregate was then mixed in, followed by addition of the appropriate amount of water. The mix water was increased to correct for absorption of the aggregates. Thorough mixing was then performed manually. The concrete mix design proportions consisted of cement: sand: coarse aggregate ratio of 1:2:2. With the exception of specimens used to evaluate the effect of water-cement ratio on expansion, all specimens were prepared using mixes with a water-cement ratio of 0.5.

The steel molds were oiled and sealed with modeling clay. The molds were filled in three equal layers, with each layer being rodded twenty-five times using a five-eighths inch diameter rod. During the first twenty-four hours, the molds were stored in a moist curing room at 23 C and covered with a plastic sheet. The specimens were then removed from the molds and stored in the curing room. All specimens were moist cured for seven days with the exception of those used to evaluate the effect of curing duration.

After the specimens were moist cured, they were cored using a Milwawkee model 4099 electric drill. Diamond tipped drill bits of internal diameters 25 mm (1 inch) and 57 mm (2-1/4 inch) were used to extract the cores from the specimens. The 25 mm diameter cores were obtained from the 75x75x380 mm prisms, while the 57 mm diameter cores were obtained from the 150 mm cubes. The cores were cut using a high speed

diamond masonry saw to obtain a length-to-diameter ratio of two. Aside from evaluating size effects, the core size used in this study was the 25 mm (1 inch) diameter size with a nominal length of 50 mm (2- inches).During the coring and cutting process, the specimens were stored in plastic containers that contained tap water at a temperature equal to that of the curing room. Containers for cores to be processed were removed from the curing room one at a time, the cores processed, and then returned to the curing room. Figure 3.3 shows the 25 mm and 57 mm diameter cores.

Five 25 mm diameter cores and three 57 mm diameter cores were used in each set of expansion measurements. For these measurements, the 25 mm diameter cores were stored in 114x127x75 mm (4.5x5x3 inch) deep plastic containers, each with a volume of 1 litre. The 57 mm diameter cores were stored in 2.5 litre circular containers with a diameter of 178 mm (7 inches) and a depth of 127 mm (5 inches). Each core was given a label designating the core and mix number. For example, a core labelled 1-A1 indicates that the specimen is core number one from mix A1.

3.3.1.2 Test Measurements

Length measurements were carried out on saturated specimens. A specimen was removed from the container, blotted with a damp cloth to remove excess free moisture, and inserted into the measuring apparatus. A vertical line drawn on the surface of each specimen enabled the specimen to be placed in the same position each time in the measuring apparatus. After three individual measurements, the specimen was returned to its container prior to measurement of the next specimen. Latex rubber gloves were worn at all times for the handling of test specimens. The room in which the specimens were

stored and measured was maintained at about 50 % relative humidity and 23 C. Length measurements were taken every three days for the first fifteen days, then every five days for a minimum of 15 days. In many of the test series, the duration of the test measurement was extended beyond 30 days.

Figures 3.4 shows the measuring apparatus. A converted drill press acts as the holding device, a piece of angle fixed to the base plate maintained a vertical positioning of the cores. The base on which the core rested and the vertical column fixed to the drill press had small steel ball bearings to ensure point contacts at the top and bottom of the core. A linear variable differential transformer (LVDT) fixed to the drill press measured the change in distance between the two ball bearings. A steel calibration bar was used to re-calibrate the system prior to the core measurements. A 50.800 mm bar was used for the small core device and a 114.300 mm bar was used for the larger core device. Figure 3.4 shows a calibration bar in the measuring apparatus.

The LVDT was connected to a data acquisition unit which recorded the voltage differential. The data acquisition unit is shown in Figure 3.5. A computer program converted the voltage to a linear core length measurement through application of a calibration factor. During the calibration process, the calibration factor was varied until the difference between the calibration bar length and the computer measurement was within 0.005 mm. The calibration factor was rarely altered by more than 0.0005 volts/mm. The computer printout obtained showed the core number, mix designation, the three individual length measurements (the computer took two readings for each measurement) and the average of three measurements.

The length change data were used to calculate expansion (or contraction) of the cores based on the initial length measurements. The average percent expansion of the five cores (three for 57 mm cores) was computed for each measurement period.

3.3.1.3 Scanning Electron Microscope Studies

The scanning electron microscope (SEM) equipped with an energy dispersive x-ray analyzer provides a valuable tool in the identification of reaction products. A JEOL JXA-840 SEM in the Faculty of Engineering at the University of Manitoba was used in this study. The system is also equipped with an energy dispersive x-ray analyzer which allows for rapid determination of the elemental and oxide compositions of materials. A Trecor Northern computer unit enables the system to perform semi-quantitative analysis. Figure 3.6 shows the SEM and the x-ray analysis system.

For the SEM examination, small fractured specimens, approximately 6 mm (1/4 inch) thick by 12 mm (1/2 inch) long by 6 mm (1/4 inch) high, were prepared from 6 mm thick slices. The slices were removed from selected core specimens at the conclusion of the length measurements using a high speed diamond masonry saw. A typical SEM specimen, as mounted on a stud, is shown in Figure 3.7. To obtain clear photomicrographs, the top surface of the SEM specimens was rendered conductive with a layer of gold-palladium about 0.02 micrometers thick. No conductive coating was used on specimens for the energy-dispersive x-ray analysis.

3.3.2 Test Results

Table 3.3 shows a typical output obtained from the core length measurement process. The length measurements were used to compute the expansion of the cores. Table 3.4 shows typical results consisting of measurement period, core number, initial length of core, measured length, change in length, percent expansion and the average percent expansion.

A typical photomicrograph of needlelike crystals within the microstructure of a test specimen is shown in Figure 3.8. The corresponding elemental energy-dispersive spectrum of the crystals is shown in Figure 3.9, and the oxide compositions of the crystals are shown in Table 3.5.

3.4 ALKALI-AGGREGATE REACTION

3.4.1 Test Procedure

In the assessment of alkali-aggregate reaction, both the accelerated and standard tests were performed. The accelerated test was based on the method proposed by Oberholster and Davies (10), while the standard test was based on the CSA concrete prism test (2). In the accelerated test, the primary storage medium for the test specimens was a one molar sodium hydroxide solution. The effect of a three molar potassium chloride solution was also investigated. One inch diameter cores were used in the test program. The concrete cores were extracted from cubes that had been moist cured for seven days. The cores were conditioned by immersing them in the storage medium at room temperature and then placing them in an oven at 80 C for 24 hours. This conditioning process ensured that the specimens did not undergo thermal shock. The initial measurement of the

specimens were taken after the conditioning. Subsequent length measurements were taken at selected time intervals.

In order to enhance the reaction, the effect of pretreating the test specimens by subjecting them to wet-dry cycles was investigated. The possible enhancement in reaction would be due to formation of microcracks in the test specimens to facilitate movement of the NaOH solution within the specimens. The wet-dry cycle procedure is as shown in Figure 4.7. Upon the final oven drying segment of the cycle, the specimens were allowed to cool, immersed in 1 M sodium hydroxide solution and placed in the oven at 80 C. A control batch of specimens from the same mixes were used for comparison purposes. Instead of being immersed in NaOH solution, the control group was immersed in distilled water, and placed in the 80 C oven.

All the seven aggregates were utilized in the test program. For comparison purposes, the standard CSA concrete prism expansion test (2) was conducted alongside the accelerated test. In order to investigate the effect of cement alkali content only, no alkali was added to the concrete mixes for the CSA prism test.

3.4.1.1 Test Specimens

Test specimens for the accelerated test were fabricated in the same manner as those used in the study pertaining to late formation of ettringite. Section 3.3.1.1 provides a complete description of specimen fabrication. The concrete mixes were designed for a water-cement ratio of 0.5.

The mix design for the CSA concrete prism test was similar to that for the accelerated test. However, the desired consistency was based on slump. The slump was

in the range of 70-90 mm, and the water-cement ratio ranged from 0.48-0.51. The size of the test specimens was 75x75x380 mm (3x3x15 inches). As specified in the CSA procedure, the test specimens were stored over water at 38 C in a tank. Wicks were placed on the sides of the tank.

3.4.1.2 Test Measurements

The specimens in the accelerated test were measured in the 'hot-wet' condition after being wrapped in a sheet of plastic to diminish the effects of thermal contraction. The remainder of the length measurement process was identical to that described in section 3.3.1.2.

All test specimens were monitored for a minimum of 30 days. The frequency of measurement consisted of measurements every two days for the first 14, then every three days for the next 18 days. Any additional measurements taken were at five to seven- day intervals. Five test specimens were used for each concrete mix.

The concrete prisms were measured at the intervals prescribed by the CSA standard. The measurements were taken at 7, 14, 28, 56, 84, 112, 168 and 365 days. Additional measurements were obtained at 60-day intervals beyond 168 days. Measurement of the prisms was accomplished using an LVDT apparatus similar to that used for the core specimens. A metal stand with a fixed base and a spring loaded LVDT attached to the top of the stand was used. Figure 3.5 also shows the prism measuring apparatus with a calibration bar in place. The computer program used to measure the prisms was the same as the one used for the cores. The program calibration number was always checked prior to any series of prism measurements. Three independent measurements were taken on

each prism. Three prisms were used for each concrete mix.

The length data were related to the initial length measurement to obtain percent change in length or expansion. Expansion versus time relationships were then obtained.

3.4.1.3 Scanning Electron Microscope Studies

To determine the nature of reaction products, SEM examination and energy dispersive x-ray analysis was performed on selected specimens at the end of length measurements. The SEM procedure is as described in Section 3.3.1.2.1.

3.4.2 Test Results

Table 3.6 shows typical expansion results for test specimens stored in 1 M NaOH solution at 80 C. A typical photomicrograph of alkali-silica gel within the microstructure of a test specimen is shown in Figure 3.10. The corresponding elemental energy-dispersive spectrum of the gel is shown in Figure 3.11 and the oxide compositions of the gel are shown in Table 3.7. The molar ratio of calcium oxide to silica (CaO/SiO_2) for the gel is 0.22. This value is much lower than the values of between 2 and 3 for the normal cement paste matrix, indicating the high silica content of the reaction product.

4. EVALUATION AND DISCUSSION OF TEST RESULTS

4.1 GENERAL

In this chapter, the test results described in Chapter 3 are used to evaluate and discuss the potential of the different mixes to undergo chemical attack due to either late formation of ettringite or alkali-aggregate reaction. Test specimen expansion and the effect of different factors on the magnitude of expansion are discussed. Photomicrographs and chemical composition of the test specimen microstructure are used to evaluate the nature of the reaction products. Test procedures are proposed for evaluating cements for late formation of ettringite, and aggregates for alkali-aggregate reaction.

4.2 EXPANSION DUE TO LATE FORMATION OF ETTRINGITE

A plot of expansion versus time for cement paste specimens made with the five cements is shown in Figure 4.1. The average results for five test specimens are shown in the figure and in subsequent figures. The expansions for Mixes B and C are much larger than those for Mixes A and E. The expansion for Mixes B and C is about 1.2 % after 30 days compared to 0.2 % for Mixes A and E and 0.1 % for Mix D. For all test series, the Type 30 cements produced in eastern Canada exhibit much larger expansions than those produced in central and western Canada. Mixes B and C specimens exhibited extensive cracking whereas Mixes A, D and E specimens were uncracked. Figure 4.2 shows a cross-section of an uncracked specimen, and Figures 4.3 and 4.4 show cross-sections of cracked specimens at the conclusion of the tests. As will be discussed later in Section 4.2.7.2,

cement paste specimens which exhibit large expansions contain massive formations of ettringite.

As discussed earlier, Heinz and Ludwig (7) found that cements with molar ratios of SO_3 to Al_2O_3 below 0.55 showed little or no expansion. Of the cements used in this study, A, B, C and D have SO_3 to Al_2O_3 ratios greater than 0.55. The ratios are 0.83 for cement A, 1.03 for cement B, 1.21 for cement C and 1.18 for cement D. However, only cements B and C produced large expansions. This seems to suggest that the ratio of SO_3 to Al_2O_3 is not the only factor which controls the degree of expansion.

It is interesting to note that cements B and C which produced the largest expansions also have the highest alkali contents, 0.99 % and 1.17 % respectively (Table 3.1). Cements A and D have alkali contents of 0.52 % and 0.57 %, respectively. In the cement clinker, the alkalis occur preferentially in the form of sulphates (17). Since the alkali sulphates dissolve readily when in contact with water, sulphate ions are released to react with tricalcium aluminate in the cement to form ettringite. This implies that higher alkali cements would release more sulphate ions into the pore solution for ettringite formation than lower alkali cements. As such, larger quantities of ettringite, and accompanying larger expansions, could be obtained for high alkali cements than for lower alkali cements. This conclusion is supported by the results obtained in this study. It seems therefore that low molar ratios of SO_3 to Al_2O_3 and low alkali contents are required in cements to avoid large expansions due to late formation of ettringite.

Large expansions of cement paste specimens can also occur due to slow hydration of uncombined lime which may be present in large cement particles and is not detected by current tests (22). Vivian (22) showed that the uncombined lime content of re-ground

large cement particles was higher than that of the bulk cement. Specimens made with 20-40 micrometer and greater than 40 micrometer size particles expanded by significant amounts, whereas those made with the bulk cement expanded by negligible amounts. To determine if significant quantities of undetected uncombined lime were present in the cements used in this study, different size fractions of the cements were analyzed. The uncombined lime contents of the different size fractions were approximately the same as that of the bulk cement. The uncombined lime content of the cement particles larger than 44 micrometers was slightly lower than that of the bulk cement. This indicates that hydration of uncombined lime did not contribute to the expansions measured in this study.

4.2.1 Effect of Drying

Figure 4.5 shows the expansion-time plot for Mix D cement paste specimens subjected to one wet-dry cycle and for specimens subjected to a distilled water bath heated to 80 C for 48 hours. The specimens show expansion when subjected to the wet-dry cycle and no expansion when subjected to heating in the water bath. The difference in expansion shows that drying is required to induce the expansion.

4.2.2 Effect of Number of Wet-Dry Cycles

Expansion versus time results for specimens subjected to one and two wet-dry cycles are compared in Figure 4.6. The figure shows that the expansion for two wet-dry cycles is larger than that for one cycle. For both cycles, Mix B specimens exhibit larger expansions than Mix A specimens. Increasing the number of wet-dry cycles beyond two caused rapid disintegration of Mix B specimens. Two wet-dry cycles are therefore

recommended for evaluating cements, as illustrated in Figure 4.7.

4.2.3 Effect of Water-Cement Ratio

The effect of water-cement ratio (w/c) on cement paste expansion is shown in Figure 4.8. The data points are expansion values for specimens subjected to one wet-dry cycle and immersed in distilled water for 15 days. Similar relationships are obtained for other periods of immersion in the distilled water. For all water-cement ratios, Mix B specimens exhibit larger expansions than Mix A specimens. The expansions are larger for a w/c of 0.5 than for w/c of 0.3, 0.7, and 1.0. The lower expansions for the higher w/c pastes (w/c= 0.7 and 1.0) could be attributed to the higher porosity of these pastes. The high porosity could enable these materials to deform into voids with little or no changes in the external dimensions of the specimens. The lower expansion for the lower w/c paste (w/c= 0.3) could be explained by the lower permeability of this paste. The low permeability reduces the amount of water absorbed by the specimen and could therefore reduce the extent of the reaction which induces expansion. A w/c of 0.5 was therefore used throughout the remainder of this study.

4.2.4 Effect of Curing Duration

The results obtained for the effect of curing duration on expansion are shown in Figure 4.9 for Mix B specimens. The figure shows that specimens cured for seven days expand more than those cured for two days. The lower expansion of specimens cured for two days could be attributed to the higher porosity of these specimens. As explained in Section 4.2.3, a high porosity could enable the specimen material to deform into voids with

little or no change in external dimension. A curing duration of seven days was used throughout the remainder of this study.

4.2.5 Effect of Storage Medium

The effect of storage medium on expansion is shown in Figure 4.10 for cement paste specimens and in Figure 4.11 for concrete specimens. The specimens were stored in distilled water and in saturated sodium chloride (NaCl) solution. For both cement paste and concrete, specimens stored in water expand whereas those stored in NaCl solution contract. The large expansions of Mix B and Mix B2 specimens stored in distilled water contrast sharply with the contraction of the same specimens stored in NaCl solution.

Expansion of the specimens is attributed to formation of ettringite, as discussed in Section 4.2.7.2. Contraction of the specimens in NaCl solution is therefore not surprising since ettringite is soluble in the presence of chloride ions (17). Alkali ions in NaCl solution enhance expansion due to alkali-aggregate reaction (AAR) for specimens made with reactive aggregates (3). As such, the contraction of concrete specimens made with reactive aggregates and stored in NaCl solution suggests that ettringite and not AAR is the cause of the expansion of concrete specimens stored in water. While massive formations of ettringite are found in photomicrographs presented in a subsequent section, no AAR products are found in any of the concrete specimens.

4.2.6 Effect of Specimen Size

The effect of specimen size on expansion is shown in Figure 4.12. The figure shows a comparison of expansions for 25 mm and 57 mm diameter cores. The figure shows that

the smaller specimens exhibit larger expansions. Figure 4.13 shows the coefficient of variation for the 25 mm and 57 mm diameter cores. The coefficient of variation generally decreases with increase in specimen immersion time. After 32 days immersion, the coefficient of variation values are 8 % for the 25 mm diameter core and 13 % for the 57 mm diameter core. The smaller coefficient of variation, in addition to the larger expansions (Figure 4.12), suggest that the small cores are preferable to the larger ones for evaluating cements.

4.2.7 Cement Paste vs Concrete Specimens

4.2.7.1 Expansion

Expansion results obtained for concrete specimens are shown in Figure 4.14. Figure 4.15 shows the results for mixes B1 and B2 only. Figures 4.1 and 4.14 show that the cement paste specimens expand more than the concrete specimens. The ratio of cement paste to concrete core expansion is at least two. This indicates that the aggregate provides a restraining effect on expansion. Concrete mixes made with cement B exhibit large expansions, regardless of the aggregate type. Concrete mixes made with cement A, on the other hand, exhibit very little expansion. These results are similar to the results in Figure 4.1 which shows that cement B specimens exhibit very large expansions whereas cement A specimens exhibit very small expansions. The expansion of the concrete specimens therefore seems to depend solely on the cement used. As will be discussed in the next section, both cement paste and concrete specimens which exhibit large expansions contain massive formations of ettringite.

Cement B concrete mixes show differences in the magnitude of expansion. As such, the question arises as to the role the coarse aggregate plays in the observed expansion. As stated earlier, aggregate 1 is a known non-reactive aggregate, aggregate 2 is alkali-silica reactive, and aggregate 3 is alkali-carbonate reactive.

The large expansions for Mix B1, the non-reactive aggregate mix, cast doubt on aggregate reactivity as the cause of the differences in expansion of the cement B concrete mixes. This observation is supported by SEM examination and analysis which revealed no trace of gel due to alkali-aggregate reaction. To understand the effect of aggregate on the observed expansion, the lengths of selected concrete specimens were measured at the end of each phase of the pretreatment process. Figure 4.16 shows that cement paste contraction due to drying is approximately five times that of concrete specimens, reflecting the restraining effect of aggregate. Figure 4.16 also shows that there is a difference in contraction of mixes B1 and B2 specimens. Since both mixes are made with the same cement, the difference in contraction is attributed to difference in restraining effect provided by the aggregates. The fact that the test specimens exhibit differences in contraction at the end of pretreatment seems to explain the different expansions obtained for the concrete specimens made with the same cement. Thus it is concluded that aggregate reactivity does not contribute to the expansion of the concrete specimens.

Since the expansion of the test specimens depends solely on the cement used, cement paste specimens are preferred to concrete specimens in evaluating the potential expansion of a mix made with a particular cement.

4.2.7.2 Scanning Electron Microscope (SEM) Analyses

Micrographs: Photomicrographs of features found within the microstructure of test specimens are presented in Figures 4.17-4.26. These features are found within the paste matrices and voids in cement paste and concrete, on crack surface in cement paste, and at the paste-aggregate interface in concrete. The photomicrographs shown in Figures 4.17-4.21 were obtained from cement paste specimens while those in Figure 4.22-4.26 were obtained from concrete specimens.

Figure 4.17 shows needlelike features within the paste matrix and Figure 4.18 shows globular needlelike features within a void. A higher magnification micrograph of the features in Figure 4.18 is shown in Figure 4.19. Figure 4.20 and 4.21 are micrographs of globular needlelike features found on a crack surface in cement paste. Needlelike features within the paste matrix of concrete are shown in Figure 4.22. Figure 4.23 and 4.24 show features within a void in concrete and their morphology at a higher magnification. Figure 4.25 is a micrograph showing the paste surface of a paste-aggregate interface. A higher magnification micrograph of the paste surface, Figure 4.26, shows needlelike features. These features appear to be flattened, compared to those located in a void (Figure 4.24), probably due to pressure imposed by the interface aggregate.

The microstructural features shown were found primarily in those mixes which exhibited large expansions. These mixes were made with cements B and C. Mixes made with cements A, D and E contained very little or no visible amounts of these features. Thus, the extent to which the features formed within the microstructure of the test specimens correlates very well with the degree of specimen expansion.

Energy-dispersive analysis: As the photomicrographs show, all the microstructural features are made up of needlelike crystals, suggesting that they are ettringite products. This observation is supported by the composition of the features as shown by the energy-dispersive spectra presented in Figures 4.27-4.32. A typical spectrum for the microstructural feature in Figure 4.17 is shown in Figure 4.27, while that for the feature in Figures 4.18 and 4.19 is shown in Figure 4.28. Figure 4.29 is typical for the feature in Figures 4.20 and 4.21. The spectrum in Figure 4.30 is typical for the needlelike feature in the paste matrix of concrete (Figure 4.22). A typical spectrum for the feature in Figures 4.23 and 4.24 is shown in Figure 4.31, while that for the feature in Figures 4.25 and 4.26 is shown in Figure 4.32.

The elemental spectra show that the microstructural features are predominantly composed of calcium (Ca), sulphur (S) and aluminum (Al). This confirms that the features are calcium sulphoaluminate or ettringite products.

Stoichiometric oxide compositions of the microstructural features as obtained from the energy-dispersive analysis are presented in Table 4.1. Also shown are the stoichiometric oxide ratios, CaO/SO_3 and CaO/Al_2O_3. The theoretical values of CaO/SO_3 and CaO/Al_2O_3 for ettringite are 2 and 6, respectively. In general, the oxide ratios obtained for the microstructural features in both cement paste and concrete specimens compare well with the theoretical ratios for ettringite. The high oxide ratios obtained for the feature on the crack surface of a cement paste specimen indicate that this feature has a high calcium content, probably due to leaching onto the crack surface.

The source of ettringite formation in the test specimens could be due to one or both of the following mechanisms:

(i) reaction between aluminate and sulphate ions that are bound within the hydration products when moisture becomes available;

(ii) dissolution of previously formed ettringite by water circulating through the specimen and its subsequent precipitation from solution.

The different morphologies of ettringite observed in the test specimens could have been formed from both of these mechanisms. The formation of ettringite due to the second mechanism is not likely to give rise to excessive expansion and cracking (11,18). It is therefore believed that the formation of ettringite in accordance with the first mechanism is largely the cause of the expansion and cracking of the test specimens.

The formation of ettringite in the test specimens due to the first mechanism implies that the expansion and cracking phenomena could be described as internal sulphate attack, where sulphates are supplied by the cement paste itself.

4.2.7.3 Proposed Test Method

The procedure utilized in this study is proposed as a test method to evaluate cements for their potential to cause expansion and cracking due to late formation of ettringite.

A summary of the proposed test method is as follows:

1. Fabricate cement paste specimens with a water-cement ratio of 0.5 in accordance with ASTM C 305-82 specification.
2. Moist cure the specimens for seven days.
3. Obtain cores with a nominal diameter of 25 mm (1 in). Saw cut the cores to obtain test specimens with a length of 50 mm. Use five cores to evaluate each cement.

4. Pretreat the test specimens using the two wet-dry cycle procedure shown in Figure 4.7. Each wet-dry cycle consists of two days saturation, three days drying, and a final two days saturation.
5. Measure the length of the test specimens at the end of the pretreatment. Store the specimens in distilled water at room temperature for one to two weeks and measure their lengths every two to three days.
6. The critical limit of expansion, based on the limited results of this study, is proposed to be 0.2 percent after seven days in distilled water. The expansion limit may need to be refined after more cements have been evaluated.

4.2.8 Summary of Findings

1. Cement paste specimens made with cements produced in different regions of Canada exhibit significant differences in the magnitude of expansion when pretreated by subjecting them to wet-dry cycles. Specimens for some cements expand by negligible amounts, whereas those for other cements expand by very large amounts.
2. Cement paste specimens expand more than concrete specimens made with the same cement. The magnitude of expansion in both types of specimen depends upon the cement used.
3. A water-cement ratio of 0.5 appears to be the optimum water-cement ratio for expansion under the test procedure used in this study.
4. Expansion and cracking of test specimens increase with increase in the number of wet-dry cycles. Pretreatment involving two wet-dry cycles is recommended for evaluating cements.

5. The duration of curing affects the magnitude of test specimen expansion. Specimens cured for seven days expand more than those cured for two days, probably due to the higher porosity of the latter specimens.

6. Based on the magnitude of expansion and the coefficient of variation of the expansion data, the small test specimens, 25 mm diameter, used in this study are preferable to the larger 57 mm diameter ones for evaluating cements.

7. Both cement paste and concrete specimens which exhibit large expansions contain massive formations of ettringite, whereas those which exhibit very small expansions contain little or no visible amounts of ettringite. This strongly suggests that late formation of ettringite is the cause of expansion of the test specimens.

8. For concrete specimens, SEM analysis indicates the absence of alkali-aggregate reaction, even in concretes made with known reactive aggregates.

9. The different magnitudes of expansion for concretes made with the same cement but different coarse aggregates appears to be due to differences in the length change of the test specimens at the end of pretreatment.

10. Test specimens stored in sodium chloride solution contract, in contrast to expansion of similar specimens stored in water.

11. The contraction of test specimens in sodium chloride solution and the absence of visible ettringite in these specimens are attributed to the high solubility of ettringite in the presence of chloride ions.

12. The contraction of test specimens in sodium chloride solution further suggests that ettringite is the cause of expansion of the test specimens stored in water.

13. Expansion and cracking of concrete due to late formation of ettringite could be prevented by using cements with low molar ratios of SO_3 to Al_2O_3 and low alkali contents.

14. The procedure utilized in this study could be used as a test method to identify cements that could cause expansion and cracking due to late formation of ettringite when concrete is subjected to alternate wet and dry conditions.

4.3 EXPANSION DUE TO ALKALI-AGGREGATE REACTION

Figure 4.33 shows an expansion versus time plot comparing expansion results of test specimens fabricated with aggregate 2, the alkali-silica reactive aggregate, in two different storage media. In the figure and in subsequent figures, each data point is an average of results for five test specimens. One set of specimens was stored in a 3 M KCl solution, and the other set in a 1 M NaOH solution, both at 80 C. The figure shows that a NaOH storage medium is more effective in accelerating expansion in concrete cores. Thus, a 1 M NaOH solution at 80 C was utilized as the storage medium for the remainder of the accelerated tests.

4.3.1 Specimens in Sodium Hydroxide Solution

Figures 4.34 and 4.35 show expansion versus time results for test specimens subjected to two different conditioning media. Each figure shows the results for a particular concrete mix subjected to the two different conditioning media. One set of specimens was conditioned in distilled water at 80 C, whereas the second set was conditioned in NaOH solution at 80 C. The figures show that specimens conditioned in

NaOH start expanding immediately, whereas those conditioned in water have a 4-6 day lag prior to expansion. Reaction products were observed on the surface of the NaOH-conditioned specimens within 2 days, whereas it took 4-6 days before any reaction products were seen on the water-conditioned specimens.

The reason for the expansion lag in water conditioned specimens is probably due to a dilution of alkalis by water in the specimens. By conditioning in NaOH, the alkali is able to immediately penetrate the matrix and instigate the reaction. Conditioning in NaOH was therefore utilized in the remainder of the study.

Figure 4.36 shows expansion versus time results for specimens made with aggregate 2, and different cements. The cements had different alkali-contents ranging from 0.52 % to 1.17 %, as shown in Table 3.1. The figure shows that the expansions do not correlate with the alkali content of the cements. The NaOH solution appears to override the cement alkalis. Thus, expansion appears to be independent of cement alkali content for the test method used in this study. The magnitudes of expansion obtained for the test specimens clearly show that the test method is suitable for evaluating aggregate reactivity, utilizing concrete specimens.

Figure 4.37 shows expansion versus time results for test specimens made with alkali-silica and alkali-carbonate reactive aggregates. The magnitudes of expansion for both types of reactivity are essentially the same.

Figure 4.38 shows expansion versus time results for specimens made with reactive and non-reactive aggregates. The magnitude of expansion for Mixes A2 and B2 specimens is approximately 0.3 % in about one month. Mixes A1 and B1 specimens on the other hand, contract, clearly showing that the test method used in this study discriminates

between reactive and non-reactive aggregates. Figure 4.39 shows the expansion results for Mix A2 and B2 specimens over a period of 68 days. The figure shows that expansion continues to increase even after two months. The expansion-time relationships are essentially linear.

Figure 4.40 shows expansion versus time results for specimens made with aggregate 4, an alkali-silica reactive aggregate. Figure 4.40, when compared to Figure 4.38, shows that expansion levels, though significant, are markedly less than those obtained for aggregate 2, the other alkali-silica reactive aggregate. SEM examination, as discussed later in Section 4.3.1.2, revealed smaller amounts of reaction product inside the aggregate 4 specimens than in the aggregate 2 specimens.

Figure 4.41 shows expansion results for specimens fabricated with aggregate 6, which is obtained from a quarry near Winnipeg, Manitoba. Expansions for Mix B2 specimens are also plotted for comparison purposes. The figure shows that virtually no expansion occurred in the Mix B6 specimens. Aggregate 6 has a good service record with regard to AAR.

Figure 4.42 shows expansion versus time results for specimens fabricated with aggregate 5, the alkali-silicate reactive aggregate, and for Mix B2 specimens. The figure shows that no expansion was obtained for specimens fabricated using aggregate 5. This result contrasts sharply with that obtained by Hudec and Larbi (8), in which large expansions were obtained for specimens fabricated with the same aggregate. Hudec recorded expansion levels as high as 0.6 % within 30 days. These different results could be due to the fact that in Hudec and Larbi's work, additional alkali was added to the concrete mix whereas no alkali was added in this study. In addition it was determined from

Hudec (telephone conversation) that not all specimens made with aggregate 5 expanded and that only the results for specimens which expanded were published. The test method may need to be modified for the evaluation of alkali-silicate reactive aggregates.

The appearance of the test specimens at the conclusion of the tests is represented in Figures 4.43-48. Figures 4.43 and 4.44 show cross-sections of uncracked specimens for aggregates 1 and 5, respectively, Cracked specimens for aggregate 2 are shown in Figures 4.45 and 4.46, while that for aggregate 3 is shown in Figure 4.47. White spots of gel are observed on the surface of an aggregate 3 specimen in Figure 4.48.

4.3.1.1 Effect of Wet-Dry Cycles

Figure 4.49 shows expansion versus time results for specimens which were pretreated by subjecting them to two wet-dry cycles prior to their immersion in NaOH solution. In comparison with expansion of specimens that were not pretreated (Figure 4.38), it is apparent that the wet-dry pretreatment does not enhance the expansion. The expansion values after 30 days immersion for mixes A2 and B2 specimens that were not pretreated are 0.30 and 0.27 %, respectively. Expansion values for similar specimens which were pretreated are 0.26 and 0.22 %, respectively. Specimens made with aggregate 1 showed a contraction of about 0.06 to 0.08 % with and without pretreatment. Thus, no apparent advantage exists for incorporating pretreatment in the test procedure.

Figure 4.50 shows the results for specimens placed in distilled water at 80 C instead of in NaOH solution. The figure shows that the pretreated specimens contract. The NaOH bath is therefore necessary to induce AAR expansion in the pretreated specimens.

4.3.1.2 Photomicrographs and Microstructure Composition

Photomicrographs of reaction products and their elemental spectra obtained from the SEM examination and analysis are presented in Figures 4.51 to 4.79. The oxide compositions and the molar ratios of CaO/SiO_2 are given in Table 4.2. All the ratios are less than the values of between 2 and 3 for normal cement paste matrix of concrete (6), indicating high silica content of the reaction products.

Figures 4.51 to 4.61 are photomicrographs and elemental compositions obtained for specimens made with aggregate 2, an alkali-silica reactive aggregate. Figures 4.51 and 4.52 are low and higher magnification micrographs of a rosette-like morphology at a paste-aggregate interface. This morphology is identical to that obtained by Oberholster and Davies (5), both from their tests and from concrete structures undergoing AAR. The rosette morphology was found only in test specimens made with aggregate 2. Figures 4.54 and 4.55 show a different morphology obtained at the aggregate-paste interface, near the same area as the rosettes. The higher magnification micrograph in Figure 4.55 shows the fibrous texture of this morphology. The morphology was found only in test specimens made with aggregate 2. Figure 4.57 shows a sponge-like morphology also at the paste-aggregate interface. Figure 4.59 and 4.60 show low and higher magnification micrographs of a reaction product within the paste matrix adjacent to the paste-aggregate interface. This morphology appears to be oriented in a particular direction and was found only in specimens made with aggregate 2.

Figures 4.62 and 4.63 are micrographs for specimens fabricated with aggregate 3, the alkali-carbonate reactive aggregate. Figure 4.62 shows a low magnification micrograph of

a reaction product within a void. Figure 4.63 is a higher magnification shot of the same area. The morphology is sponge-like, as in the case of Figure 4.57 for ASR. A sponge-like morphology is also observed at the paste-aggregate interface, as shown in Figure 4.65. Figure 4.67 is a micrograph of a reaction product scraping obtained from the surface of a test specimen. The reaction product has a plate-like structure. No brucite (MgOH) reaction products were observed in the test specimens for the alkali-carbonate reactive aggregate. Rather, reaction products which are very high in silica are obtained, as shown in Table 4.2. The source of the silica may be the clay minerals which are present in reactive carbonate aggregates.

Figure 4.69 and 4.70 are micrographs of reaction products obtained from specimens made with aggregate 4, an ASR aggregate. Figure 4.69 shows a feature with worm-like ridges at the base of a void where an aggregate appears to have been pulled out. Figure 4.70 shows a higher magnification micrograph of the same feature. These ridge-like formations were found only in specimens made with aggregate 4. Figure 4.72 is a micrograph of a scraping obtained from the surface of a test specimen. The sponge-like morphology is very similar to those shown in Figure 4.57 and 4.65. A reaction product with sponge-like morphology was also observed in the matrix of the test specimens. Smaller quantities of reaction product were observed in the aggregate 4 specimens than in the aggregate 2 specimens. This seems to explain the lower expansion of the aggregate 4 specimens compared to the aggregate 2 specimens.

Figures 4.74 and 4.75 are gel scrapings obtained from specimens made with aggregate 5, the alkali-silicate reactive aggregate. Figure 4.74 is a low magnification micrograph, while Figure 4.75 is a higher magnification micrograph of the area shown in

the bottom centre of Figure 4.74. No gel was observed in the matrix of the test specimens. This seems to correlate with the lack of expansion obtained for these test specimens.

Figure 4.77 and 4.78 are micrographs of a test specimen made with aggregate 6, a local aggregate. The gel has a morphology not unlike dried mud. Very small amounts of this gel were observed, correlating well with the lack of expansion obtained for the test specimens.

The SEM examination and analysis therefore reveal the formation of different morphologies of reaction product due to AAR. The sponge-like morphology appears to be the most common. Specimens fabricated from aggregates 2 and 3 which exhibit large expansions contain massive amounts of gel with various morphologies. Specimens fabricated from aggregate 4 which exhibit smaller expansions contain smaller amounts of gel. Specimens made with aggregates 5 and 6 which showed no expansion yielded very little gel.

Thus, the magnitude of expansion appears to be an excellent indicator of the quantity of gel formed. The presence of reaction products does not necessarily result in the deleterious expansion of the test specimens.

4.3.2 Expansion Results for the Standard Test

Figure 4.80 shows expansion versus time results for Mixes A2 and B2 prisms. The average results for three prisms are shown for each mix. After 112 days, Mix B2 specimens made with high alkali cement expand by 0.02%. Mix A2 made with low alkali cement, on the other hand, showed no expansion. Figure 4.81 shows the expansion versus time results for Mix B2 prisms up to one year. The prisms initially expand and then contract by the end of the test. This result is typical of the behaviour of the prisms in the test.

Closer examination of the results for individual prisms indicated that specimens located close to the moisture wicks expanded the least and those located furthest away from the wicks expanded the most. This phenomenon is illustrated in Figure 4.82 and is attributed to the leaching of alkalis from the test specimens. Rogers and Hooton (13) have also found that wicks tend to cause alkalis to be leached from the test specimens, resulting in lower expansions. These results suggest that the use of wicks in the concrete prism test should be discontinued.

4.3.3 Proposed Test Method

The procedure utilized in this study is proposed as a test method to evaluate aggregates for their potential to cause expansion and cracking due to alkali-aggregate reaction.

A summary of the proposed test method is as follows:

1. Fabricate concrete specimens with a water-cement ratio of 0.5.
2. Moist cure the specimens for seven days.
3. Obtain cores with a nominal diameter of 25 mm. Saw cut the cores to obtain test specimens with a length of 50 mm. Use five cores to evaluate each concrete mix.
4. Condition the test specimens in sodium hydroxide solution at 80 C for 24 hours.
5. Measure the length of the test specimens at the end of the conditioning period. Store the specimens in the sodium hydroxide solution at 80 C for two to three weeks and measure their lengths every two days.
6. The critical limit of expansion, based on the limited results of this study, is proposed to be 0.1 percent after two weeks in the sodium hydroxide solution. The expansion

limit may need to be refined after more aggregates have been evaluated.

4.3.4 Summary of Findings

1. A one molar sodium hydroxide solution (1 M NaOH) at 80 C is more effective than a 3 M potassium chloride (KCl) solution at 80 C in accelerating expansion due to alkali-aggregate reaction.
2. Conditioning of test specimens in NaOH solution instead of distilled water prior to storage in the NaOH solution at 80 C expedites the reaction process.
3. Specimens made with reactive aggregates and stored in the NaOH solution at 80 C expand significantly within 30 days. Reaction products are observed on the surface of the specimens within 2-6 days of the start of the test.
4. The test method is sensitive to both the alkali-silica and alkali-carbonate reactions.
5. The test method does not appear to be sensitive to the alkali-silicate reaction.
6. The alkali content of the cement does not seem to affect the magnitude of expansion of the test specimens. The NaOH bath appears to override the cement alkalis.
7. After a period of more than two months, specimens made with an alkali-silica reactive aggregate do not show any decrease in the expansion rate.
8. Pretreating the test specimens using two wet-dry cycles does not seem to enhance the reaction. Expansion levels for pretreated specimens are about the same as those for specimens which are not pretreated.
9. Pretreated test specimens stored in distilled water at 80 C contract. The NaOH bath is therefore necessary to induce alkali-aggregate expansion in the pretreated

specimens.

10. SEM examination and analysis reveal that the alkali-aggregate reaction products have many morphologies. A sponge-like morphology appears to be the most common.

11. A rosette morphology was found in specimens made with an alkali-silica reactive aggregate. The same morphology was observed by Oberholster and Davies (5) in concrete structures undergoing ASR.

12. There is an excellent correlation between the magnitude of expansion and the amount of gel observed in the test specimens.

13. The use of wicks in the storage tank for the concrete prism test affects the magnitude of expansion of the test specimens. Specimens closest to the wicks expand the least, while those furthest from the wicks expand the most.

14. The effect of the wicks on expansion is attributed to leaching of alkalis from the test specimens.

15. The accelerated test utilizing 25 mm diameter concrete cores and a 1 M NaOH solution at 80 C is more effective than the concrete prism test for identifying alkali-silica and alkali-carbonate reactive aggregates.

5. SUMMARY AND CONCLUSIONS

5.1 SUMMARY

Many concrete structures are not surviving through their expected life span due to premature deterioration. Degradation arises through many mechanisms which are either physical or chemical in nature. In this study, two forms of chemical attack, late formation of ettringite and alkali-aggregate reaction (AAR), are evaluated.

The experimental program is designed to develop and evaluate test methods for expansion due to late formation of ettringite and AAR in concrete. Five cements from various regions of Canada are used in the experimental program. Seven aggregates from various Canadian quarries are utilized. The aggregates varied in reactivity, ranging from innocuous to highly reactive. Cement paste and concrete specimens are fabricated. The test specimens consist of cores with nominal diameters of 25 mm and 57 mm and a length-to-diameter of two. Reactivity is gauged by specimen expansion. The effect of various factors on specimen expansion are evaluated. For the experimental program pertaining to late formation of ettringite, those factors include: specimen drying, number of wet-dry cycles, water-cement ratio, curing duration, storage medium, specimen size and the effect of aggregate on expansion. Regarding AAR, the factors evaluated include: storage medium and wet-dry cycles. The CSA standard concrete prism test is also conducted for comparison purposes.

Scanning electron microscopy coupled with energy-dispersive x-ray analysis is utilized in the identification of reaction products.

The results obtained in the experimental program are used to propose test procedures for (i) evaluation of cements that could cause concrete expansion due to the late formation of ettringite, and (ii) evaluation of concrete expansion due to alkali-aggregate reaction.

5.2 CONCLUSIONS

Late Formation of Ettringite: The conclusions drawn from the test results pertaining to the late formation of ettringite are as follows:

1. Cement paste specimens made with cements produced in different regions of Canada exhibit significant differences in the magnitude of expansion when pretreated by subjecting them to wet-dry cycles. Specimens for some cements expand by negligible amounts, whereas those for other cements expand by very large amounts.
2. Cement paste specimens expand more than concrete specimens made with the same cement. The magnitude of expansion in both types of specimen depends upon the cement used.
3. A water-cement ratio of 0.5 appears to be the optimum water-cement ratio for expansion under the test procedure used in this study.
4. Expansion and cracking of test specimens increase with increase in the number of wet-dry cycles. Pretreatment involving two wet-dry cycles is recommended for evaluating cements.
5. The duration of curing affects the magnitude of test specimen expansion. Specimens cured for seven days expand more than those cured for two days, probably due to the higher porosity of the latter specimens.

6. Based on the magnitude of expansion and the coefficient of variation of the expansion data, the small test specimens, 25 mm diameter, used in this study are preferable to the larger 57 mm diameter ones for evaluating cements.

7. Both cement paste and concrete specimens which exhibit large expansions contain massive formations of ettringite, whereas those which exhibit very small expansions contain little or no visible amounts of ettringite. This strongly suggests that late formation of ettringite is the cause of expansion of the test specimens.

8. For concrete specimens, SEM analysis indicates the absence of alkali-aggregate reaction, even in concretes made with known reactive aggregates.

9. The different magnitudes of expansion for concretes made with the same cement but different coarse aggregates appears to be due to differences in the length change of the test specimens at the end of pretreatment.

10. Test specimens stored in sodium chloride solution contract, in contrast to expansion of similar specimens stored in water.

11. The contraction of test specimens in sodium chloride solution and the absence of visible ettringite in these specimens are attributed to the high solubility of ettringite in the presence of chloride ions.

12. The contraction of test specimens in sodium chloride solution further suggests that ettringite is the cause of expansion of the test specimens stored in water.

13. Expansion and cracking of concrete due to late formation of ettringite could be prevented by using cements with low molar ratios of SO_3 to Al_2O_3 and low alkali contents.

14. The procedure utilized in this study could be used as a test method to identify cements that could cause expansion and cracking due to late formation of ettringite when concrete is subjected to alternate wet and dry conditions.

Alkali-Aggregate Reaction:

1. A one molar sodium hydroxide solution (1 M NaOH) at 80 C is more effective than a 3 M potassium chloride (KCl) solution at 80 C in accelerating expansion due to alkali-aggregate reaction.
2. Conditioning of test specimens in NaOH solution instead of distilled water prior to storage in the NaOH solution at 80 C expedites the reaction process.
3. Specimens made with reactive aggregates and stored in the NaOH solution at 80 C expand significantly within 30 days. Reaction products are observed on the surface of the specimens within 2-6 days of the start of the test.
4. The test method is sensitive to both the alkali-silica and alkali-carbonate reactions.
5. The test method does not appear to be sensitive to the alkali-silicate reaction.
6. The alkali content of the cement does not seem to affect the magnitude of expansion of the test specimens. The NaOH bath appears to override the cement alkalis.
7. After a period of more than two months, specimens made with an alkali-silica reactive aggregate do not show any decrease in the expansion rate.
8. Pretreating the test specimens using two wet-dry cycles does not seem to enhance the reaction. Expansion levels for pretreated specimens are about the same as those for specimens which are not pretreated.

9. Pretreated test specimens stored in distilled water at 80 C contract. The NaOH bath is therefore necessary to induce alkali-aggregate expansion in the pretreated specimens.

10. SEM examination and analysis reveal that the alkali-aggregate reaction products have many morphologies. A sponge-like morphology appears to be the most common.

11. A rosette morphology was found in specimens made with an alkali-silica reactive aggregate. The same morphology was observed by Oberholster and Davies (5) in concrete structures undergoing ASR.

12. There is an excellent correlation between the magnitude of expansion and the amount of gel observed in the test specimens.

13. The use of wicks in the storage tank for the concrete prism test affects the magnitude of expansion of the test specimens. Specimens closest to the wicks expand the least, while those furthest from the wicks expand the most.

14. The effect of the wicks on expansion is attributed to leaching of alkalis from the test specimens.

15. The accelerated test utilizing 25 mm diameter concrete cores and a 1 M NaOH solution at 80 C is more effective than the concrete prism test for identifying alkali-silica and alkali-carbonate reactive aggregates.

5.3 RECOMMENDATIONS FOR FUTURE STUDY

Late formation of ettringite:

1. The proposed test procedure should be used to evaluate a wider range of cements.
2. The limit of expansion may need to be refined based on the additional tests.
3. The test results indicate that the role the aggregate plays in the expansion process is physical in nature. Additional tests should be performed to verify this observation.
4. There may be a connection between late formation of ettringite and AAR. This connection needs to be explored.

Alkali-Aggregate Reaction:

1. The accelerated test method may need to be modified for the evaluation of alkali-silicate reactive aggregates.
2. The limit of expansion may need to be refined based on additional tests.
3. The effect of water-cement ratio on expansion should be investigated.
4. The actual role cement alkalis play in the test should be determined.

REFERENCES

1. American Society for Testing Materials, *Annual Book of ASTM Standards, Concrete and Aggregates*, Section 4, Vol. 4.02, 1988, pp. 121-125.

2. Canadian Standards Association, *Concrete Materials and Methods of Concrete Construction*, Supplement No. 2, CAN3-A23.1-M77 and CAN3-A23.2-M77, 1986, pp. 5-37.

3. Chatterji, S., Thaulow, N. and Jensen, A.D., "Studies of Alkali-Silica Reaction. Part 4. Effect of Different Alkali Salt Solutions on Expansion", *Cement and Concrete Research*, Vol. 17, No. 5, 1987, pp. 777-783.

4. Chatterji, S., Thaulow, N., Jensen, A.D., "Studies of Alkali-Silica Reaction, Part 6. Practical Implications of a Proposed Reaction mechanism", *Cement and Concrete Research*, Vol. 18, No. 3, 1988, pp. 363-366.

5. Davies, G. and Oberholster, R.E., "Alkali-Silica Reaction Products and Their Development", *Cement and Concrete Research*, Vol. 18, No. 4, 1988, pp. 621-635.

6. Diamond, S., "Identification of Hydrated Constituents Using a Scanning Electron Microscope - Energy Dispersive X-ray Spectrometer Combination", *Cement and Concrete Research*, Vol. 2, No. 5, 1972, pp. 617-632.

7. Heinz, D. and Ludwig, U., "Mechanism of Secondary Ettringite Formation in Mortars and Concretes Subjected to Heat Treatment", ACI SP100-105, *Concrete Durability*, Katherine and Bryant Mather International Conference, Vol. 2, pp. 2059-2071.

8. Hudec, P.P., Larbi, J.A., "A study of Alkali-Aggregate Reaction in Concrete: Measurements in Prevention", *Cement and Concrete Research*, Vol. 19, No. 6, 1989, pp. 905-912.

9. Mindess, S., Francis Young, R., *Concrete*, Prentice-Hall Publishers, 1981, pp. 102-104.

10. Oberholster, R.E. and Davies, G., "An Accelerated Method for Testing the Potential Alkali Reactivity of Siliceous Aggregates", *Cement and Concrete Research*, Vol. 16, 1986, pp. 181-189.

11. Pettifer, K. and Nixon, P.J., "A Reply to a Discussion by D.A. St. John of 'Alkali Metal Sulphate -- A Factor Common to Both Alkali-Aggregate Reaction and Sulphate Attack on Concrete'", *Cement and Concrete Research*, V. 11, 1981, pp. 801-802.

12. Ramachandran, V., Feldman, R., Beaudoin, J., *Concrete Science: Treatise on Current Research*, Heydon Publishing, 1981, pp. 340-353.

13. Rogers, C.A. and Hooton, R.D., "Leaching of Alkalis in Alkali-Aggregate Reaction Testing", *Proceedings of the 18th International Conference on AAR*, Kyoto, Japan, July 17-20, 1989.

14. Scott, J.F. and Duggan, C.R., "Potential New Test for Alkali-Aggregate Reactivity", *Concrete Alkali-Aggregate Reactions*, Proceedings of the 7th International Conference, Ottawa, Canada, pp. 319-323.

15. Shayan, A., Diggins, R.G., Ivanusec, I. and Westgate, P.L., "Accelerated Testing of Some Australian and Overseas Aggregates for Alkali-Aggregate Reactivity", *Cement and Concrete Research*, Vol. 18, 1988, pp. 843-851.

16. Shayan, A., "Re-examination of AAR in an Old Concrete", *Cement and Concrete Research*, Vol. 19, 1989, pp. 434-442.

17. Soroka, I., *Portland Cement Paste and Concrete*, Chemical Publishing Co., 1979, pp. 268-269.

18. St. John, D.A., "A Discussion on the paper 'Alkali Metal Sulphate -- A Factor Common to Both Alkali-Aggregate Reaction and Sulphate Attack on Concrete' by K. Pettifer and P.J. Nixon", *Cement and Concrete Research*, V. 11, 1981, pp. 799.

19. Swamy, N.R. and Al-Asali, M.M., "Expansion of Concrete Due to Alkali-Silica Reaction", *ACI Materials Journal*, Vol. 85, No. 1, Jan-Feb 1988, pp. 33-40.

20. Swamy, R.N. and Al-Asali, M.M., "Engineering Properties of Concrete Affected by Alkali-Silica Reaction", *ACI Materials Journal*, Vol. 85, No. 5, Sept-Oct 1988, pp. 367-374.

21. Tepponen, P., Eriksson, B., "Damage in Concrete Railway Sleepers in Finland", *Nordic Concrete Research*, Publication No. 6, December, 1987, pp. 199-211.

22. Vivian, H., "The Importance of Portland Cement Quality on the Durability of Concrete", ACI SP 100-86, *Concrete Durability*, V. 2, 1987, pp. 1691-1701.

TABLES

Table 3.1 Oxide composition of cements

Oxide Composition	Cement Designation				
	A	B	C	D	E
SiO_2	20.80	20.01	20.24	20.80	21.41
Al_2O_3	4.65	5.11	4.62	4.33	6.11
Fe_2O_3	3.70	2.34	2.46	3.06	2.44
CaO	62.60	61.47	61.30	61.06	62.00
MgO	3.22	2.28	4.25	4.19	2.72
SO_3	3.04	4.13	4.39	4.01	3.14
Na_2O	0.21	0.34	0.56	-	0.29
K_2O	0.48	0.99	0.93	-	0.90
Alkali Total Na_2O Equiv.	0.52	0.99	1.17	0.57	0.88

Table 3.2 Cement paste and concrete mix designations

Cement		Aggregate	
Name	Designation	Name	Designation
Edmonton	A	Nelson	1
Montreal	B	Spratt	2
St. Marys	C	Pittsburg	3
Winnipeg	D	Jolliet	4
St. Lawrence	E	Sudbury	5
		Manitoba-1	6
		Manitoba-2	7

Cement paste designation: same as cement designation
Concrete mix designation: xy, where x = cement designation
y = aggregate designation

Table 3.3 Typical computer output obtained from data acquisition system

Mix #A2		
Specimen 1		
50.630	50.630	50.632
50.630	50.630	50.631
Avg. Length = 50.630		
Mix #A2		
Specimen 2		
50.736	50.731	50.723
50.736	50.731	50.723
Avg. Length = 50.730		
Mix #A2		
Specimen 3		
50.063	50.060	50.054
50.063	50.060	50.053
Avg. Length = 50.059		
Mix #A2		
Specimen 4		
50.893	50.891	50.886
50.893	50.891	50.886
Avg. Length = 50.890		
Mix #A2		
Specimen 5		
50.571	50.557	50.557
50.571	50.557	50.557
Avg. Length = 50.562		

Table 3.4a Representative data for Cement A specimens

Time (Days)	Specimen No.	Initial Length (mm)	Measured Length (mm)	Expansion (Percent)
	1-A	50.3960	50.4240	0.0556
	2-A	50.6710	50.6970	0.0513
3	3-A	50.0510	50.0760	0.0499
	4-A	50.7480	50.7820	0.0670
	5-A	50.8800	50.9090	0.0570
				$\overline{\text{Avg.} = 0.0562}$
	1-A	50.3960	50.4500	0.1072
	2-A	50.6710	50.7270	0.1105
6	3-A	50.0510	50.1030	0.1039
	4-A	50.7480	50.8020	0.1064
	5-A	50.8800	50.9360	0.1101
				$\overline{\text{Avg.} = 0.1076}$
	1-A	50.3960	50.4700	0.1468
	2-A	50.6710	50.7480	0.1520
9	3-A	50.0510	50.1140	0.1259
	4-A	50.7480	50.8200	0.1419
	5-A	50.8800	50.9550	0.1474
				$\overline{\text{Avg.} = 0.1428}$
	1-A	50.3960	50.4790	0.1647
	2-A	50.6710	50.7590	0.1737
12	3-A	50.0510	50.1300	0.1578
	4-A	50.7480	50.8240	0.1498
	5-A	50.8800	50.9650	0.1671
				$\overline{\text{Avg.} = 0.1626}$
	1-A	50.3960	50.4870	0.1806
	2-A	50.6710	50.7660	0.1875
15	3-A	50.0510	50.1340	0.1658
	4-A	50.7480	50.8380	0.1773
	5-A	50.8800	50.9750	0.1867
				$\overline{\text{Avg.} = 0.1796}$

Table 3.4a (continued)

Time (Days)	Specimen No.	Initial Length (mm)	Measured Length (mm)	Expansion (Percent)
20	1-A	50.3960	50.5050	0.2163
	2-A	50.6710	50.7810	0.2171
	3-A	50.0510	50.1520	0.2018
	4-A	50.7480	50.8510	0.2030
	5-A	50.8800	50.9880	0.2123
			Avg. =	0.2101
25	1-A	50.3960	50.5160	0.2381
	2-A	50.6710	50.7930	0.2406
	3-A	50.0510	50.1650	0.2278
	4-A	50.7480	50.8660	0.2325
	5-A	50.8800	51.0030	0.2417
			Avg. =	0.2362
30	1-A	50.3960	50.5270	0.2599
	2-A	50.6710	50.8010	0.2566
	3-A	50.0510	50.1740	0.2457
	4-A	50.7480	50.8670	0.2345
	5-A	50.8800	50.0080	0.2516
			Avg. =	0.2497

Table 3.4b Representative data for Cement C specimens

Time (Days)	Specimen No.	Initial Length (mm)	Measured Length (mm)	Expansion (Percent)
3	1-C	50.990	51.099	0.214
	2-C	50.835	51.014	0.352
	3-C	50.871	51.017	0.287
	4-C	50.765	50.922	0.309
	5-C	50.755	50.907	0.300
			Avg. =	0.292
6	1-C	50.990	51.222	0.455
	2-C	50.835	51.415	1.141
	3-C	50.871	51.246	0.737
	4-C	50.765	51.224	0.904
	5-C	50.755	51.176	0.829
			Avg. =	0.813
9	1-C	50.990	51.324	0.655
	2-C	50.835	51.535	1.380
	3-C	50.871	51.393	1.026
	4-C	50.765	51.391	1.233
	5-C	50.755	51.346	1.164
			Avg. =	1.091
12	1-C	50.990	51.367	0.739
	2-C	50.835	51.530	1.367
	3-C	50.871	51.434	1.107
	4-C	50.765	51.436	1.322
	5-C	50.755	51.404	1.279
			Avg. =	1.163
15	1-C	50.990	51.399	0.802
	2-C	50.835	-	-
	3-C	50.871	51.469	1.301
	4-C	50.765	-	-
	5-C	50.755	51.448	1.486
			Avg. =	1.114

Table 3.4b (continued)

Time (Days)	Specimen No.	Initial Length (mm)	Measured Length (mm)	Expansion (Percent)
	1-C	50.990	51.451	0.904
	2-C	50.835	-	-
20	3-C	50.871	51.533	1.301
	4-C	50.765	-	-
	5-C	50.755	51.509	1.486
				Avg. = 1.230
	1-C	50.990	51.475	0.951
	2-C	50.835	-	-
25	3-C	50.871	51.564	1.362
	4-C	50.765	-	-
	5-C	50.755	51.541	1.287
				Avg. = 1.287
	1-C	50.990	51.479	0.959
	2-C	50.835	-	-
30	3-C	50.871	51.568	1.370
	4-C	50.765	-	-
	5-C	50.755	51.552	1.570
				Avg. = 1.300

Table 3.5 Oxide compositions obtained from energy-dispersive x-ray analysis (EDAX)

Oxide	Composition (Percent)
CaO	64.3
SO_3	27.1
Al_2O_3	6.6
SiO_2	1.6
Fe_2O_3	0.4

Table 3.6a Representative data for Mix A2 specimens

Time (Days)	Specimen No.	Initial Length (mm)	Measured Length (mm)	Expansion (Percent)
2	1-A2	51.146	51.164	0.0352
	2-A2	50.944	50.950	0.0118
	3-A2	50.730	50.738	0.0158
	4-A2	50.069	51.072	0.00587
	5-A2	50.672	50.683	0.0217
				Avg. $= \overline{0.0181}$
4	1-A2	51.146	51.169	0.0450
	2-A2	50.944	50.964	0.0393
	3-A2	50.730	50.743	0.0256
	4-A2	50.069	51.086	0.0333
	5-A2	50.672	50.688	0.0316
				Avg. $= \overline{0.0349}$
6	1-A2	51.146	51.181	0.0684
	2-A2	50.944	50.981	0.0726
	3-A2	50.730	50.754	0.0473
	4-A2	50.069	51.092	0.0450
	5-A2	50.672	50.703	0.0612
				Avg. $= \overline{0.0589}$
8	1-A2	51.146	51.199	0.104
	2-A2	50.944	50.997	0.104
	3-A2	50.730	50.764	0.0670
	4-A2	50.069	51.095	0.0509
	5-A2	50.672	50.716	0.0825
				Avg. $= \overline{0.0825}$
10	1-A2	51.146	51.207	0.119
	2-A2	50.944	51.012	0.133
	3-A2	50.730	50.777	0.0788
	4-A2	50.069	51.106	0.0725
	5-A2	50.672	50.725	0.105
				Avg. $= \overline{0.102}$

Table 3.6a (continued)

Time (Days)	Specimen No.	Initial Length (mm)	Measured Length (mm)	Expansion (Percent)
	1-A2	51.146	51.218	0.141
	2-A2	50.944	51.012	0.133
12	3-A2	50.730	50.780	0.0986
	4-A2	50.069	51.103	0.0666
	5-A2	50.672	50.725	0.105
			Avg. =	0.109
	1-A2	51.146	51.221	0.1470
	2-A2	50.944	51.035	0.1768
14	3-A2	50.730	50.794	0.1262
	4-A2	50.069	51.109	0.0783
	5-A2	50.672	50.748	0.150
			Avg. =	0.136
	1-A2	51.146	50.223	0.151
	2-A2	50.944	51.038	0.185
17	3-A2	50.730	50.799	0.136
	4-A2	50.069	51.111	0.0822
	5-A2	50.672	50.767	0.187
			Avg. =	0.148
	1-A2	51.146	51.250	0.203
	2-A2	50.944	51.067	0.241
20	3-A2	50.730	50.835	0.207
	4-A2	50.069	51.142	0.143
	5-A2	50.672	50.790	0.233
			Avg. =	0.206
	1-A2	51.146	51.275	0.252
	2-A2	50.944	51.096	0.298
23	3-A2	50.730	50.860	0.256
	4-A2	50.069	51.158	0.174
	5-A2	50.672	50.815	0.282
			Avg. =	0.253

Table 3.6a (continued)

Time (Days)	Specimen No.	Initial Length (mm)	Measured Length (mm)	Expansion (Percent)
26	1-A2	51.146	51.276	0.254
	2-A2	50.944	51.105	0.316
	3-A2	50.730	50.865	0.266
	4-A2	50.069	51.165	0.188
	5-A2	50.672	50.812	0.276
			Avg. =	0.260
29	1-A2	51.146	51.294	0.289
	2-A2	50.944	51.132	0.369
	3-A2	50.730	50.887	0.309
	4-A2	50.069	51.177	0.211
	5-A2	50.672	50.843	0.337
			Avg. =	0.303
32	1-A2	51.146	51.300	0.301
	2-A2	50.944	51.137	0.379
	3-A2	50.730	50.894	0.323
	4-A2	50.069	51.189	0.235
	5-A2	50.672	50.849	0.349
			Avg. =	0.318

Table 3.6b Representative data for Mix B2 specimens

Time (Days)	Specimen No.	Initial Length (mm)	Measured Length (mm)	Expansion (Percent)
2	1-B2	50.779	50.793	0.0276
	2-B2	51.209	51.223	0.0273
	3-B2	50.932	50.938	0.0118
	4-B2	51.128	51.133	0.00978
	5-B2	50.853	50.862	0.0177
			Avg. =	$\overline{0.0188}$
4	1-B2	50.779	50.796	0.0335
	2-B2	51.209	51.230	0.0410
	3-B2	50.932	50.938	0.0118
	4-B2	51.128	51.135	0.0137
	5-B2	50.853	50.872	0.0374
			Avg. =	$\overline{0.0275}$
6	1-B2	50.779	50.816	0.0729
	2-B2	51.209	51.247	0.0742
	3-B2	50.932	50.949	0.0334
	4-B2	51.128	51.142	0.0274
	5-B2	50.853	50.878	0.0492
			Avg. =	$\overline{0.0514}$
8	1-B2	50.779	50.841	0.122
	2-B2	51.209	51.262	0.103
	3-B2	50.932	50.956	0.0471
	4-B2	51.128	51.152	0.0469
	5-B2	50.853	50.890	0.0728
			Avg. =	$\overline{0.0785}$
10	1-B2	50.779	50.838	0.116
	2-B2	51.209	50.270	0.119
	3-B2	50.932	50.961	0.0569
	4-B2	51.128	51.158	0.0587
	5-B2	50.853	50.904	0.100
			Avg. =	$\overline{0.0902}$

Table 3.6b (continued)

Time (Days)	Specimen No.	Initial Length (mm)	Measured Length (mm)	Expansion (Percent)
	1-B2	50.779	50.849	0.138
	2-B2	51.209	51.276	0.131
12	3-B2	50.932	50.963	0.0609
	4-B2	51.128	51.159	0.0606
	5-B2	50.853	50.903	0.0983
				$\overline{\text{Avg. } = 0.0977}$
	1-B2	50.779	50.853	0.146
	2-B2	51.209	51.294	0.166
14	3-B2	50.932	50.972	0.0785
	4-B2	51.128	51.184	0.110
	5-B2	50.853	50.914	0.120
				$\overline{\text{Avg. } = 0.124}$
	1-B2	50.779	50.859	0.158
	2-B2	51.209	51.300	0.178
17	3-B2	50.932	50.970	0.0746
	4-B2	51.128	51.169	0.0802
	5-B2	50.853	50.912	0.116
				$\overline{\text{Avg. } = 0.121}$
	1-B2	50.779	50.884	0.207
	2-B2	51.209	51.341	0.258
20	3-B2	50.932	50.991	0.116
	4-B2	51.128	51.199	0.139
	5-B2	50.853	50.948	0.187
				$\overline{\text{Avg. } = 0.181}$
	1-B2	50.779	50.901	0.240
	2-B2	51.209	50.368	0.310
23	3-B2	50.932	50.008	0.149
	4-B2	51.128	51.223	0.186
	5-B2	50.853	50.955	0.201
				$\overline{\text{Avg. } = 0.217}$

Table 3.6b (continued)

Time (Days)	Specimen No.	Initial Length (mm)	Measured Length (mm)	Expansion (Percent)
	1-B2	50.779	50.905	0.248
	2-B2	51.209	51.385	0.344
26	3-B2	50.932	51.013	0.159
	4-B2	51.128	51.218	0.176
	5-B2	50.853	50.965	0.220
			Avg. =	0.229
	1-B2	50.779	50.921	0.280
	2-B2	51.209	51.411	0.394
29	3-B2	50.932	51.024	0.181
	4-B2	51.128	51.230	0.199
	5-B2	50.853	50.988	0.265
			Avg. =	0.264
	1-B2	50.779	50.937	0.311
	2-B2	51.209	51.434	0.439
32	3-B2	50.932	51.030	0.192
	4-B2	51.128	51.228	0.196
	5-B2	50.853	50.982	0.254
			Avg. =	0.278

Table 3.6c Representative data for Mix B3 specimens

Time (Days)	Specimen No.	Initial Length (mm)	Measured Length (mm)	Expansion (Percent)
2	1-B3	50.637	50.646	0.0178
	2-B3	50.712	50.721	0.0177
	3-B3	50.952	50.947	-0.0098
	4-B3	50.631	50.629	-0.0040
	5-B3	50.788	50.799	0.0217
			Avg. =	0.008683
4	1-B3	50.637	50.667	0.0592
	2-B3	50.712	50.743	0.0611
	3-B3	50.952	50.968	0.0314
	4-B3	50.631	50.656	0.0494
	5-B3	50.788	50.822	0.0669
			Avg. =	0.053619
6	1-B3	50.637	50.677	0.0790
	2-B3	50.712	50.744	0.0631
	3-B3	50.952	50.959	0.0137
	4-B3	50.631	50.657	0.0514
	5-B3	50.788	50.828	0.0788
			Avg. =	0.057188
8	1-B3	50.637	50.69	0.1047
	2-B3	50.712	50.759	0.0927
	3-B3	50.952	50.975	0.0451
	4-B3	50.631	50.667	0.0711
	5-B3	50.788	50.844	0.1103
			Avg. =	0.084770
12	1-B3	50.637	50.716	0.1560
	2-B3	50.712	50.794	0.1617
	3-B3	50.952	50.992	0.0785
	4-B3	50.631	50.682	0.1007
	5-B3	50.788	50.881	0.1831
			Avg. =	0.136011

Table 3.6c (continued)

Time (Days)	Specimen No.	Initial Length (mm)	Measured Length (mm)	Expansion (Percent)
	1-B3	50.637	50.713	0.1501
	2-B3	50.712	50.792	0.1578
14	3-B3	50.952	50.986	0.0667
	4-B3	50.631	50.679	0.0948
	5-B3	50.788	50.877	0.1752
				Avg. = 0.128922
	1-B3	50.637	50.741	0.2054
	2-B3	50.712	50.81	0.1932
20	3-B3	50.952	51.013	0.1197
	4-B3	50.631	50.702	0.1402
	5-B3	50.788	50.925	0.2697
				Avg. = 0.185666
	1-B3	50.637	50.764	0.2508
	2-B3	50.712	50.798	0.1696
23	3-B3	50.952	51.002	0.0981
	4-B3	50.631	50.705	0.1462
	5-B3	50.788	50.939	0.2973
				Avg. = 0.192398
	1-B3	50.637	50.776	0.2745
	2-B3	50.712	50.815	0.2031
26	3-B3	50.952	51.01	0.1138
	4-B3	50.631	50.721	0.1778
	5-B3	50.788	50.963	0.3446
				Avg. = 0.222753
	1-B3	50.637	50.813	0.3476
	2-B3	50.712	50.819	0.2110
29	3-B3	50.952	51.018	0.1295
	4-B3	50.631	50.721	0.1778
	5-B3	50.788	50.979	0.3761
				Avg. = 0.248386

Table 3.6c (continued)

Time (Days)	Specimen No.	Initial Length (mm)	Measured Length (mm)	Expansion (Percent)
	1-B3	50.637	50.837	0.3950
	2-B3	50.712	50.842	0.2563
32	3-B3	50.952	51.03	0.1531
	4-B3	50.631	50.732	0.1995
	5-B3	50.788	51.006	0.4292
			Avg. =	0.286624

Table 3.7 Oxide compositions obtained from energy-dispersive x-ray analysis (EDAX)

Oxide	Composition (Percent)
CaO	14.72
SiO_2	71.85
Na_2O	13.04
Fe_2O_3	0.28
MgO	0.11

Table 4.1 Oxide compositions obtained from energy-dispersive x-ray analysis (EDAX)

Material	Location of Spot Analysis (EDAX)	Oxide Composition				
		CaO Weight %	SO_3 Weight %	Al_2O_3 Weight %	CaO/SO_3	CaO/Al_2O_3
Cement Paste	Paste matrix	64.3	27.1	6.6	2.4	9.7
	Void	62.1	22.6	9.5	2.7	6.5
	Crack surface	76.2	18.6	2.3	4.1	32.9
Concrete	Paste matrix	59.1	26.9	6.4	2.2	9.1
	Void	53.5	33.9	11.8	1.6	4.5
	Paste-Aggregate interface	54.2	30.4	10.9	1.8	4.9

Table 4.2 Oxide composition of reaction products obtained from energy-dispersive x-ray analysis (EDAX)

Type of Reaction	Figure Showing Reaction Product	Oxide Composition		
		CaO Weight %	SiO_2 Weight %	Molar Ratio of CaO/SiO_2
Alkali-Silica (Aggregate 2)	Fig. 4.51 - 4.52	14.7	17.9	0.22
	Fig. 4.54 - 4.55	15.8	67.0	0.25
	Fig. 4.57	30.8	59.7	0.55
	Fig. 4.59 - 4.60	34.4	50.1	0.74
Alkali-Carbonate (Aggregate 3)	Fig. 4.62 - 4.63	38.6	50.5	0.82
	Fig. 4.65	41.5	47.7	0.93
	Fig. 4.67	35.1	45.2	0.83
Alkali-Silica (Aggregate 4)	Fig. 4.69 - 4.70	42.9	42.4	1.08
	Fig. 4.72	32.0	43.1	0.80
Alkali-Silicate (Aggregate 5)	Fig. 4.74 - 4.75	37.2	50.1	0.80
Aggregate 6	Fig. 4.77 - 4.78	18.2	48.8	0.40

FIGURES

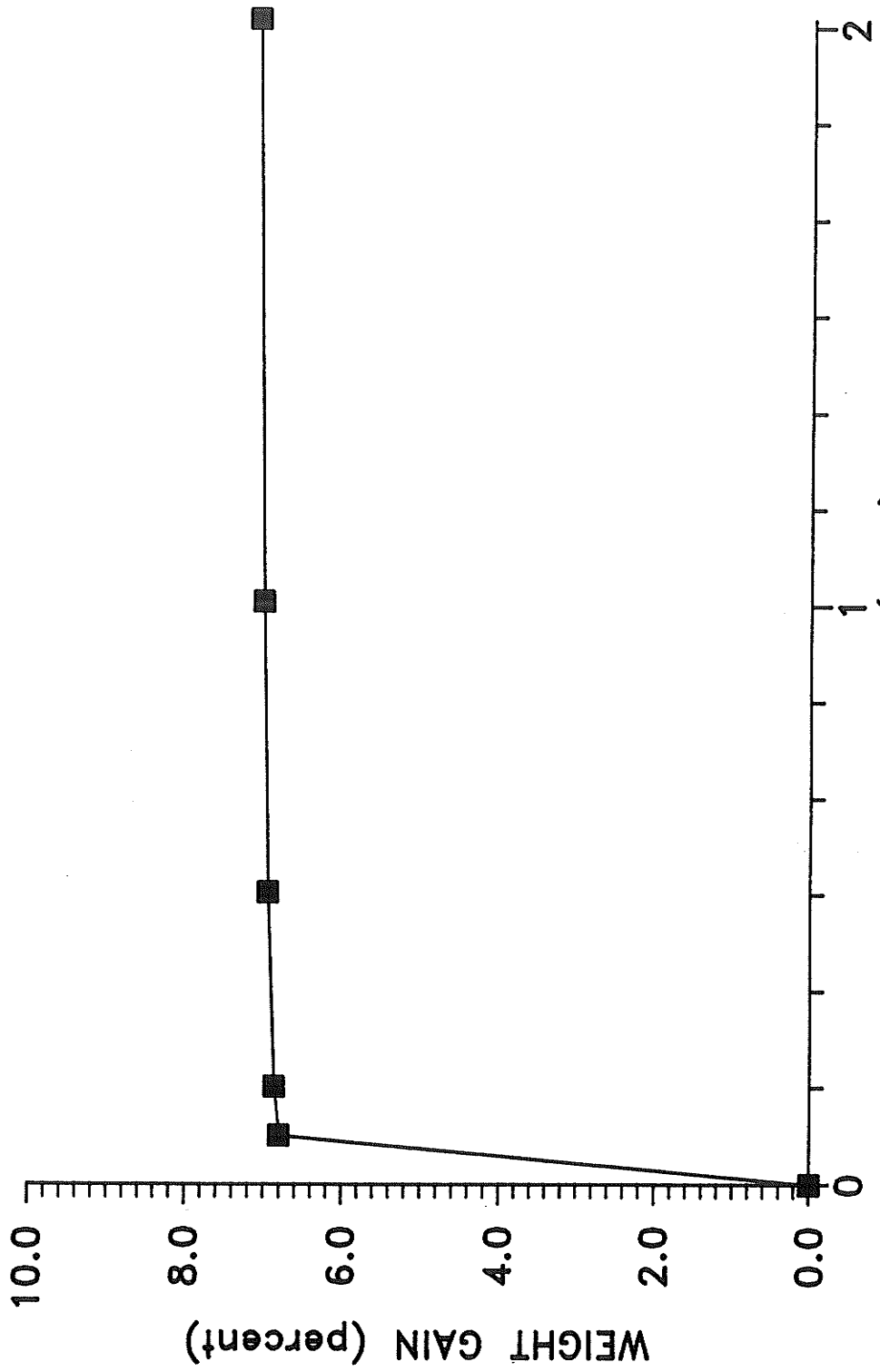

Figure 3.1 Weight gain versus time for oven-dried specimens

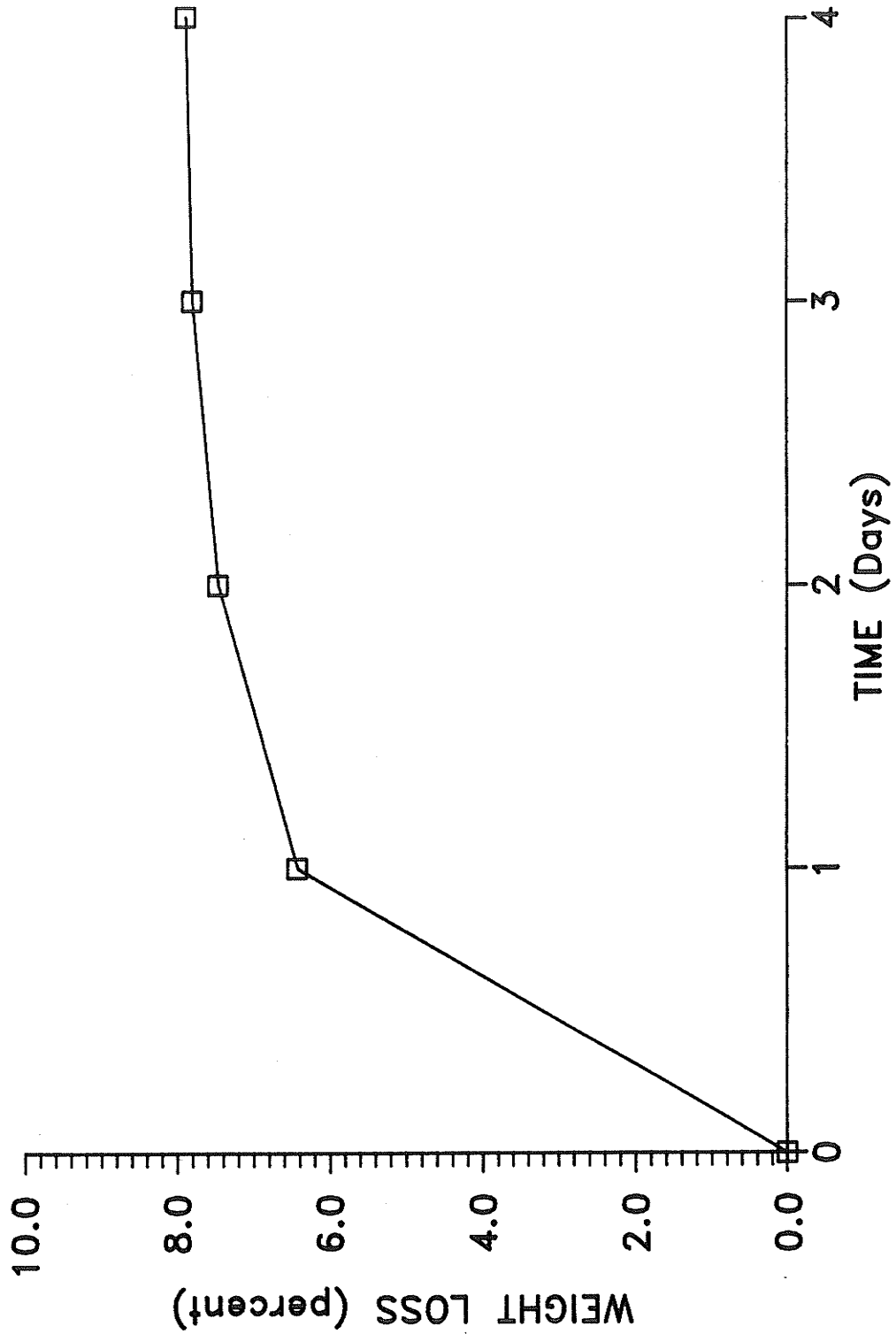

Figure 3.2 Weight loss versus time for saturated specimens

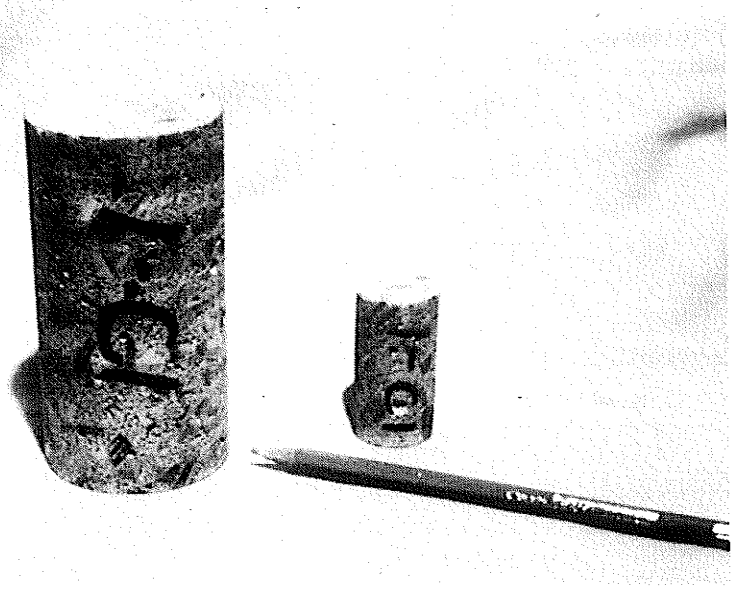

Figure 3.3 25 mm and 57 mm diameter test specimens

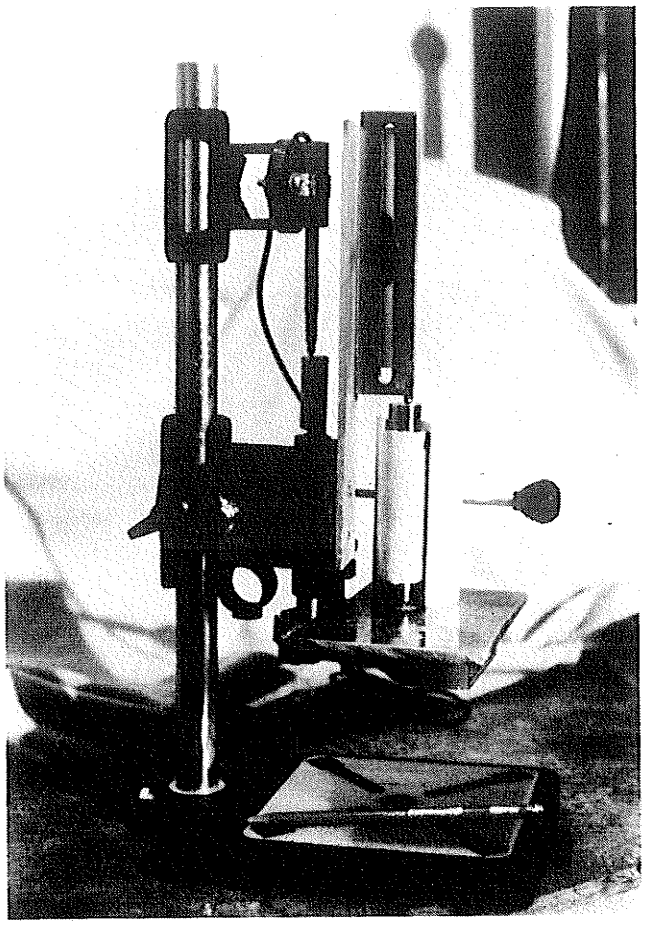

Figure 3.4 Length measurement apparatus

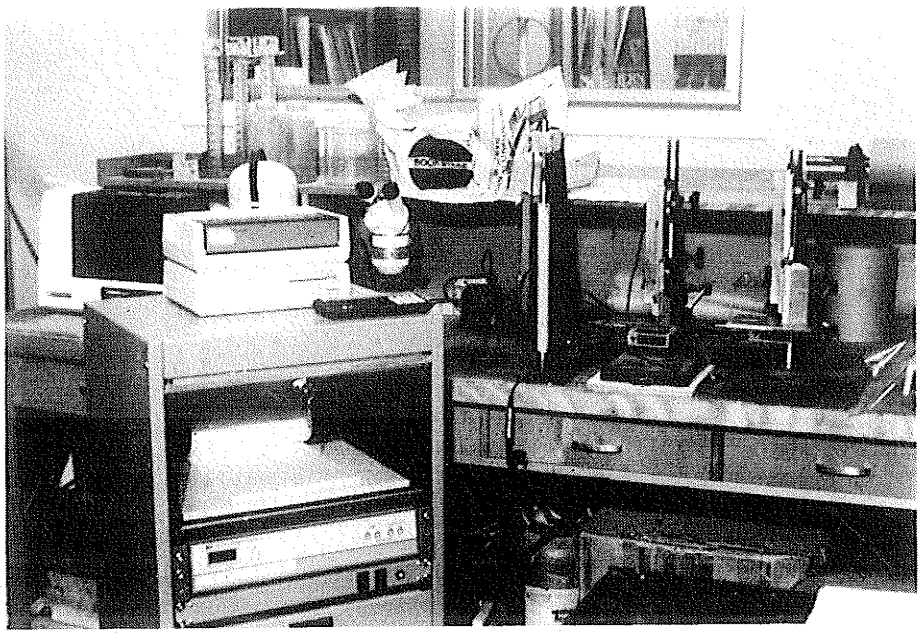

Figure 3.5 Data acquisition unit

Figure 3.6 Scanning electron microscope (SEM) and energy-dispersive x-ray analysis (EDAX) system

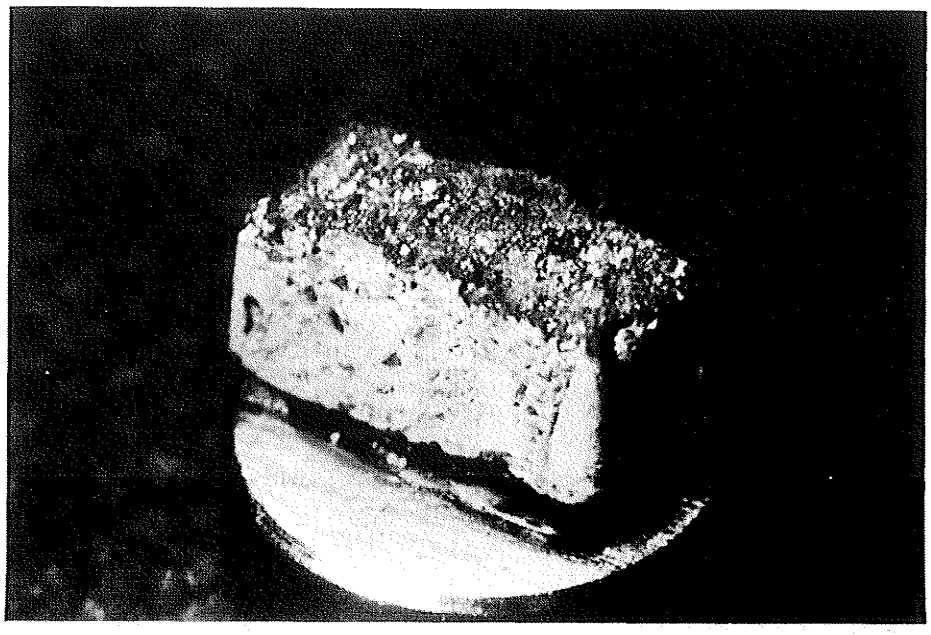

Figure 3.7 SEM specimen as mounted on stud

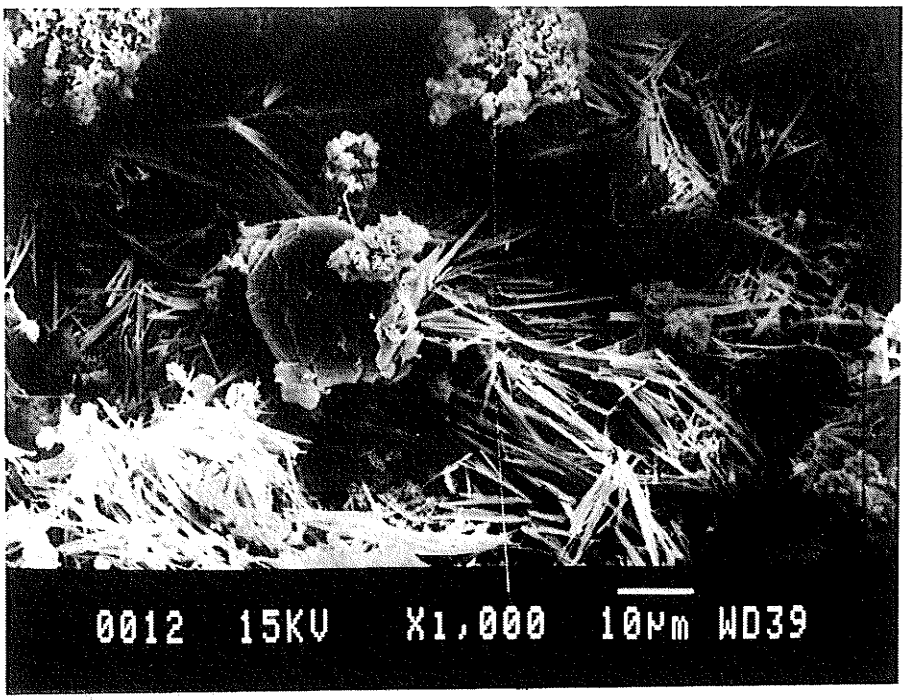

Figure 3.8 Microstructural feature within cement paste matrix

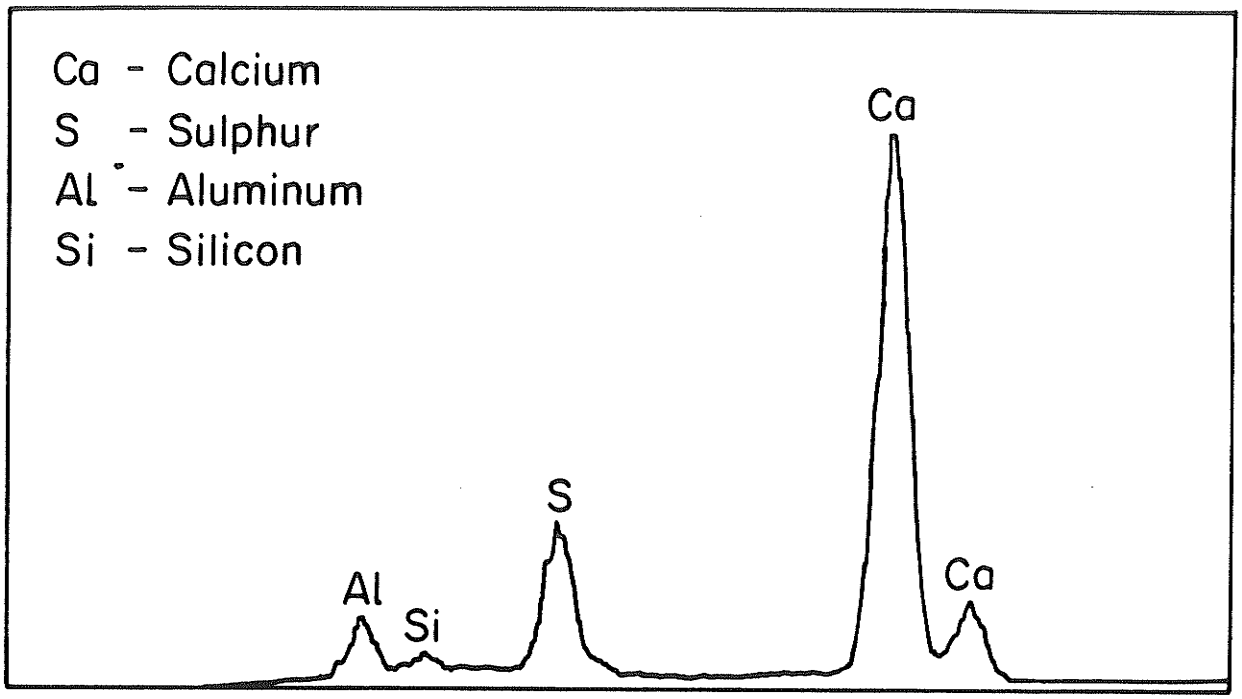

Figure 3.9 Elemental energy-dispersive spectrum for feature in Figure 3.8

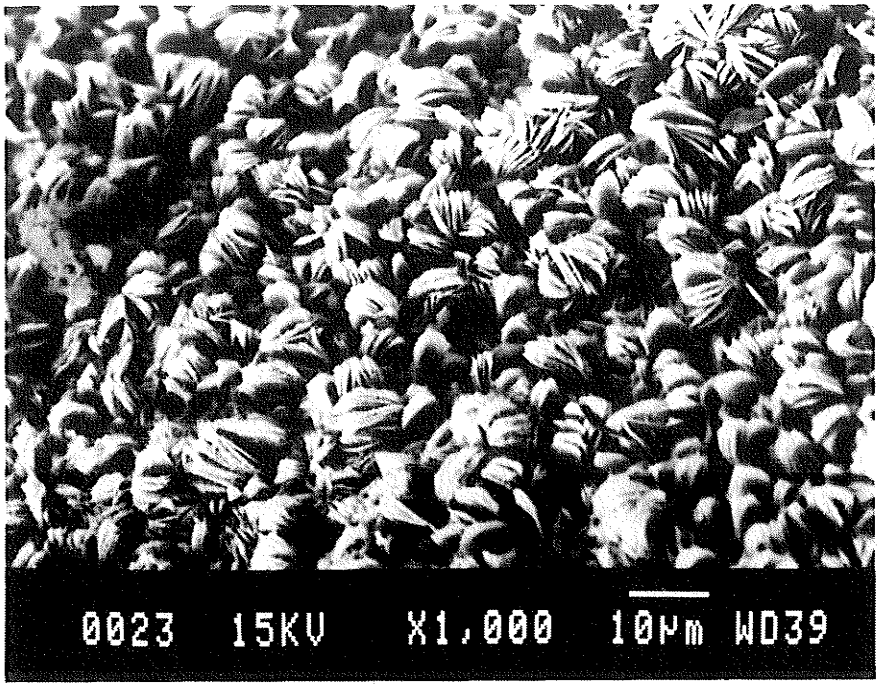

Figure 3.10 Rosette morphology of alkali-silica gel in specimen made with Aggregate 2

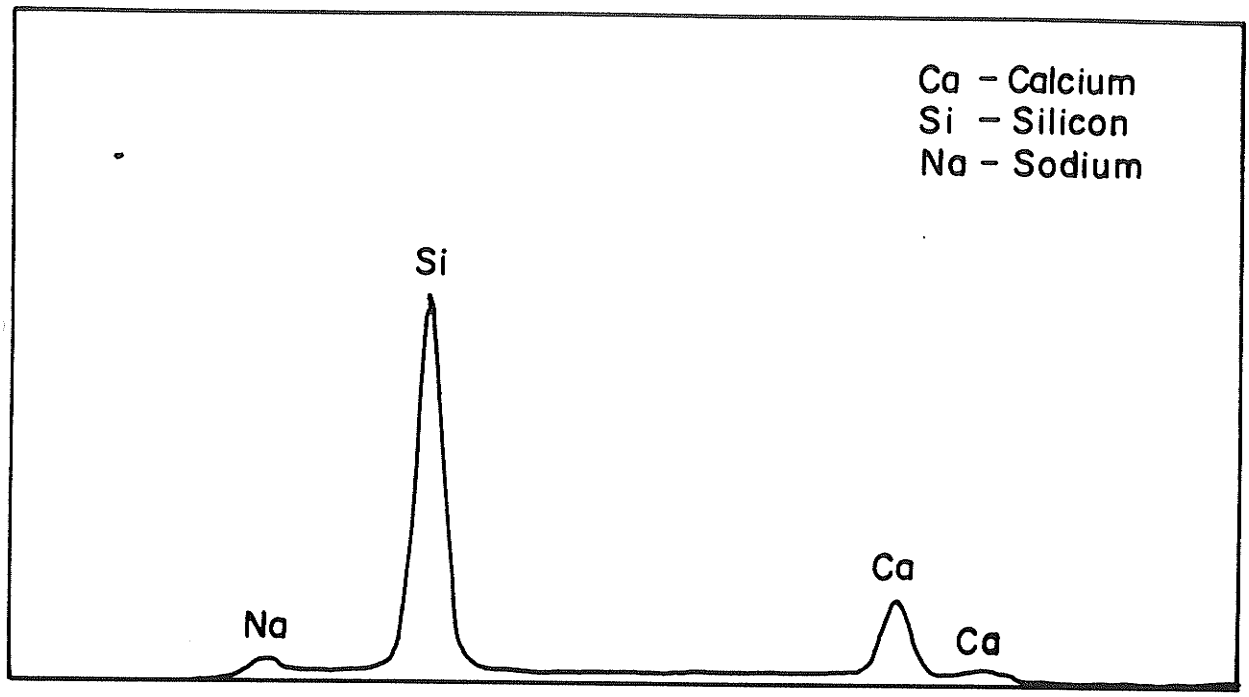

Figure 3.11 Elemental energy-dispersive spectrum for feature in Figure 3.10

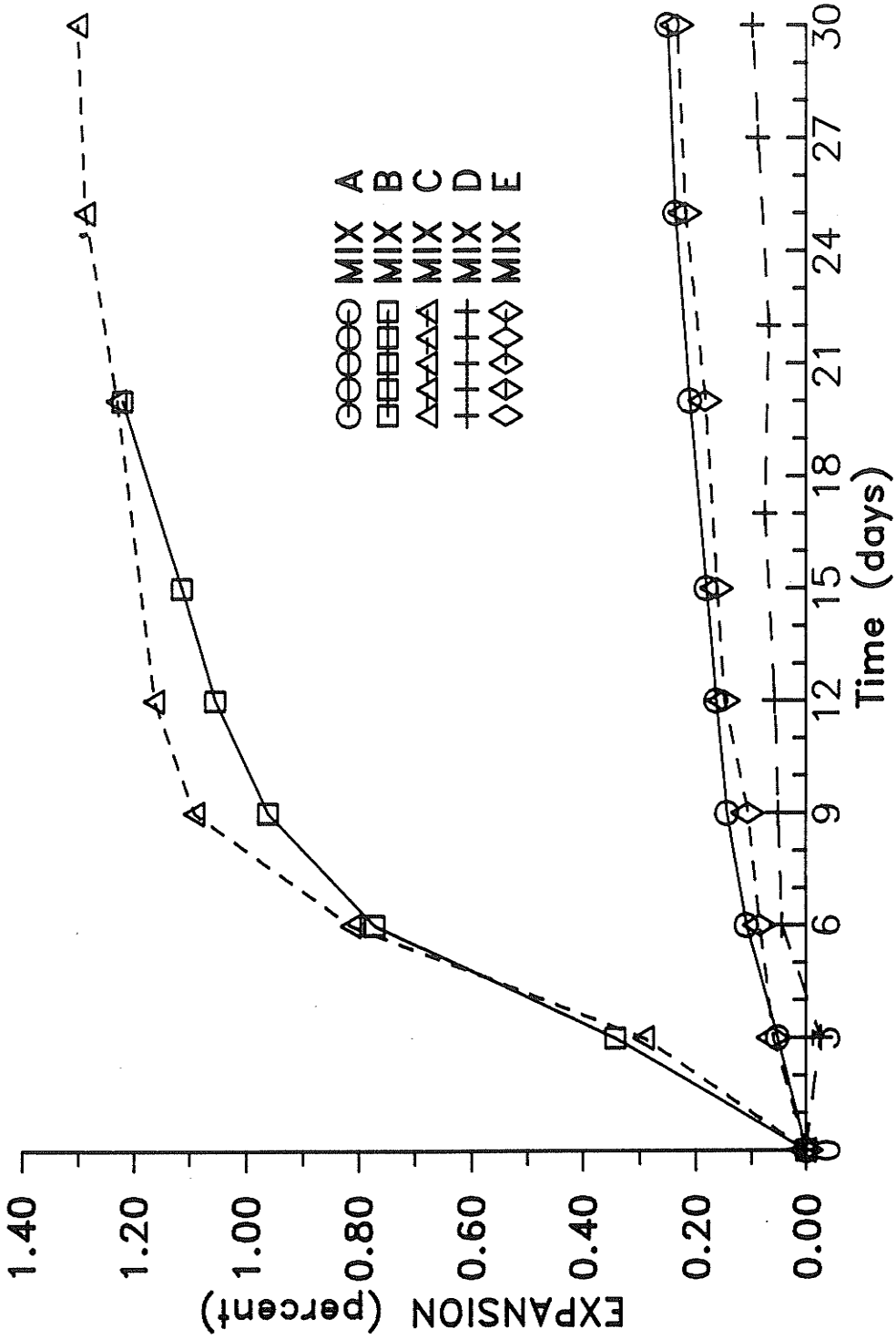

Figure 4.1 Expansion versus time for cement paste specimens

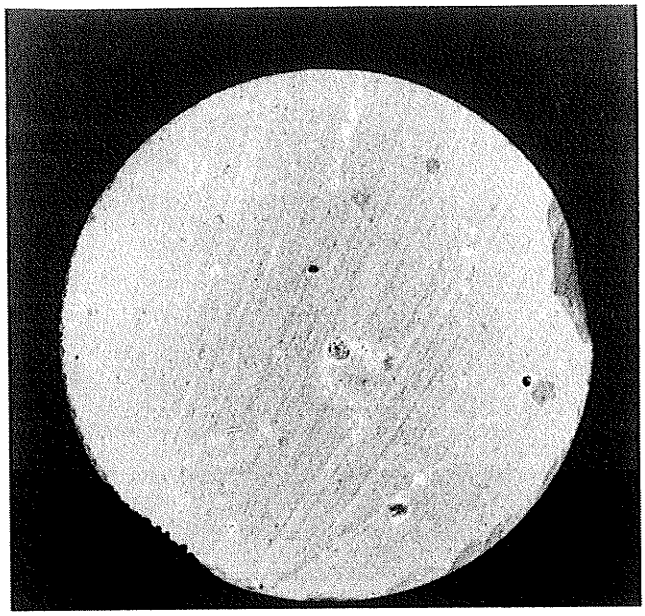

Figure 4.2 Cross-section of uncracked specimen at end of test (Mix A specimens)

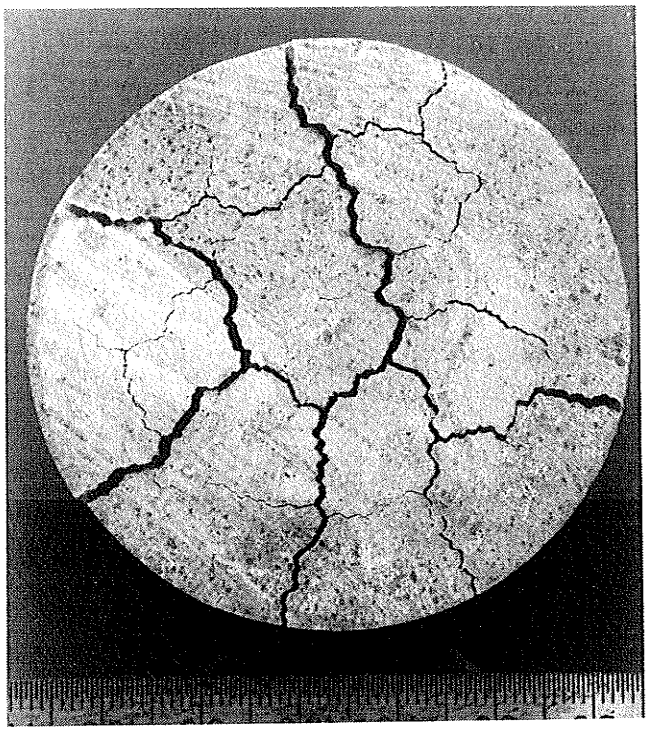

Figure 4.3 Cross-section of cracked specimen at end of test (Mix B specimen)

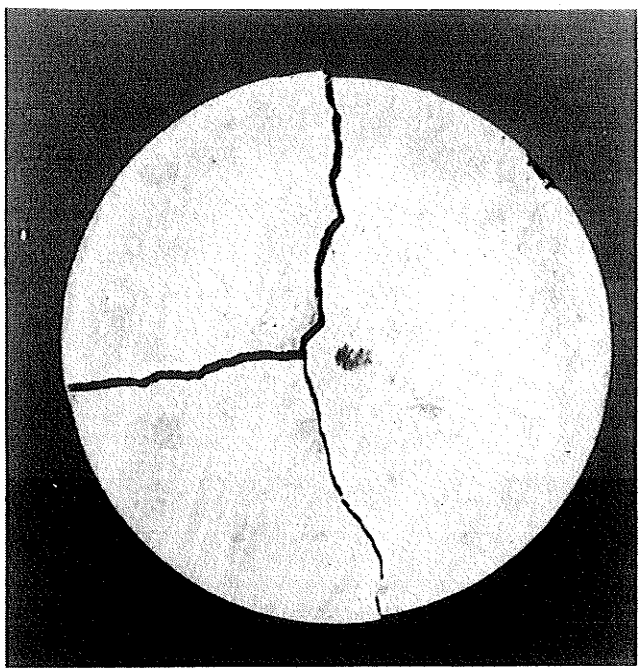

Figure 4.4 Cross-section of cracked specimen at end of test (Mix C specimen)

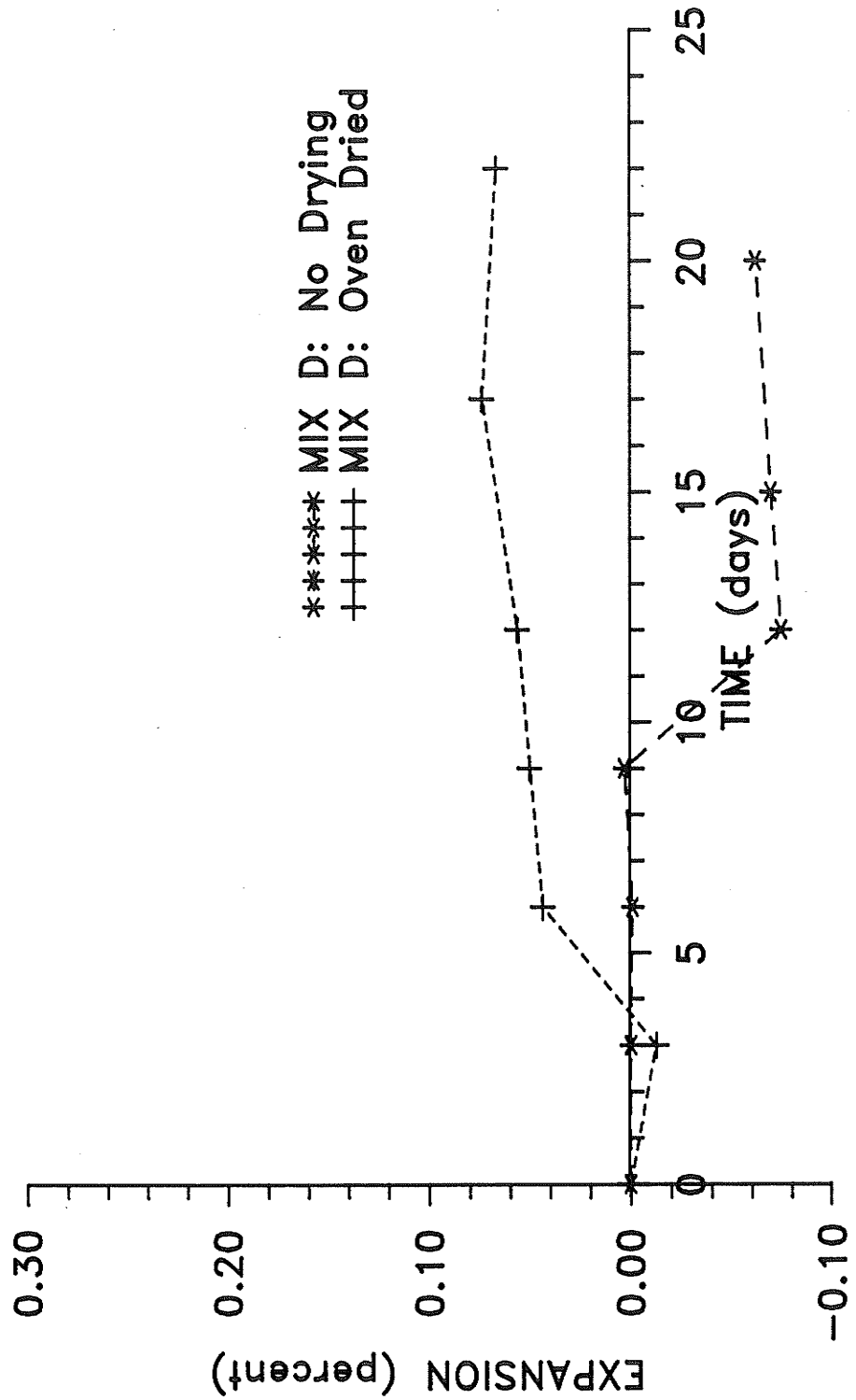

Figure 4.5 Effect of drying on expansion of cement paste specimens

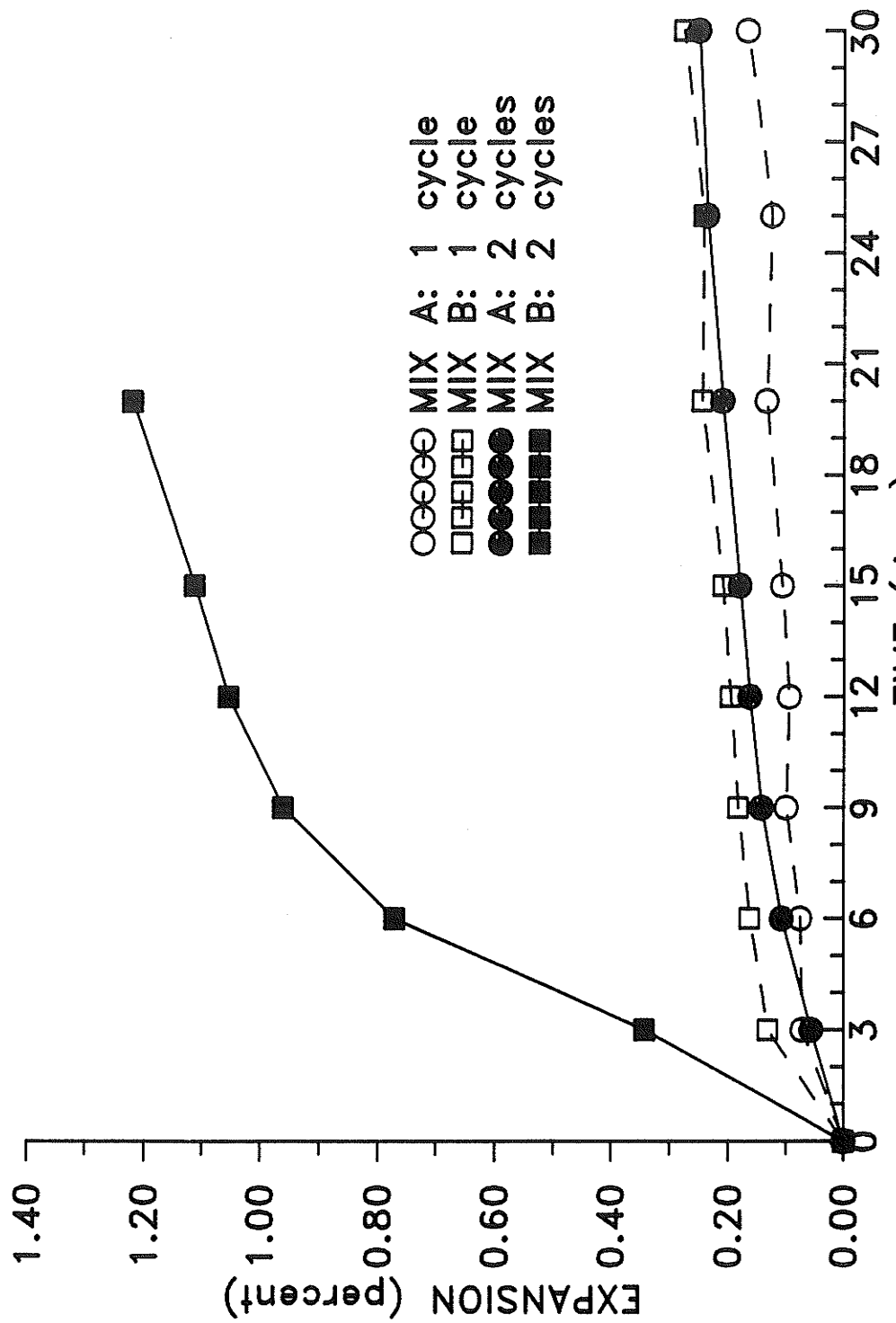

Figure 4.6 Effect of number of wet-dry cycles on expansion of cement paste specimens

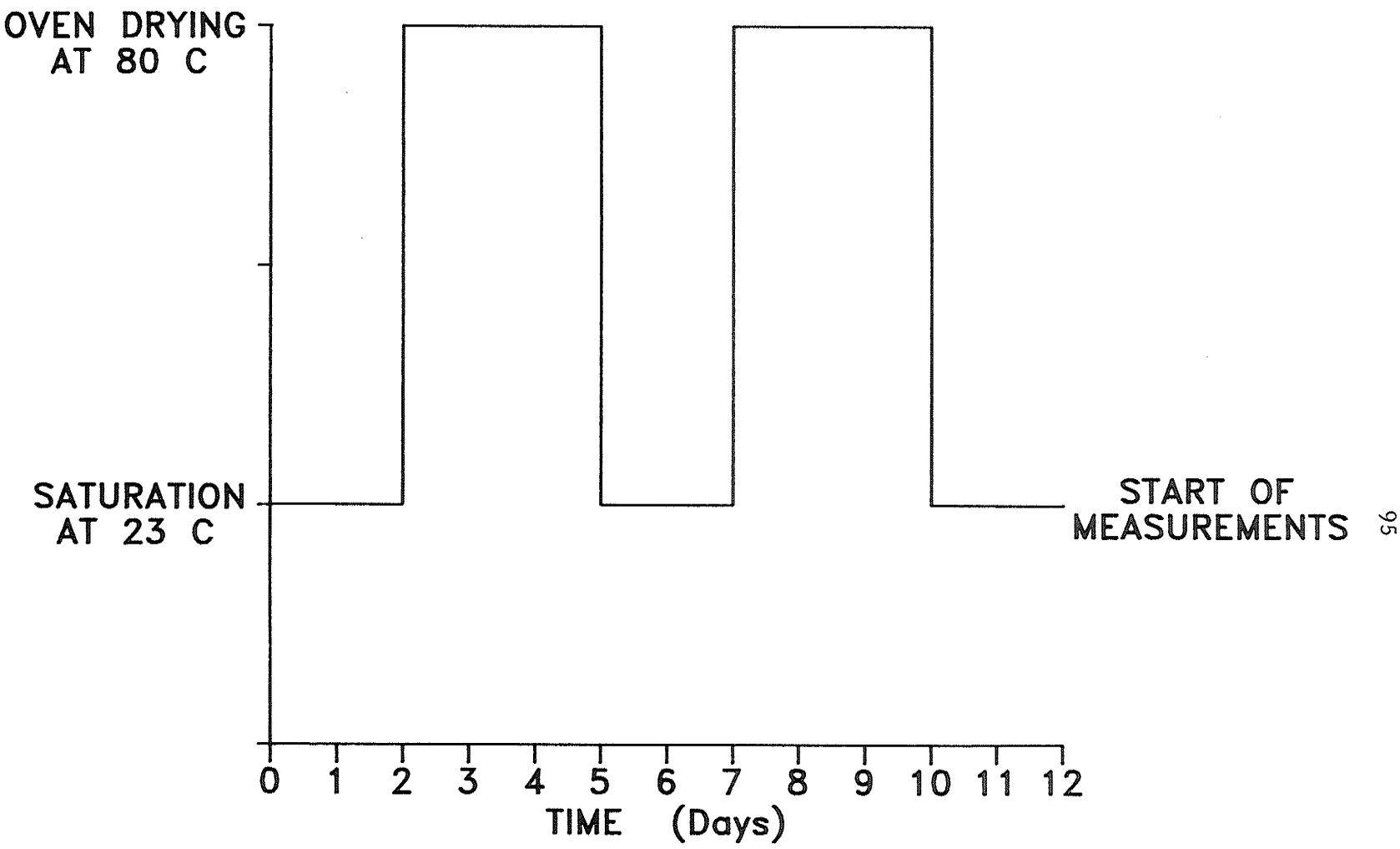

Figure 4.7 Pretreatment of test specimens: Two wet-dry cycles

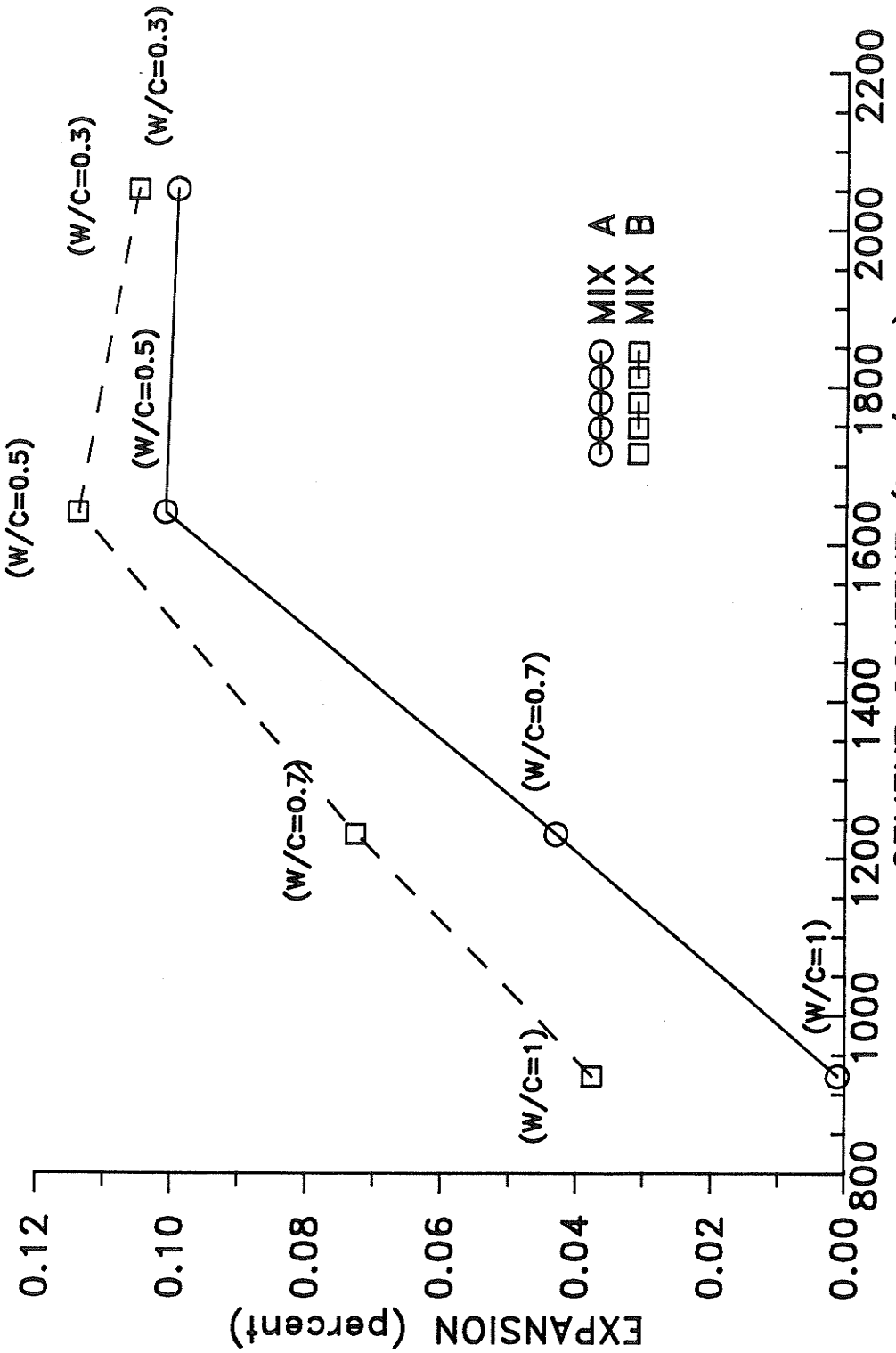

Figure 4.8 Effect of water-cement ratio on expansion of cement paste specimens

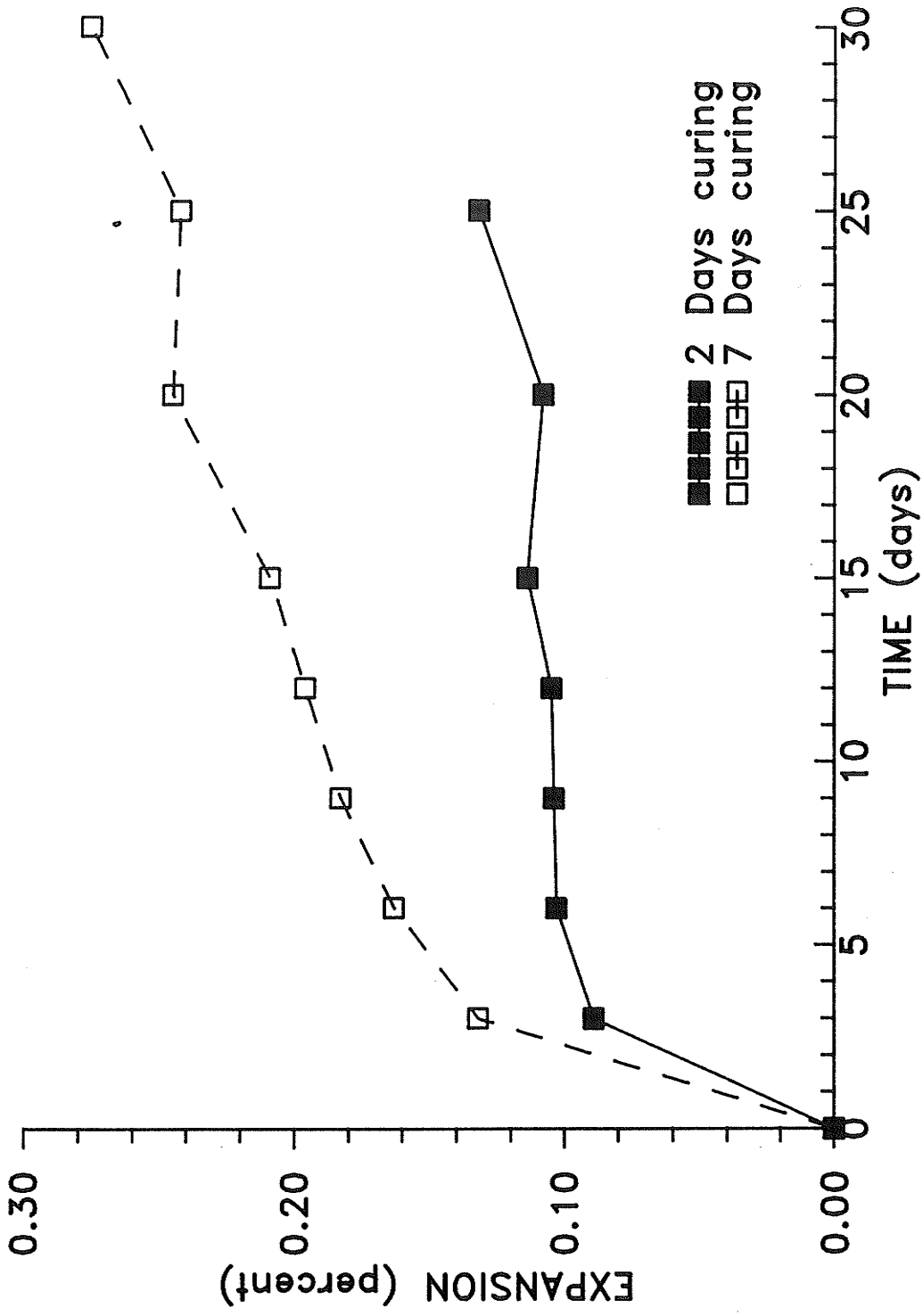

Figure 4.9 Effect of curing duration on expansion of cement paste specimens (Mix B)

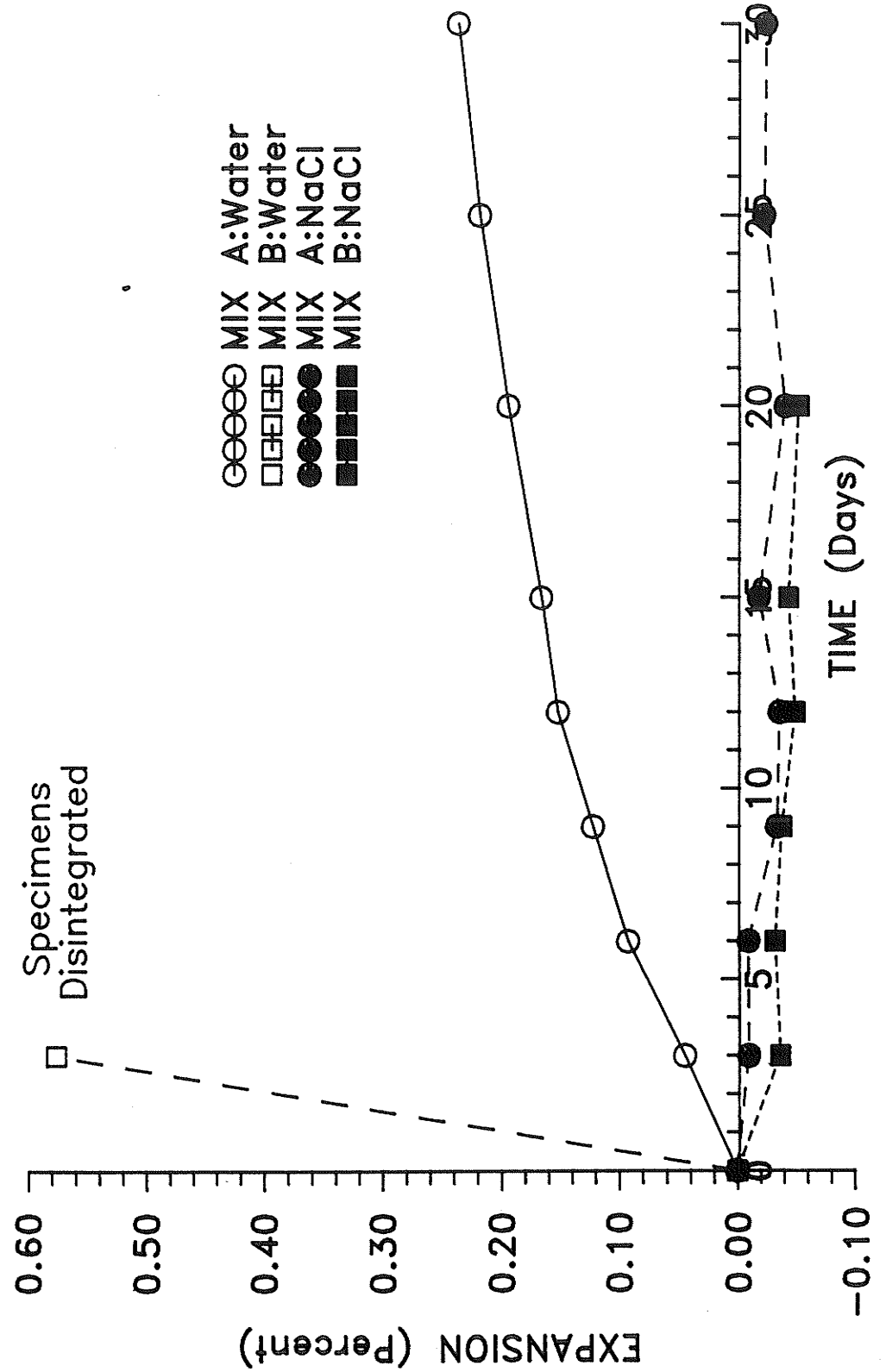

Figure 4.10 Effect of storage medium on expansion of cement paste specimens

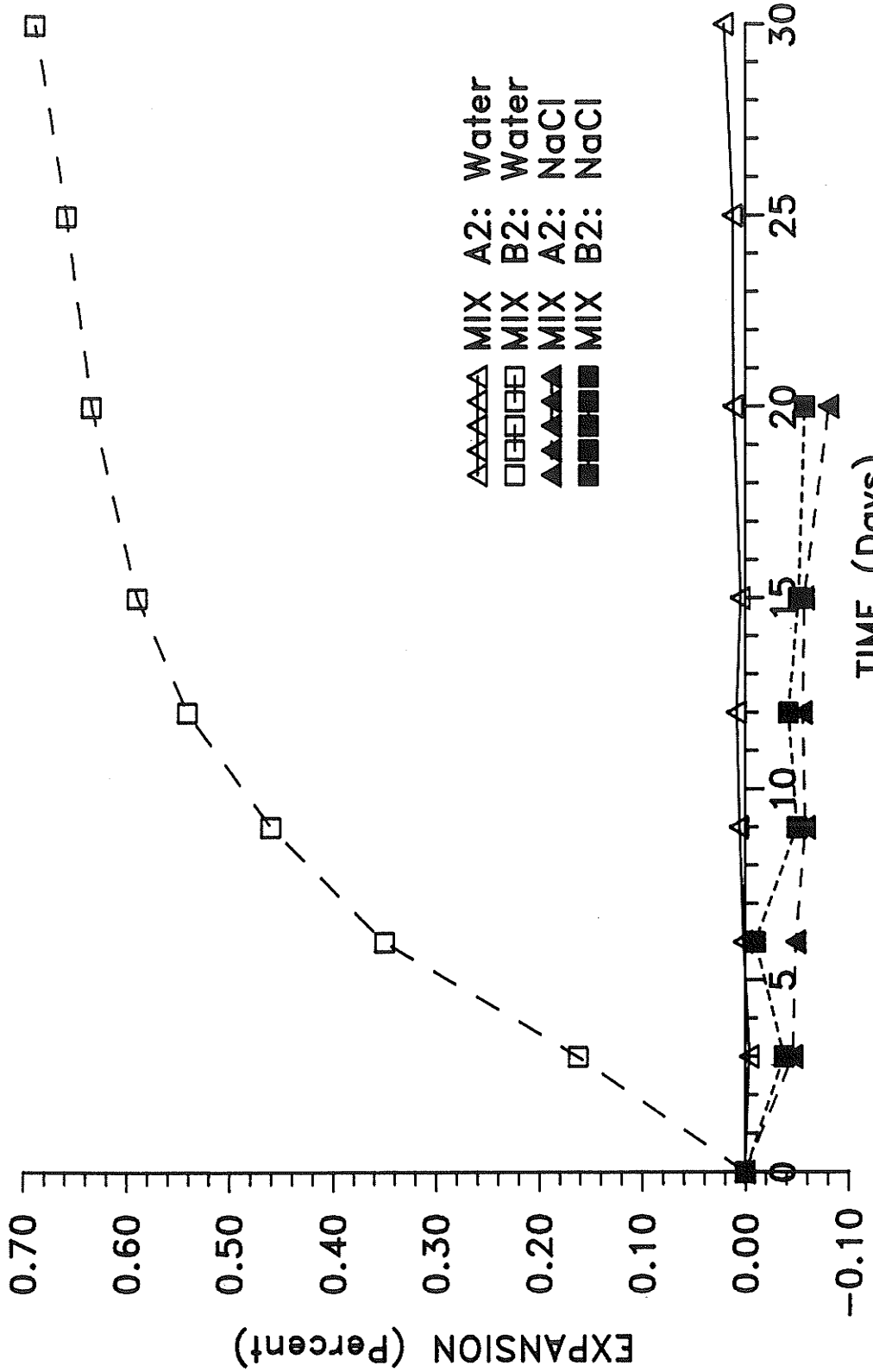

Figure 4.11 Effect of storage medium on expansion of concrete specimens

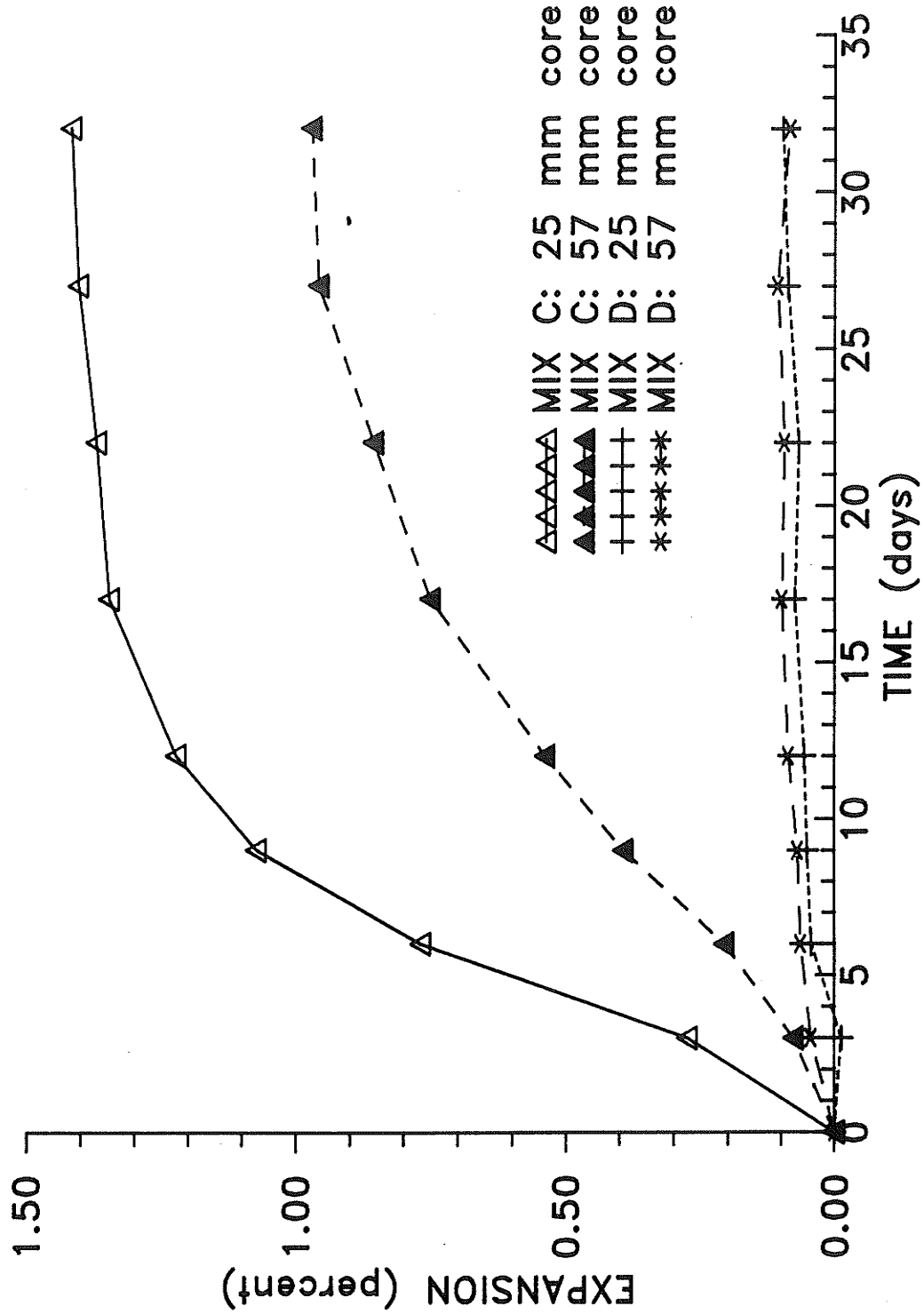

Figure 4.12 Effect of specimen size on expansion

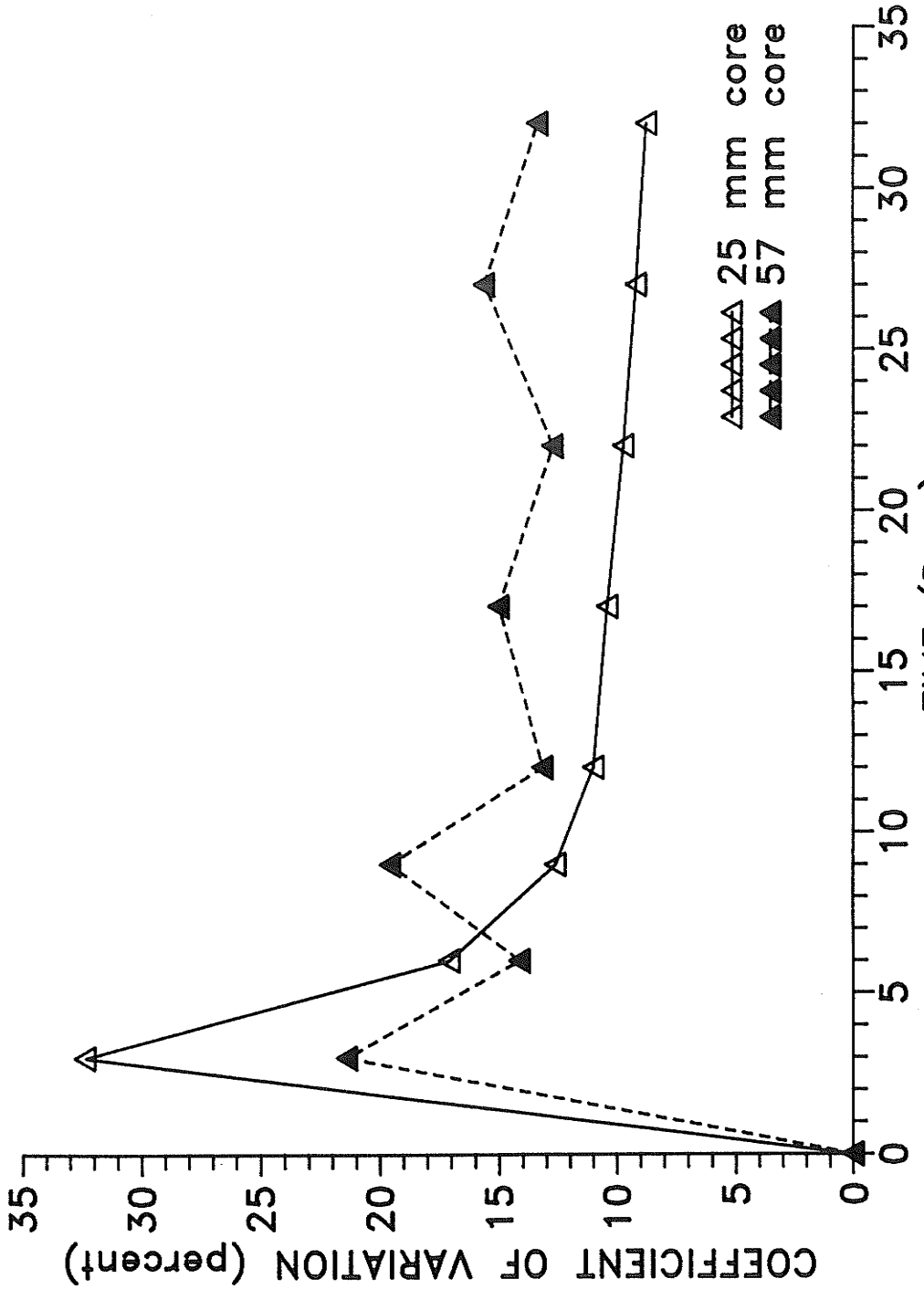

Figure 4.13 Coefficient of variation versus time (Mix C)

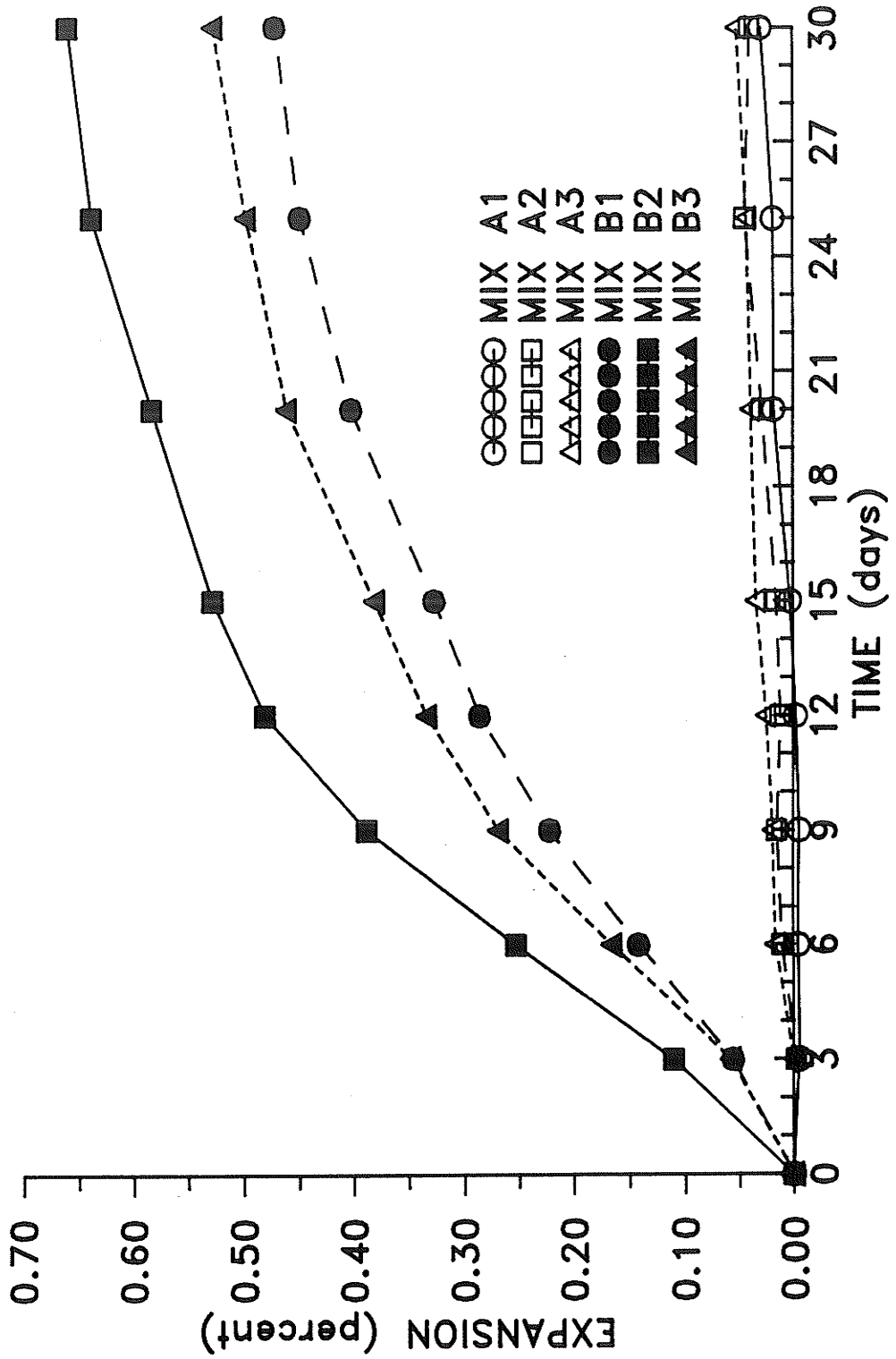

Figure 4.14 Expansion versus time for concrete specimens

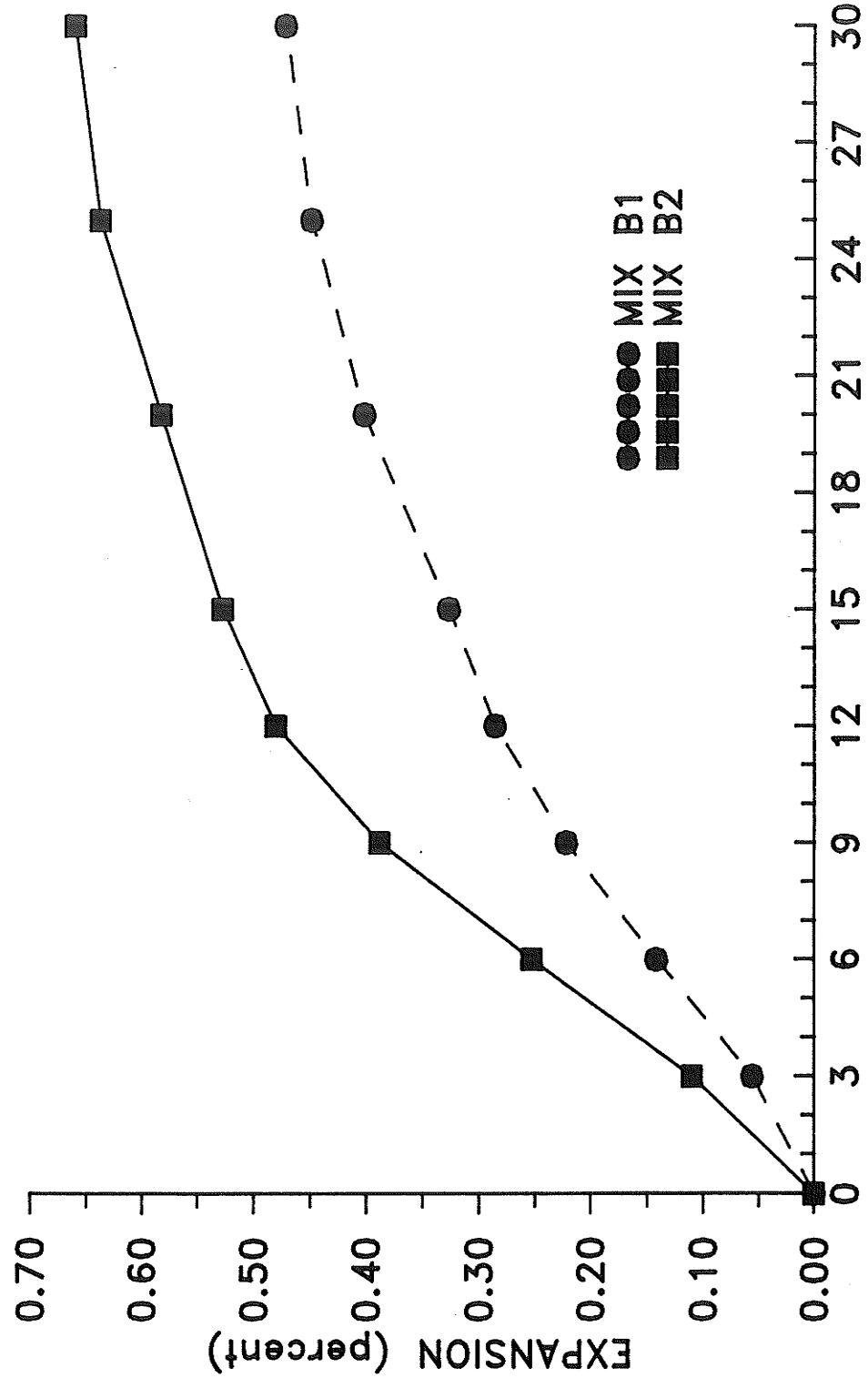

Figure 4.15 Expansion versus time for concrete specimens

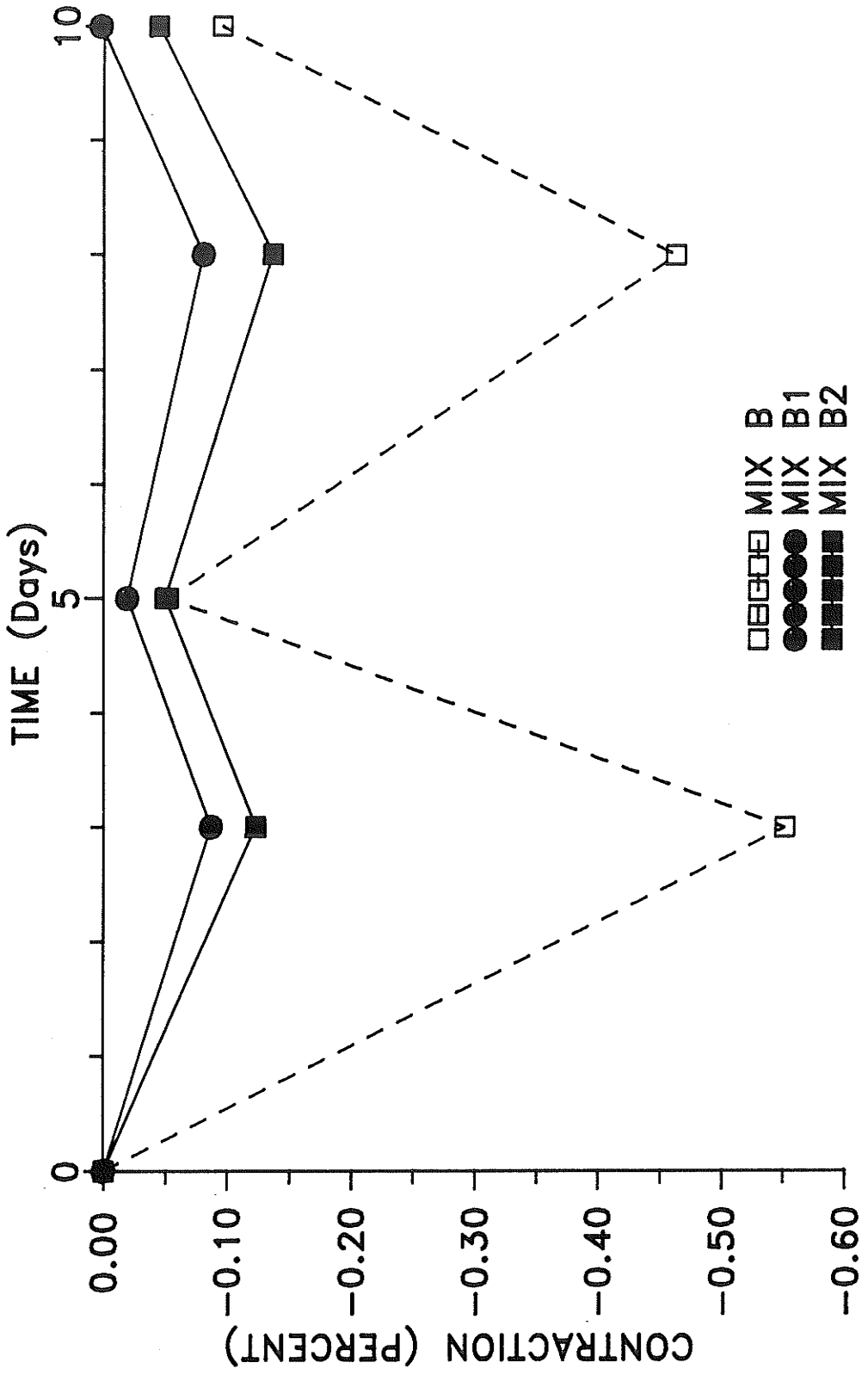

Figure 4.16 Contraction of test specimens during pretreatment

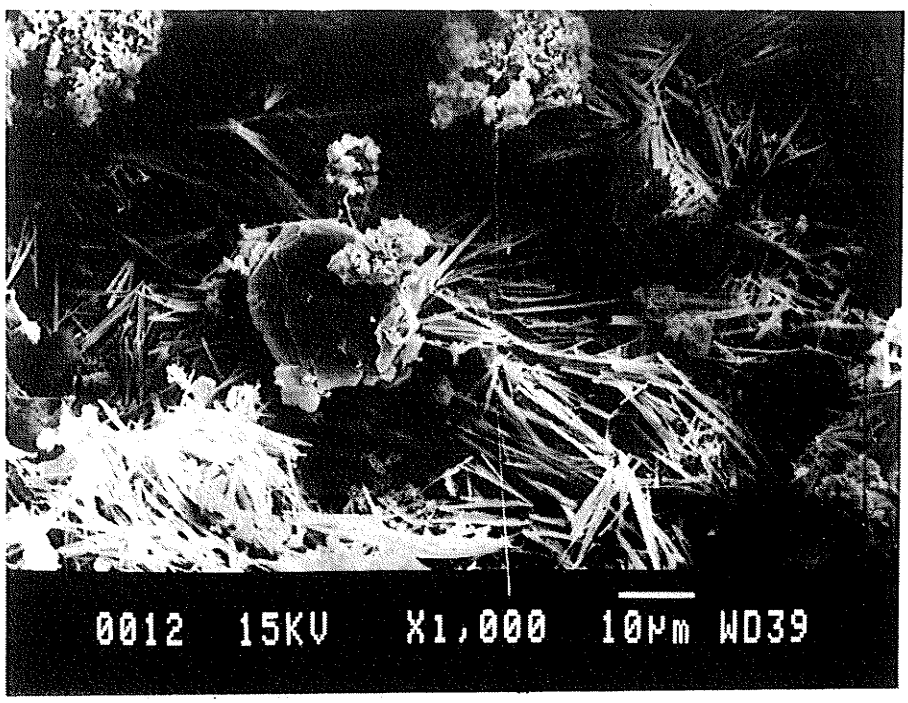

Figure 4.17 Microstructural feature within cement paste matrix

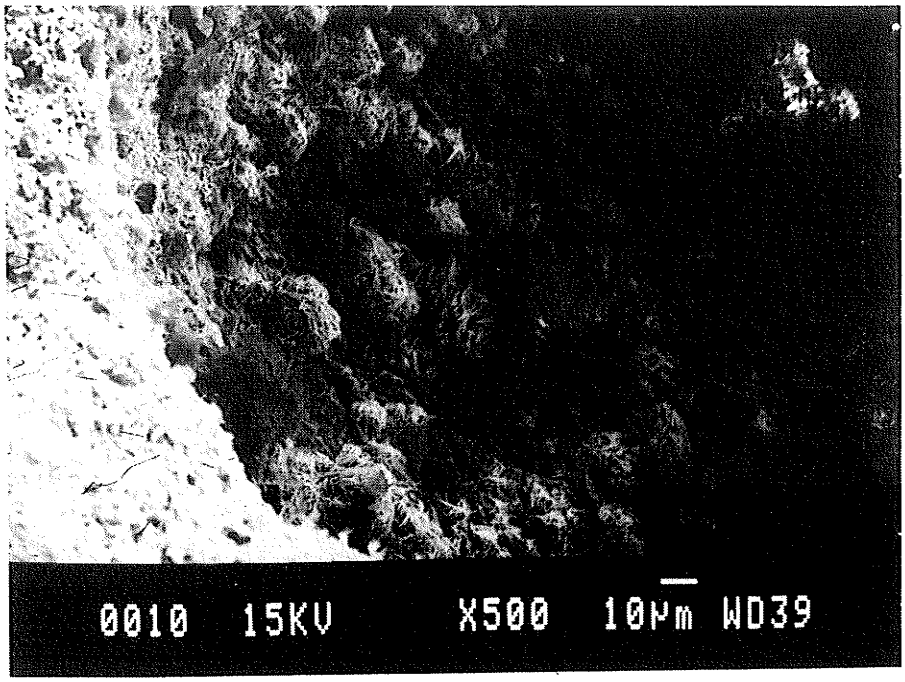

Figure 4.18 Microstructural feature in void of a cement paste specimen

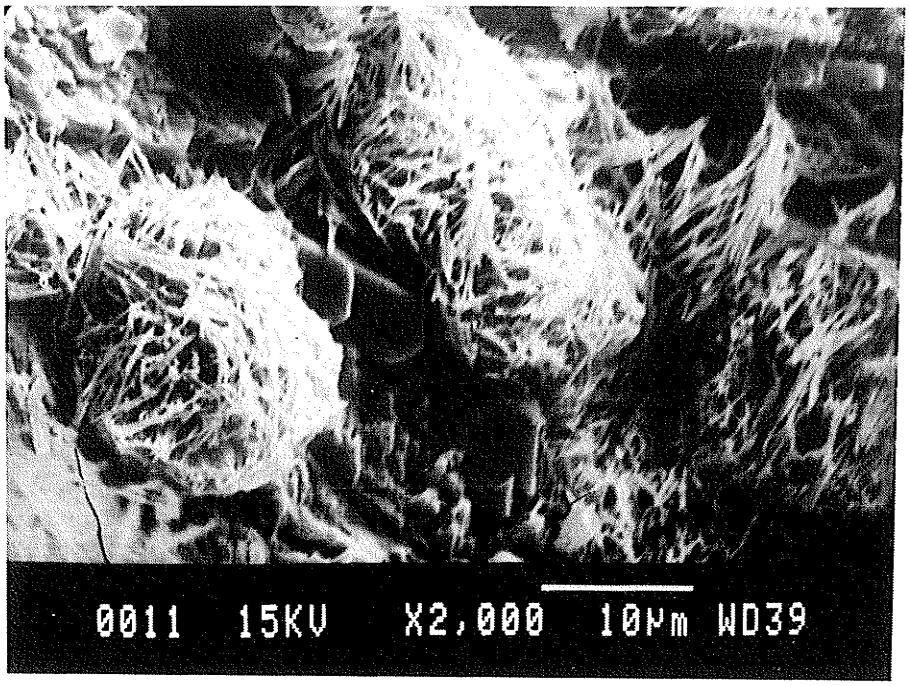

Figure 4.19 Microstructural feature in a void of a cement paste specimen (higher magnification of Figure 4.18)

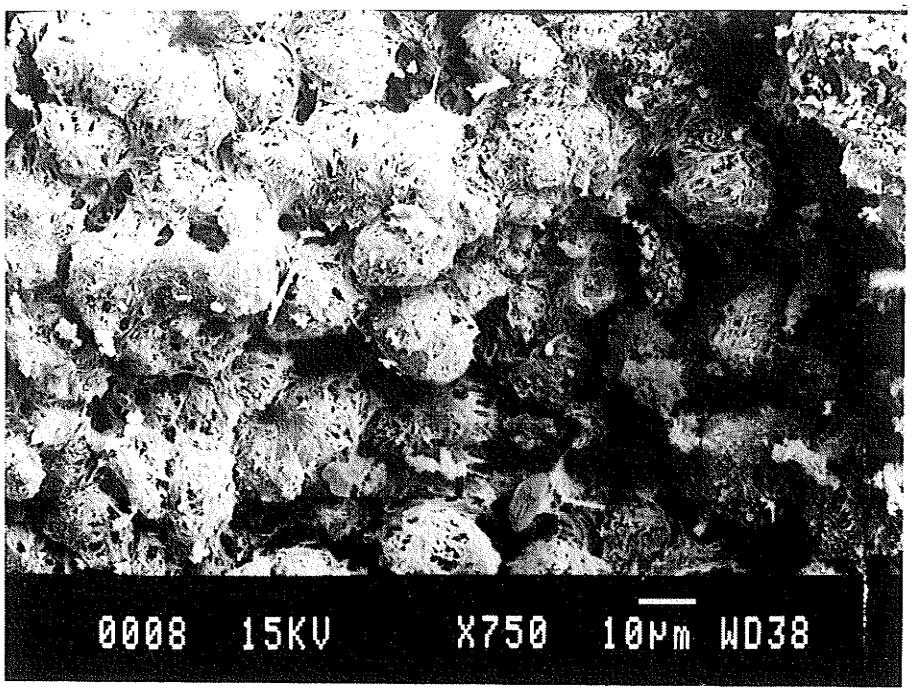

Figure 4.20 Microstructural feature on crack surface of a cement paste specimen

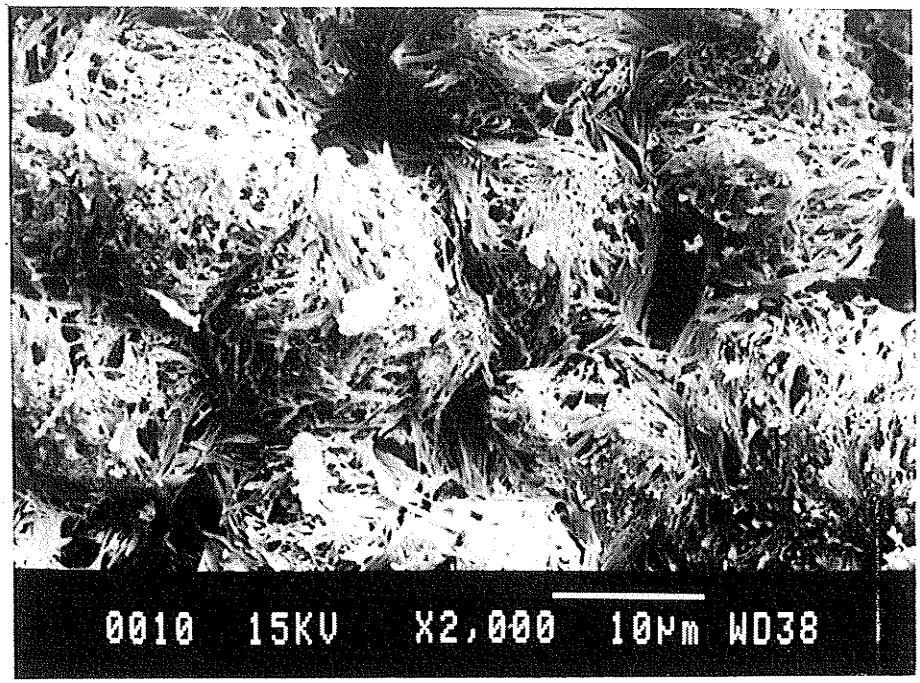

Figure 4.21 Microstructural feature on crack surface of a cement paste specimen (higher magnification of Figure 4.20)

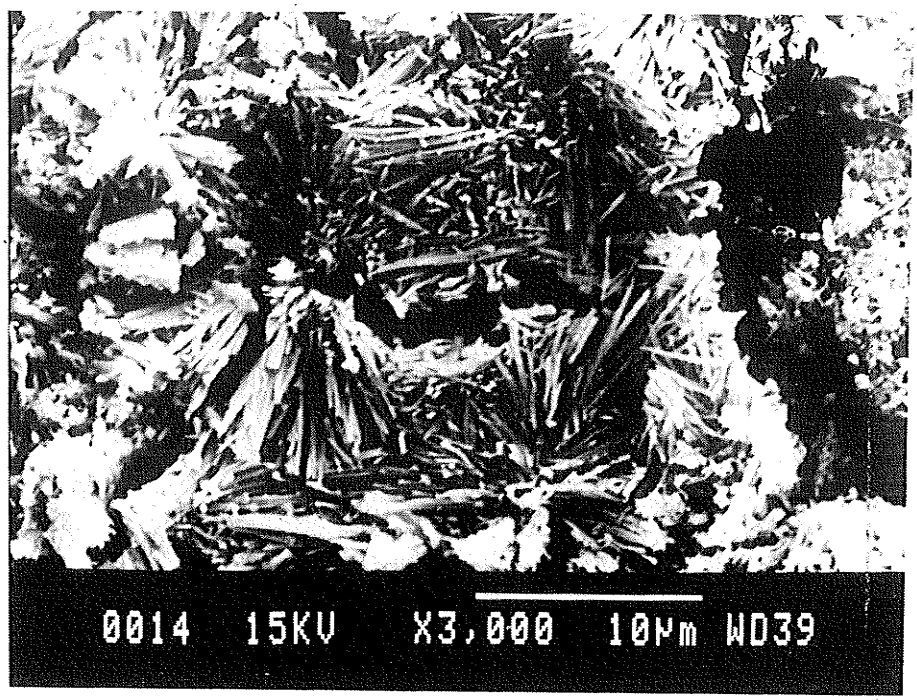

Figure 4.22 Microstructural feature in paste matrix of a concrete specimen

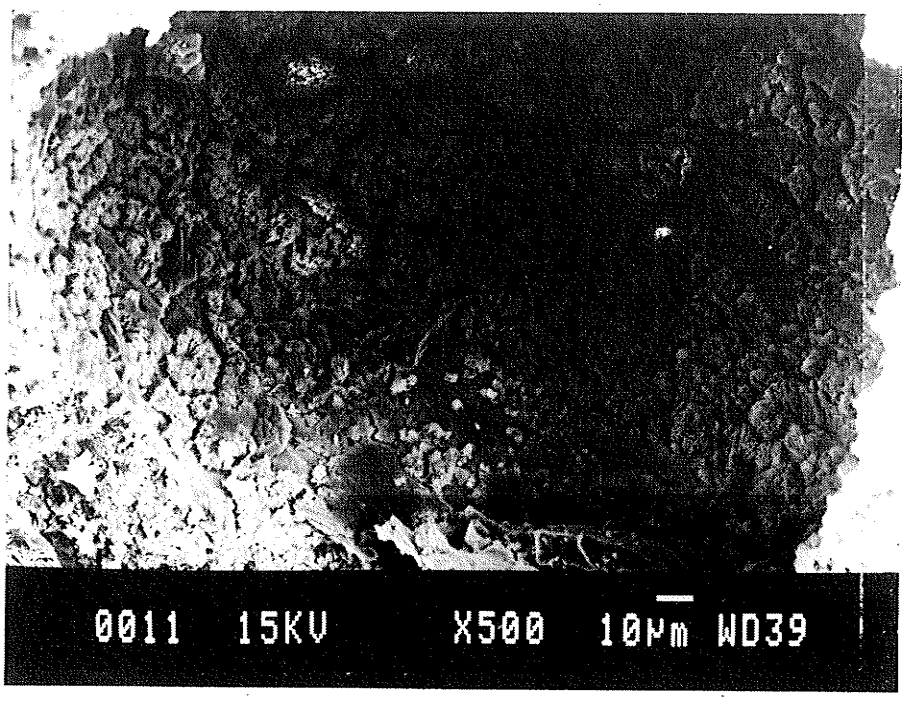

Figure 4.23 Microstructural feature in void of a concrete specimen

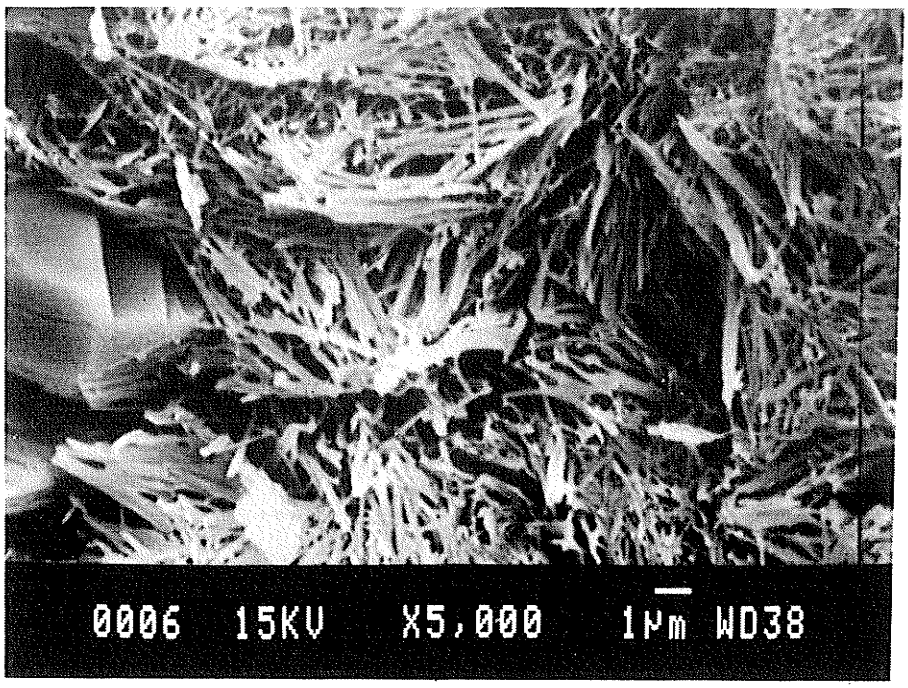

Figure 4.24 Microstructural feature in void of a concrete specimen (higher magnification of Figure 4.23)

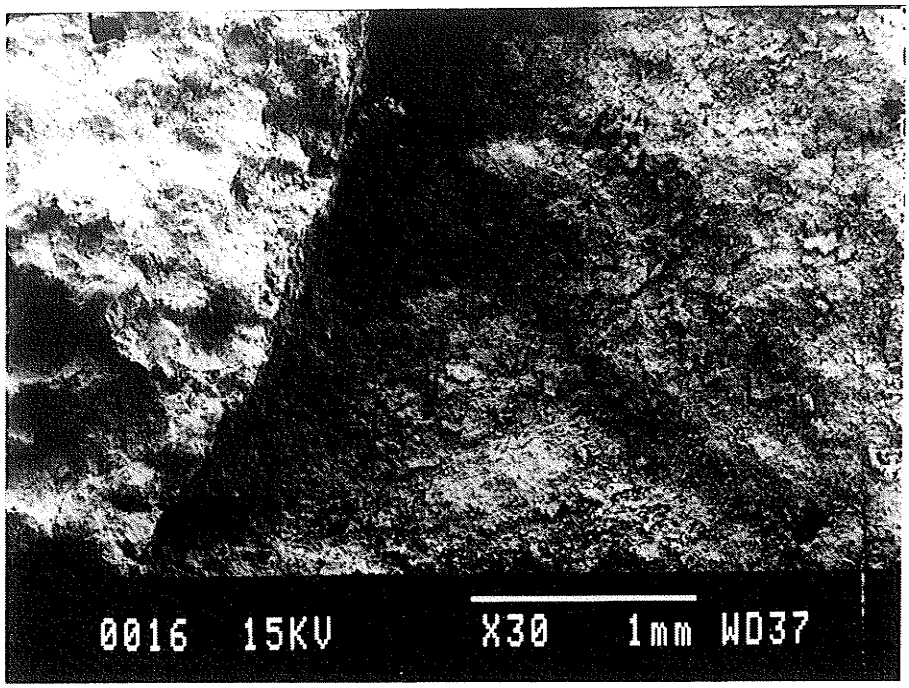

Figure 4.25 Paste-aggregate interface in a concrete specimen

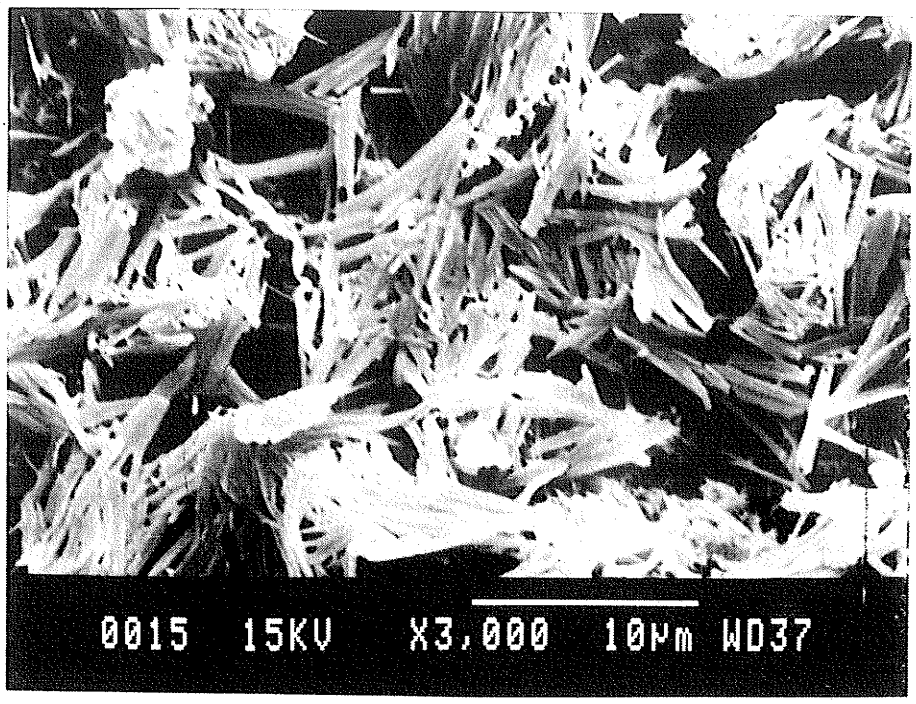

Figure 4.26 Microstructural feature at paste-aggregate interface in a concrete specimen (higher magnification of Figure 4.25)

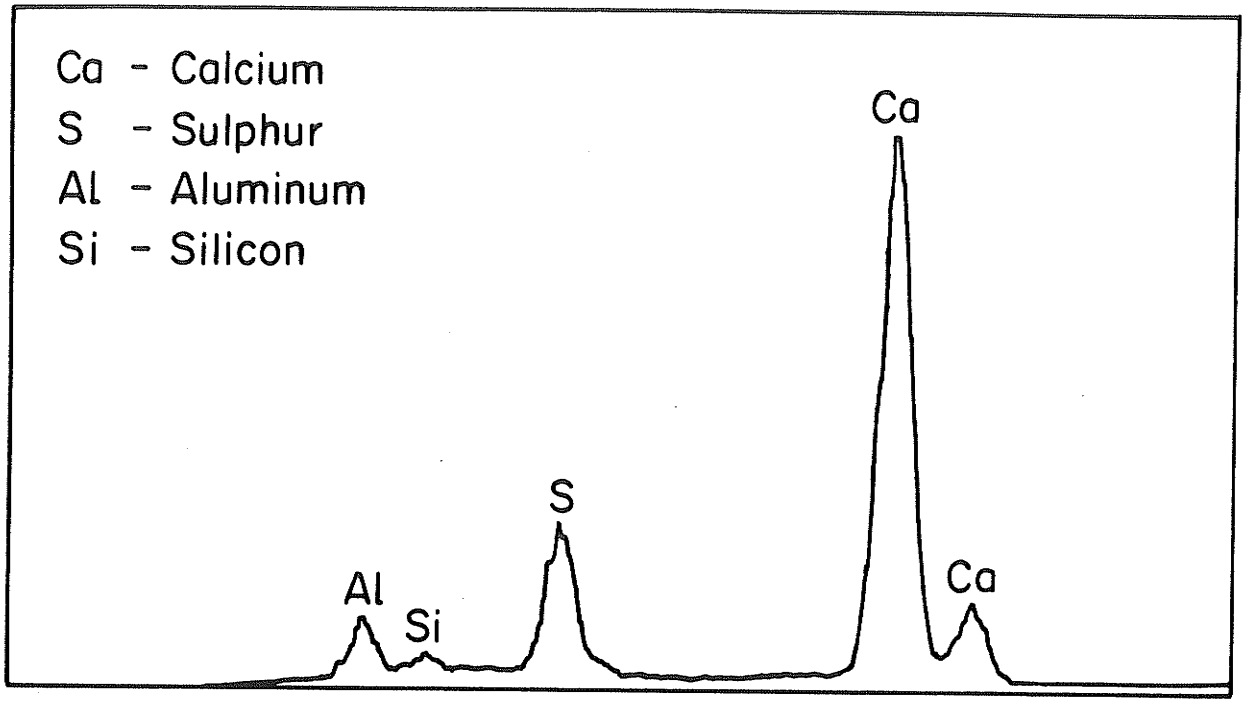

Figure 4.27 Elemental energy-dispersive spectrum for feature in Figure 4.17

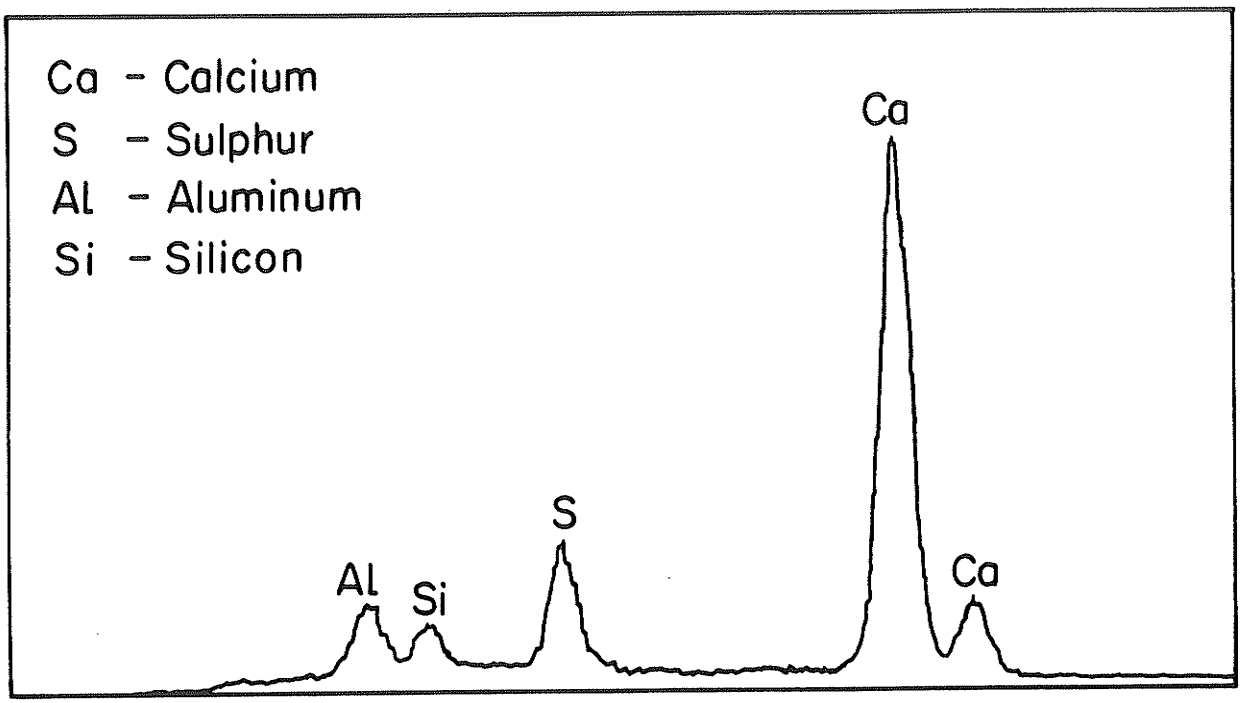

Figure 4.28 Elemental energy dispersive spectrum for feature in Figures 4.18 and 4.19

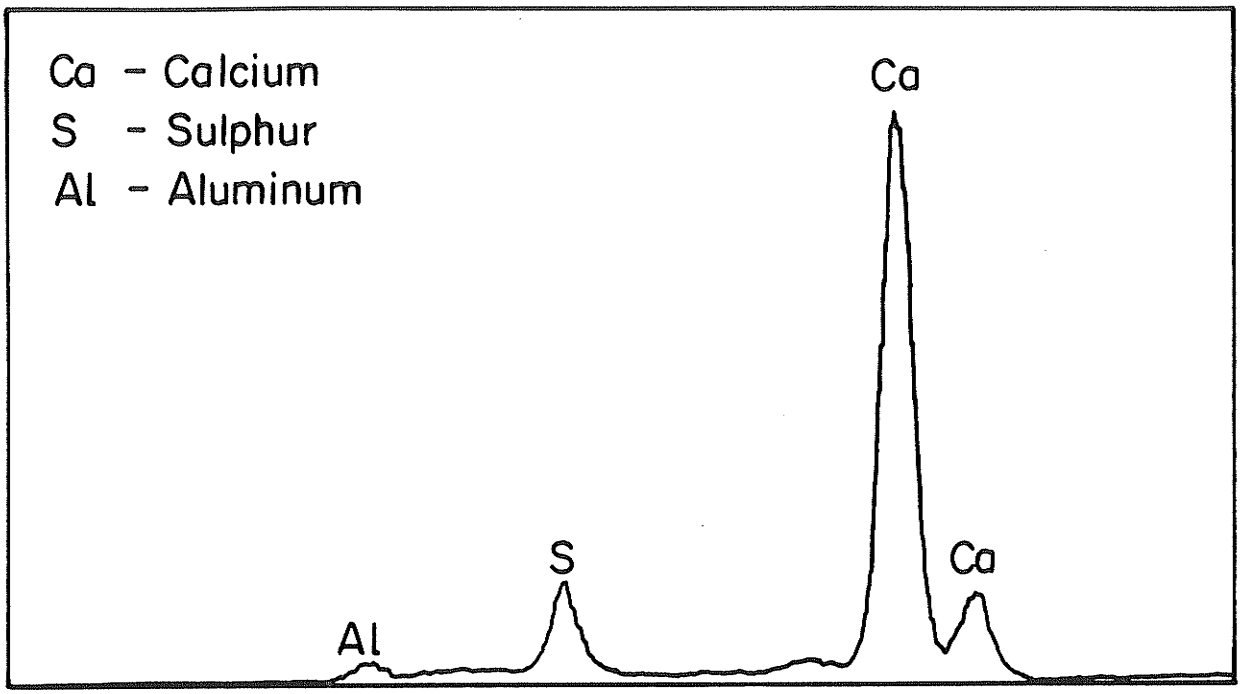

Figure 4.29 Elemental energy-dispersive spectrum for feature in Figures 4.20 and 4.21

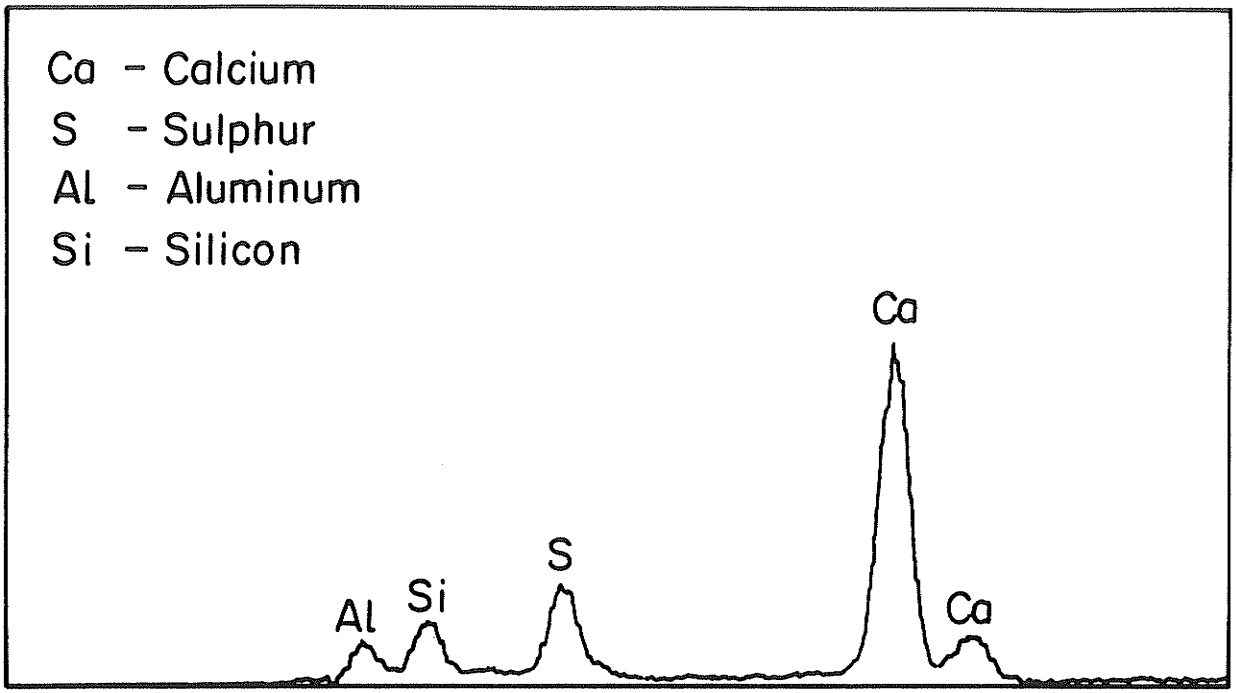

Figure 4.30 Elemental energy dispersive spectrum for feature in Figure 4.22

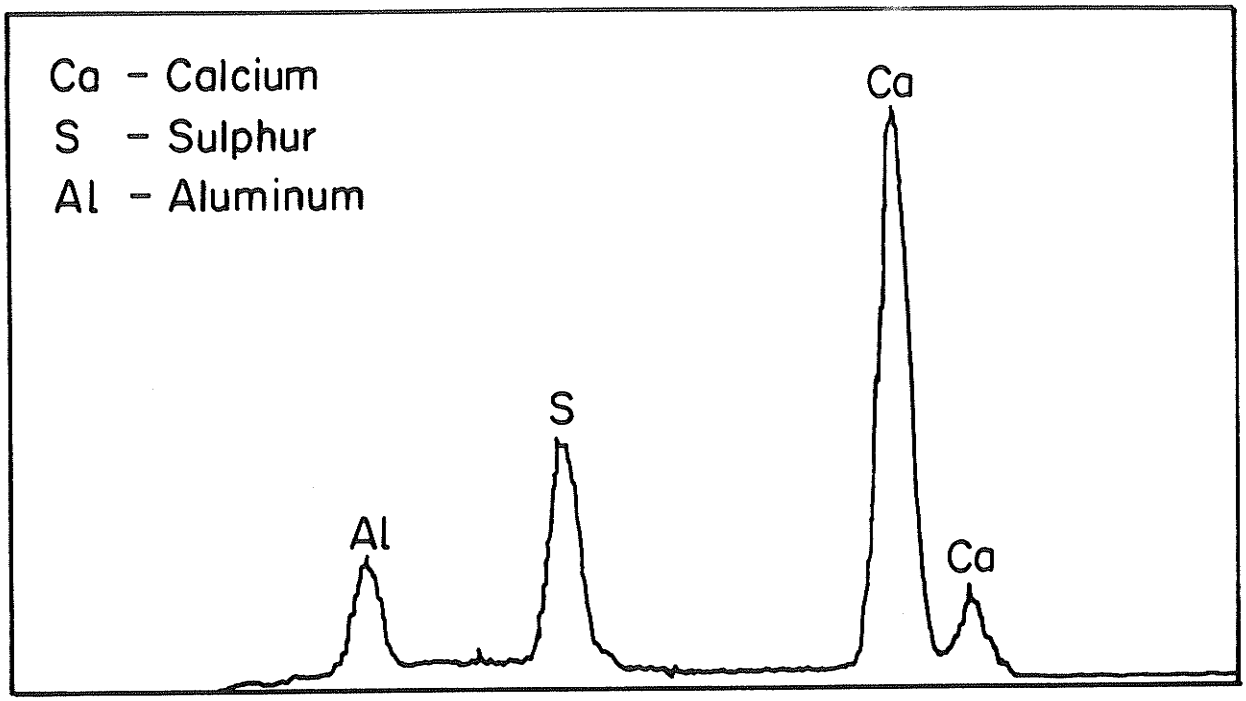

Figure 4.31 Elemental energy-dispersive spectrum for feature in Figures 4.23 and 4.24

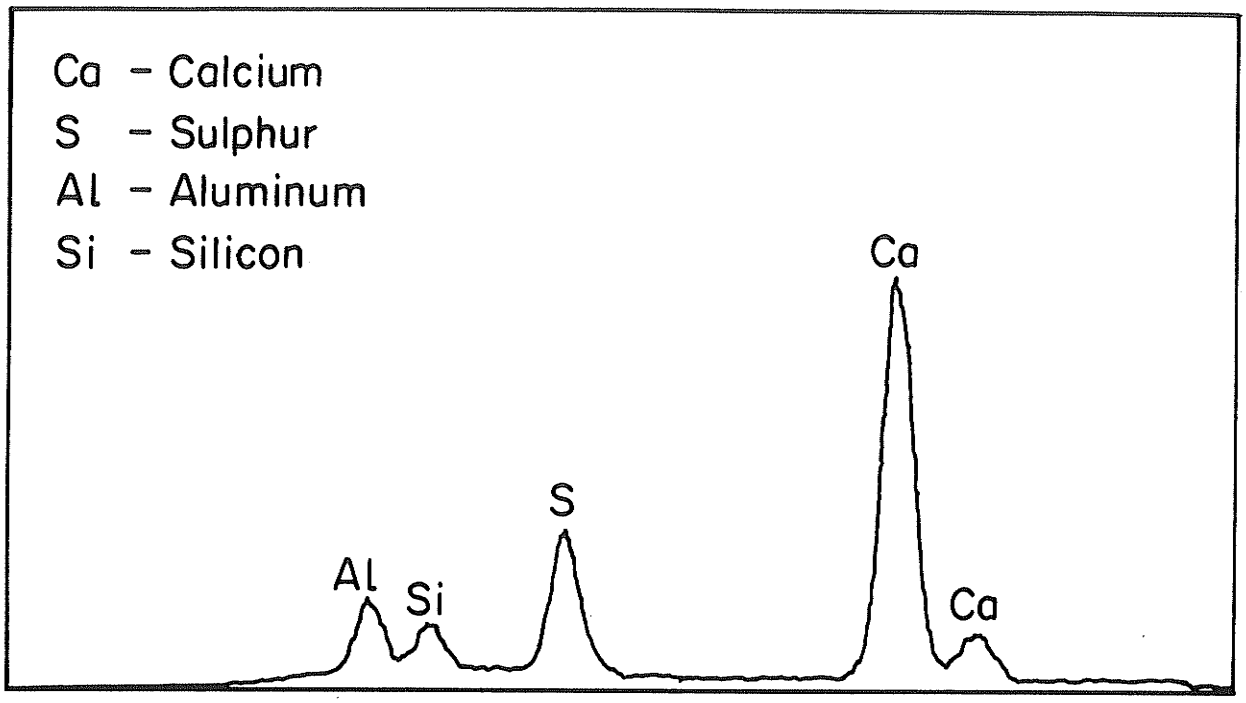

Figure 4.32 Elemental energy dispersive spectrum for feature in Figures 4.25 and 4.26

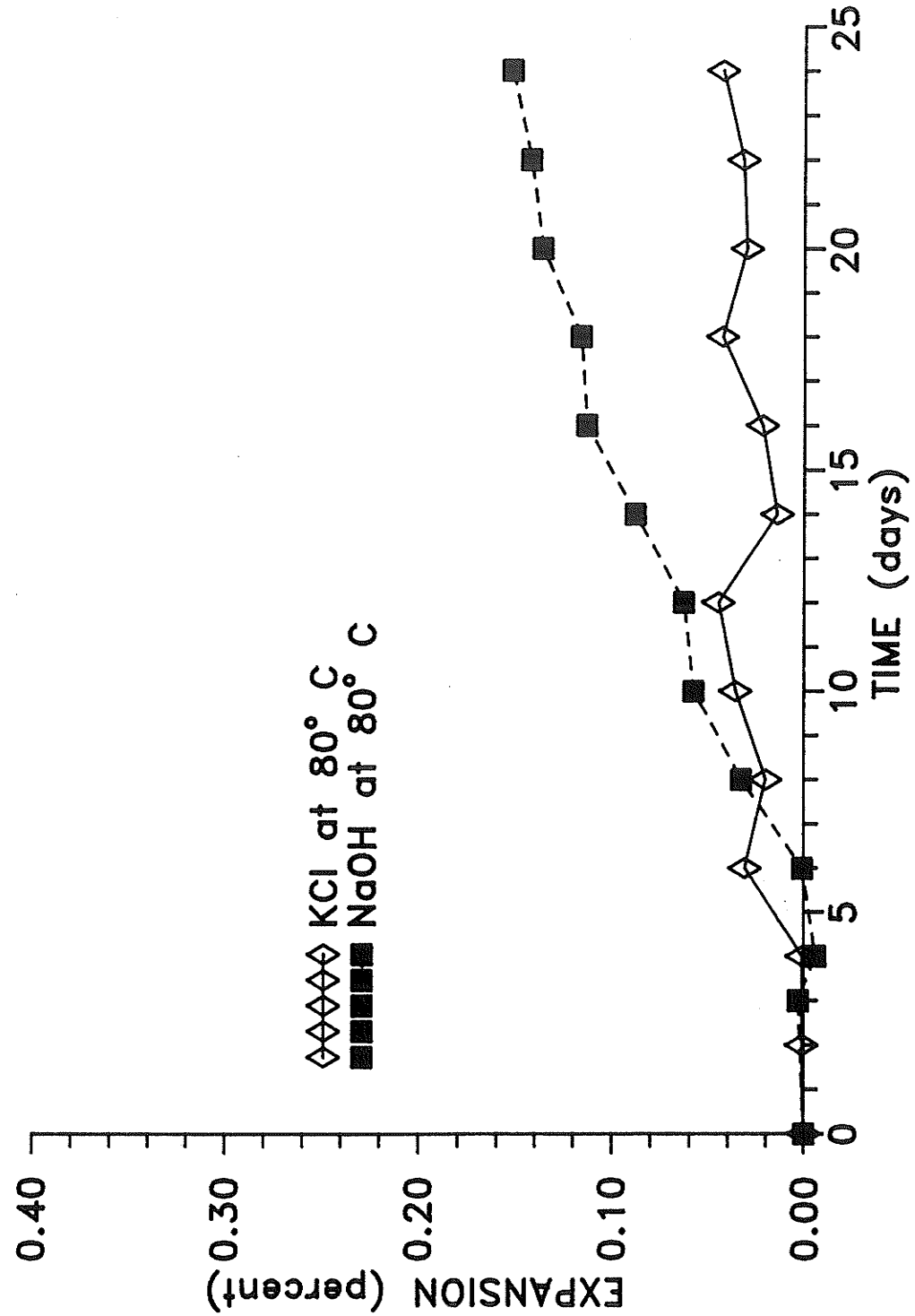

Figure 4.33 Comparison of expansion for test specimens stored in potassium chloride (KCl) and sodium hydroxide (NaOH) solutions

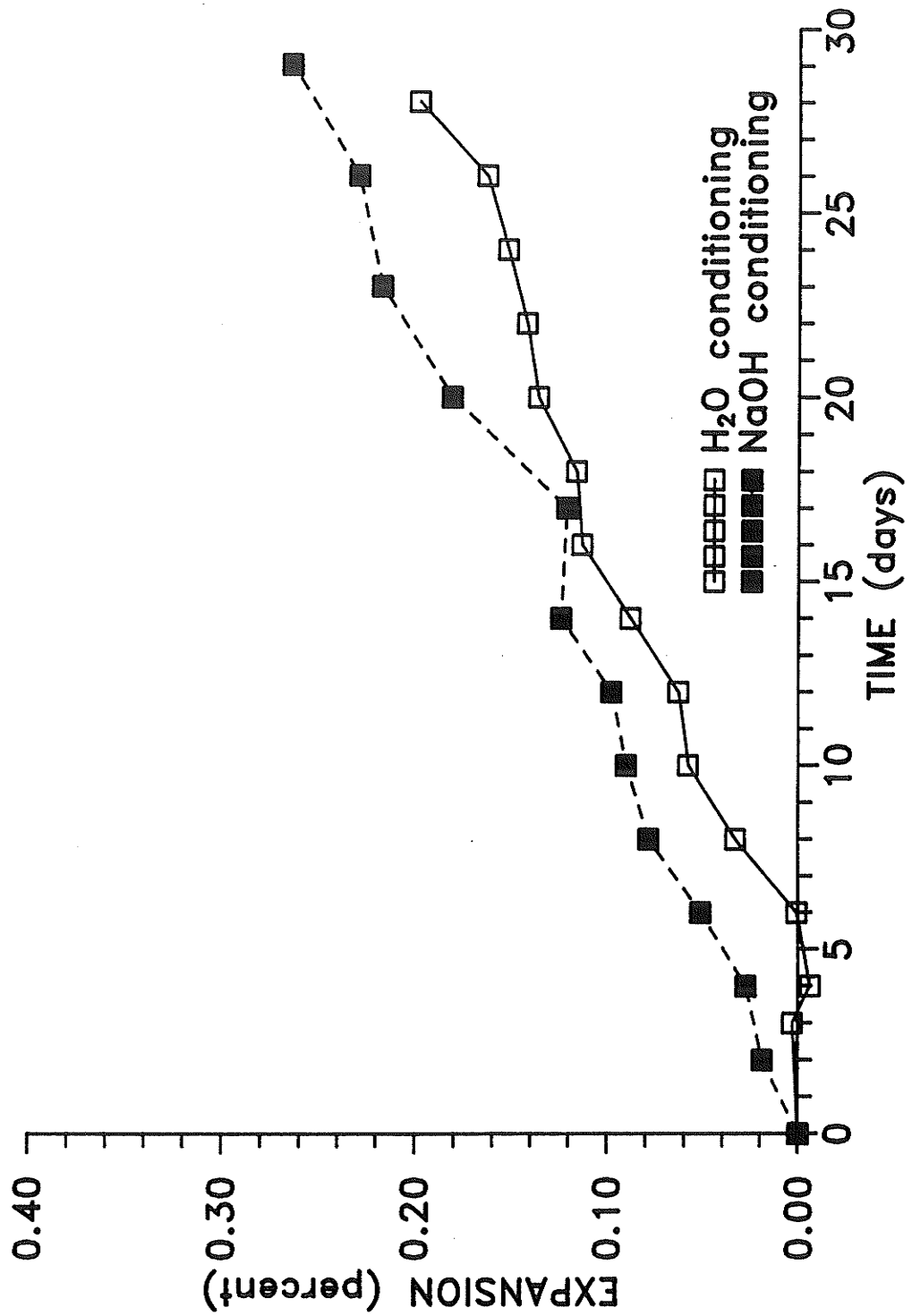

Figure 4.34 Effect of conditioning medium on expansion of Mix B2 specimens

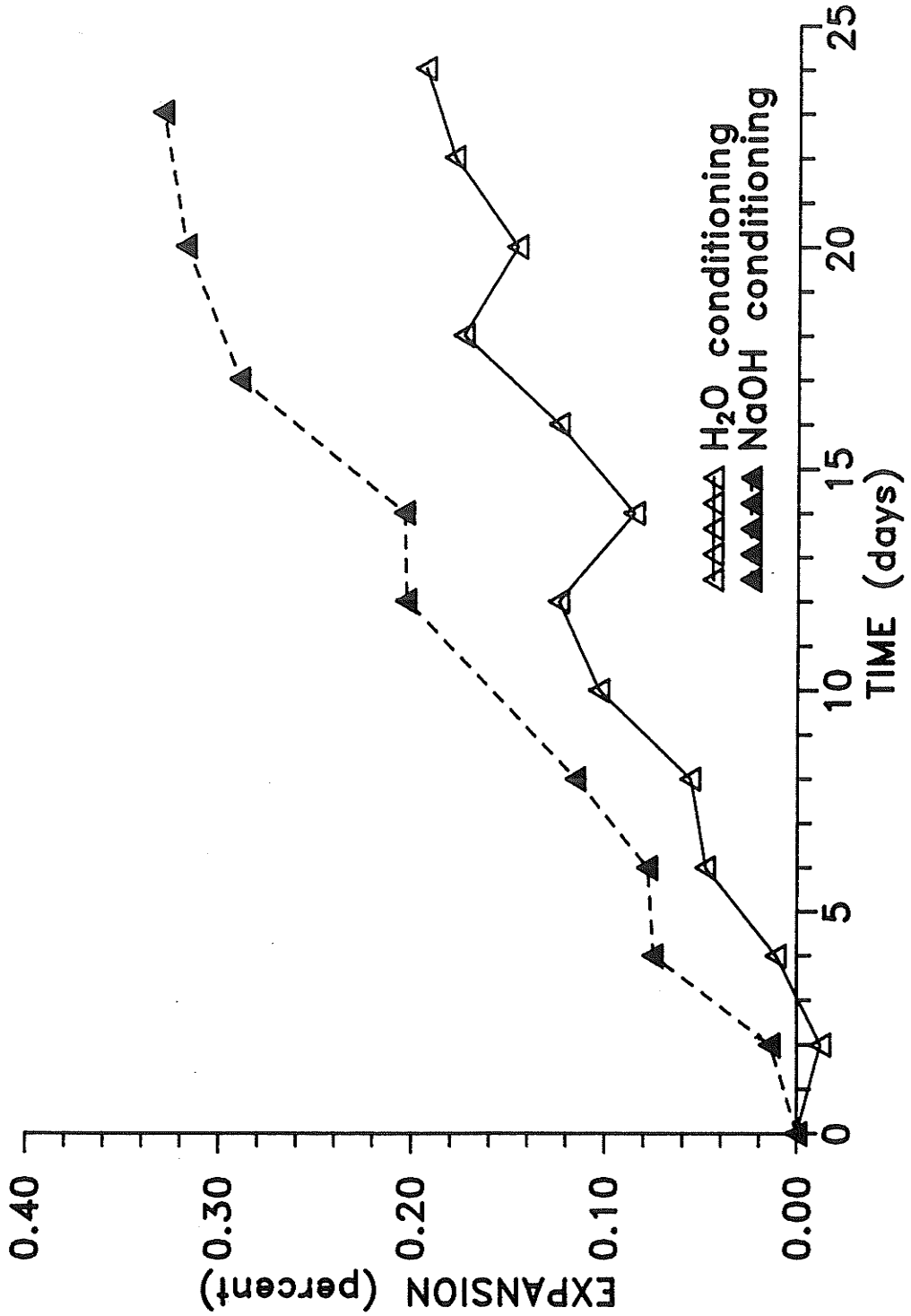

Figure 4.35 Effect of conditioning medium on expansion of Mix C3 specimens

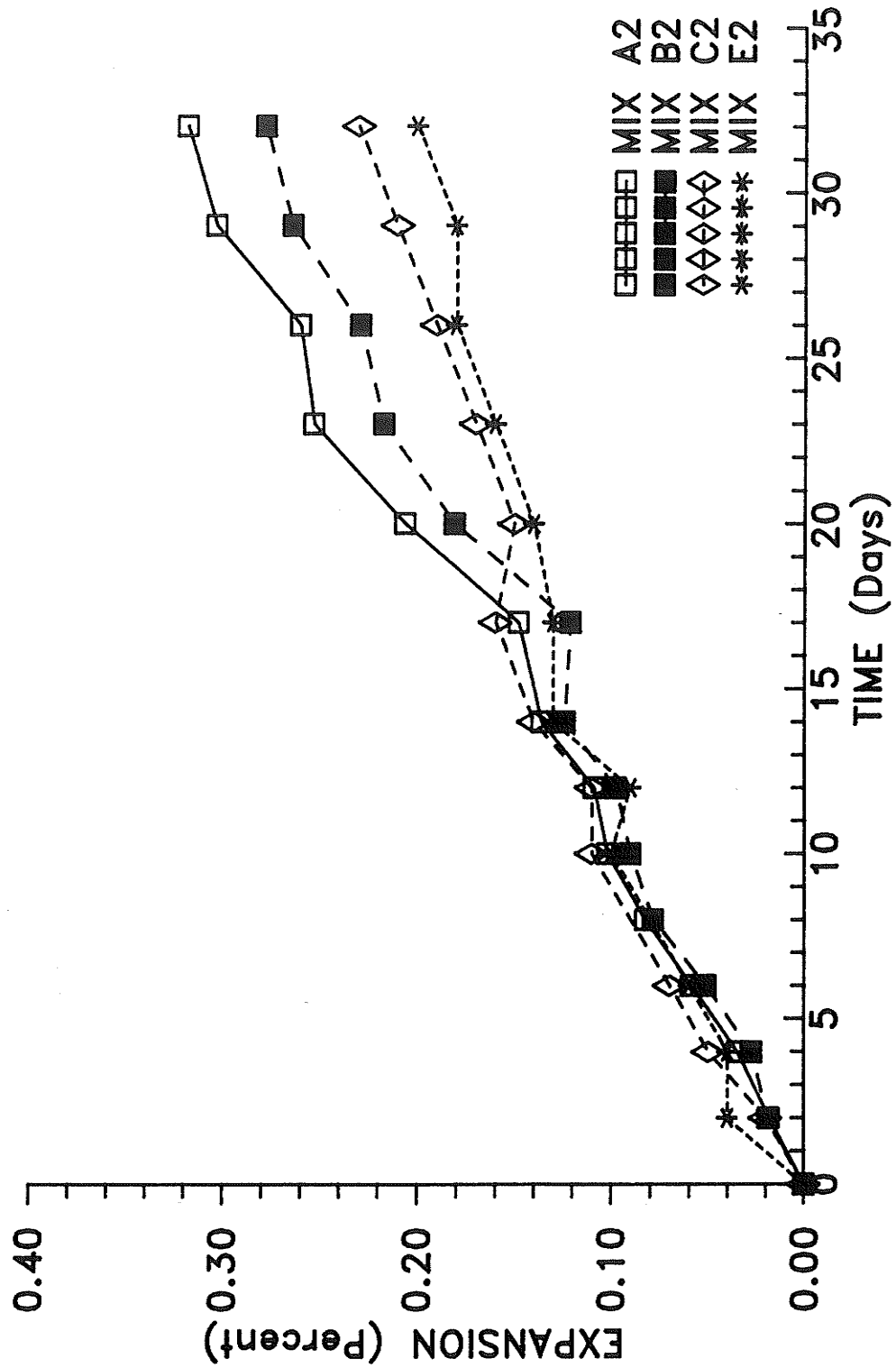

Figure 4.36 Expansion of test specimens made with alkali-silica reactive aggregate (Aggregate 2) and cements having different alkali contents

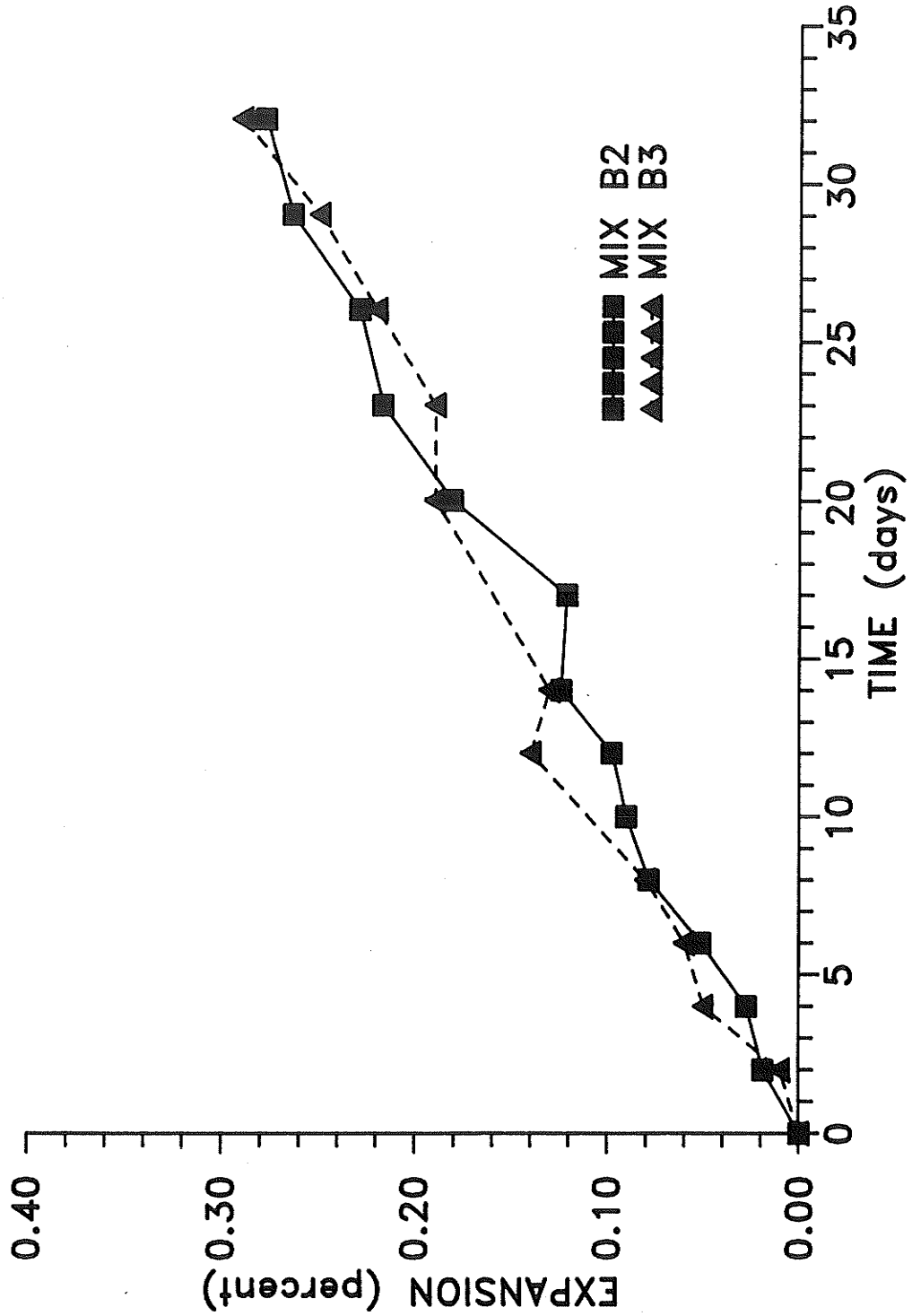

Figure 4.37 Expansion of test specimens made with alkali-silica (Aggregate 2) and alkali-carbonate (Aggregate 3) reactive aggregates.

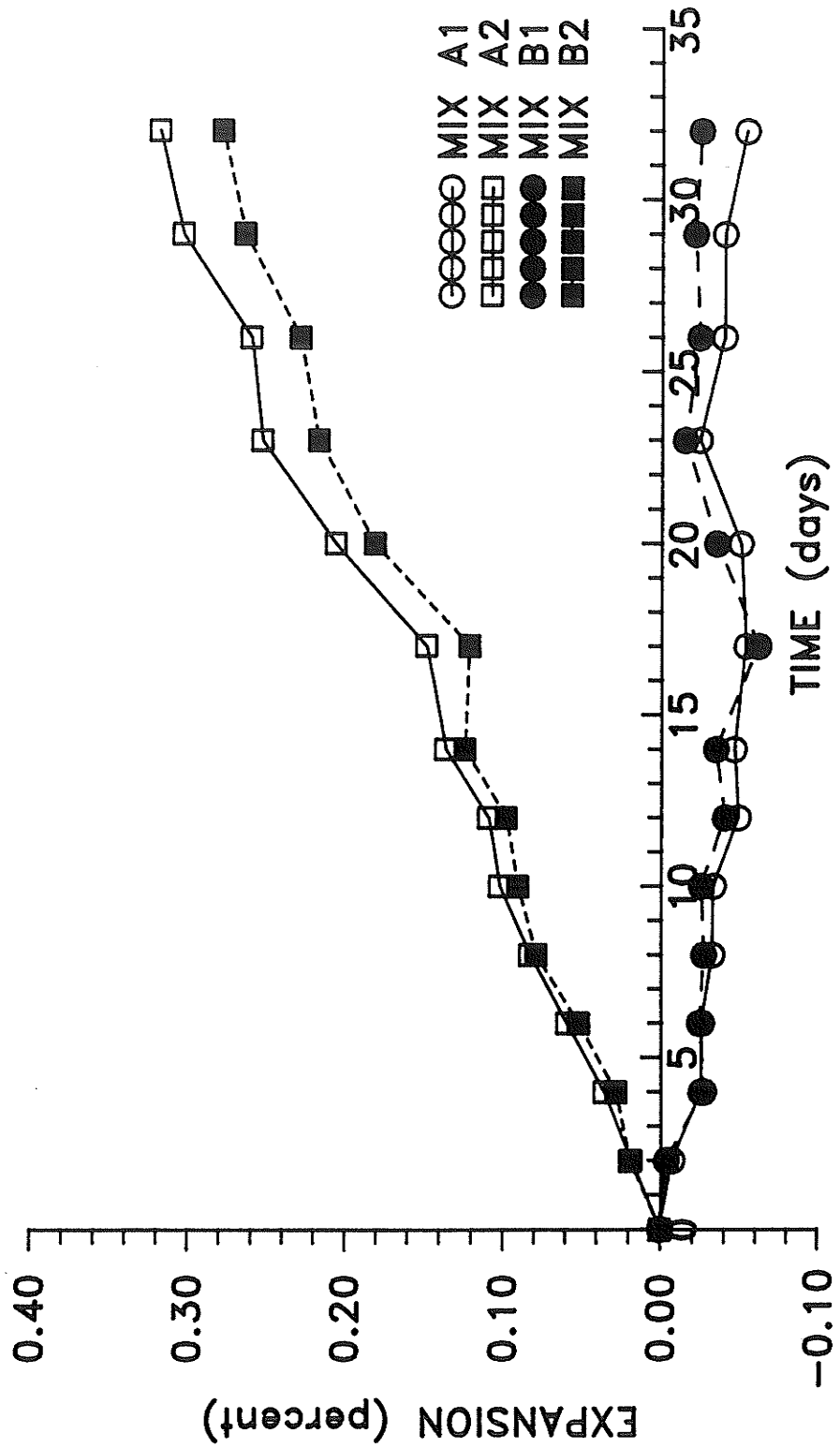

Figure 4.38 Expansion of test specimens made with non-reactive (Aggregate 1) and alkali-silica reactive (Aggregate 2) aggregates

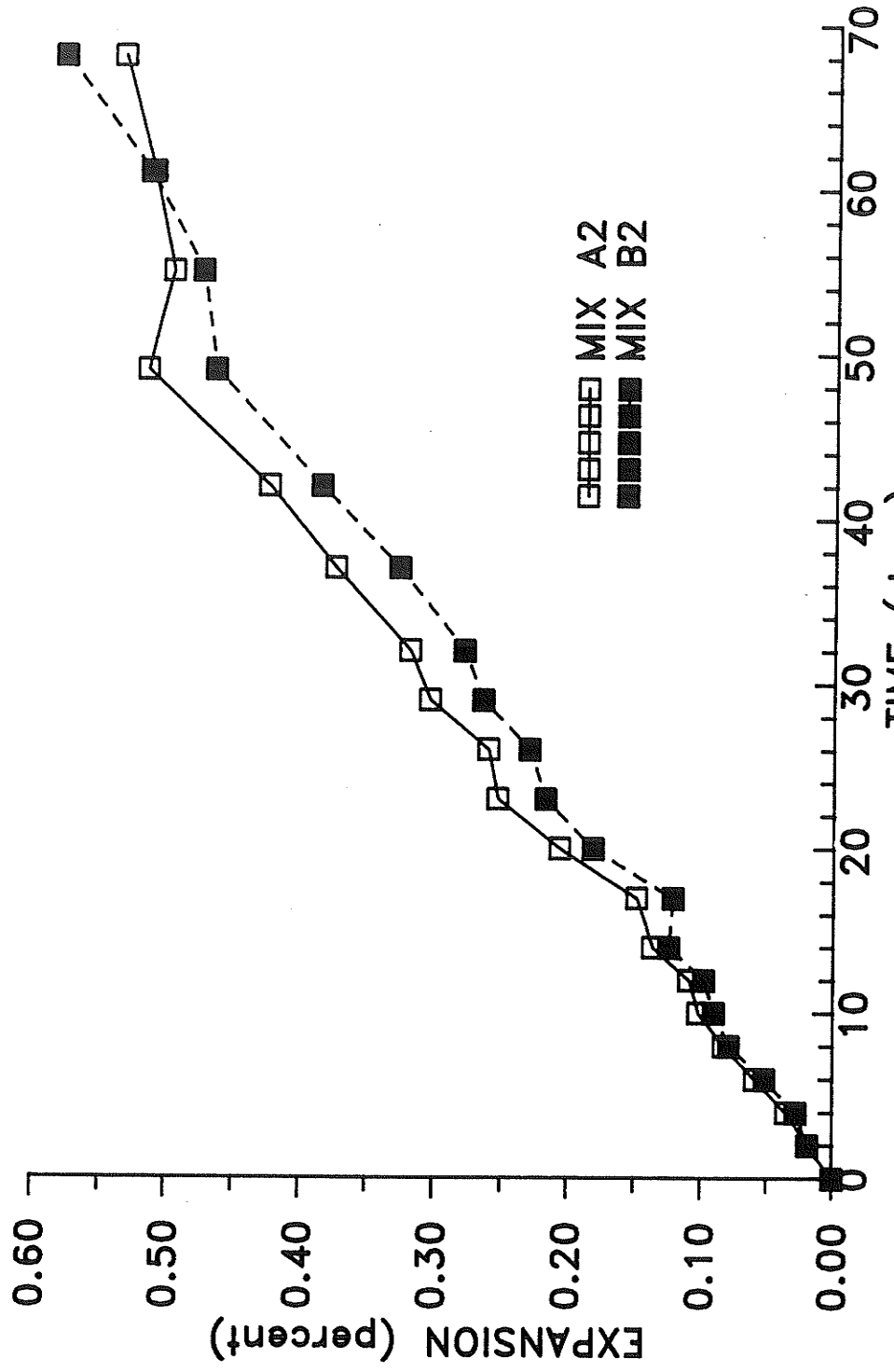

Figure 4.39 Expansion of test specimens in NaOH solution for over two months

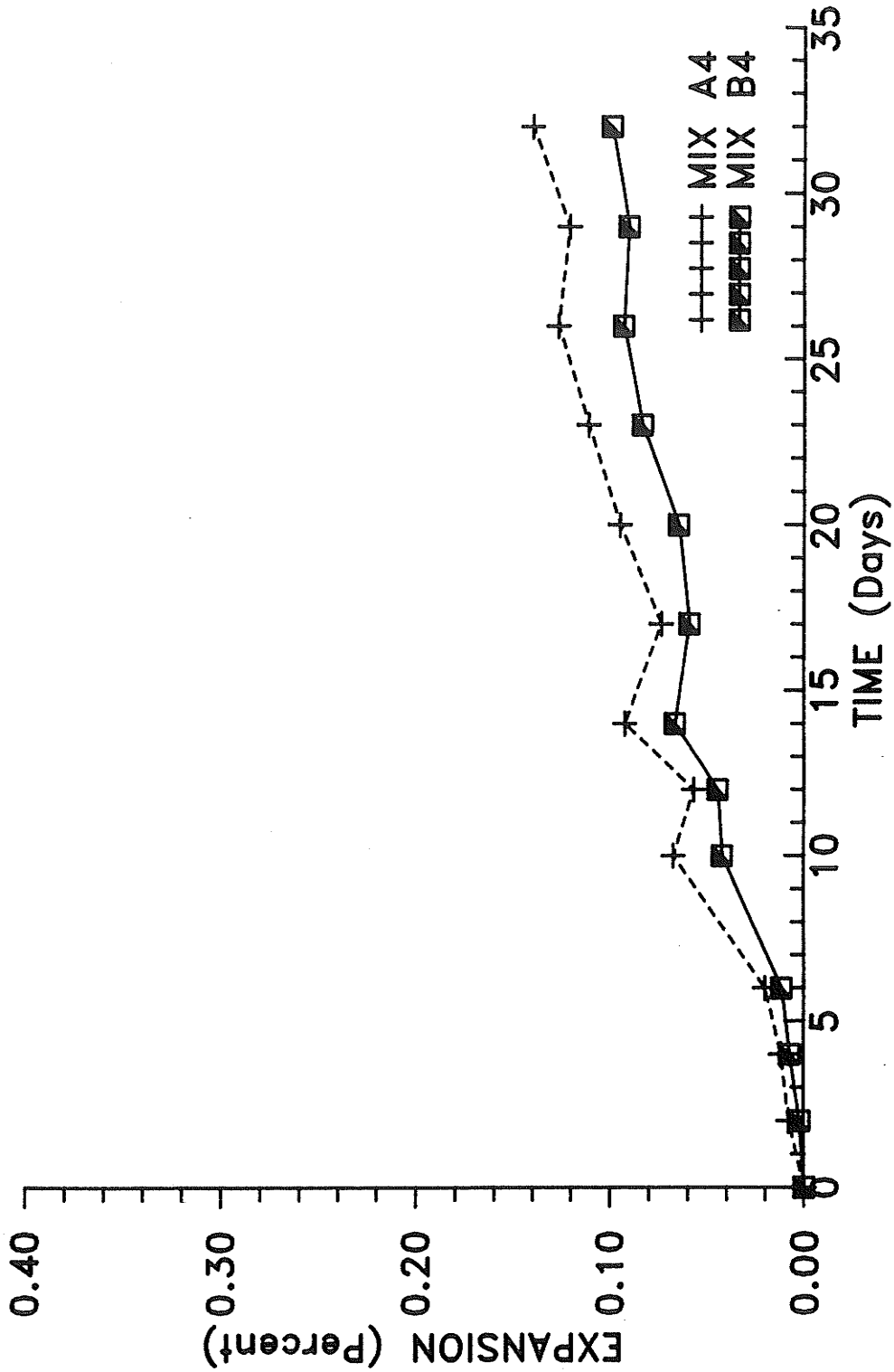

Figure 4.40 Expansion of test specimens made with Aggregate 4, on alkali-silica reactive aggregate

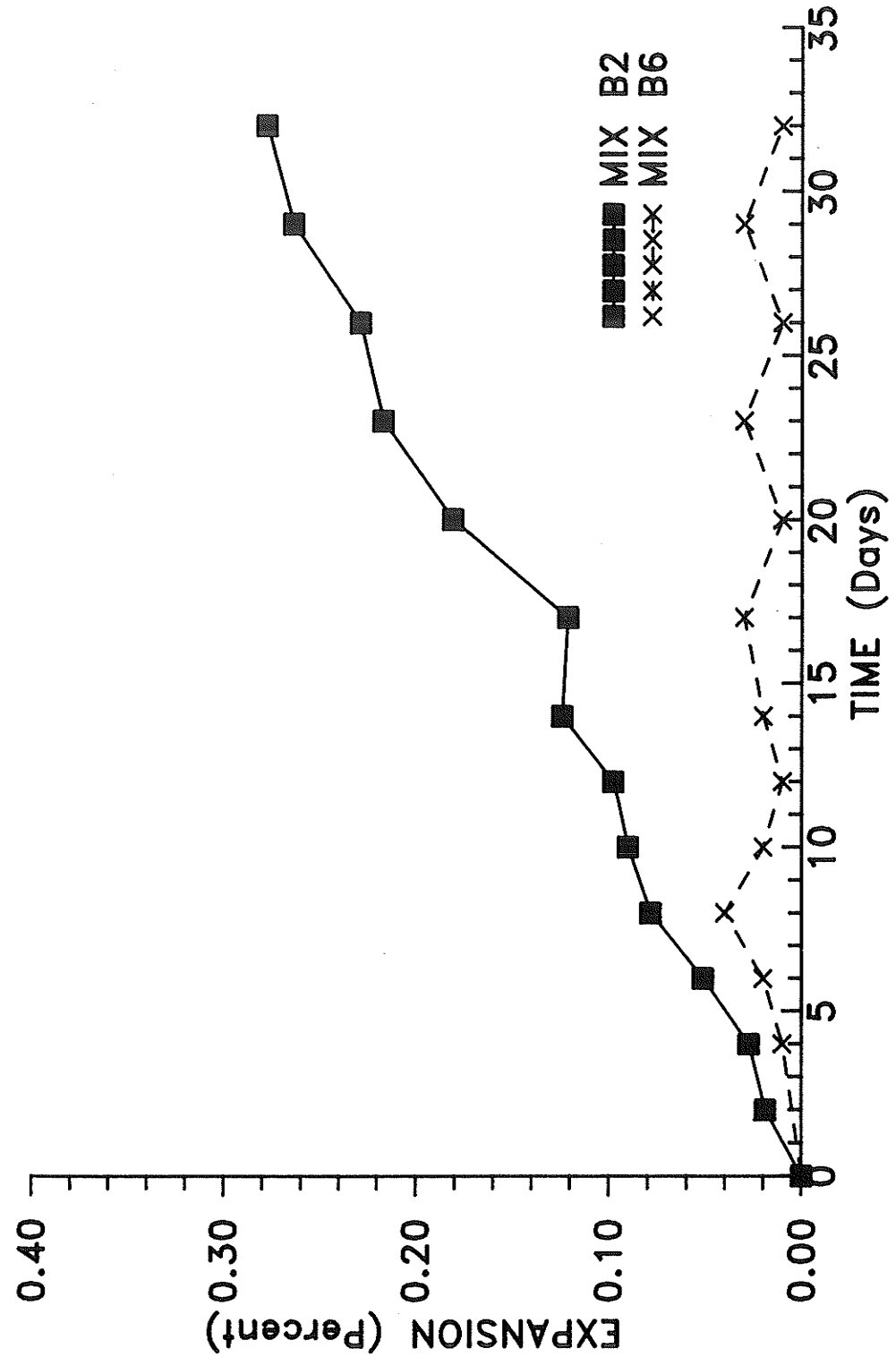

Figure 4.41 Comparison of expansion for mixes B2 and B6 specimens

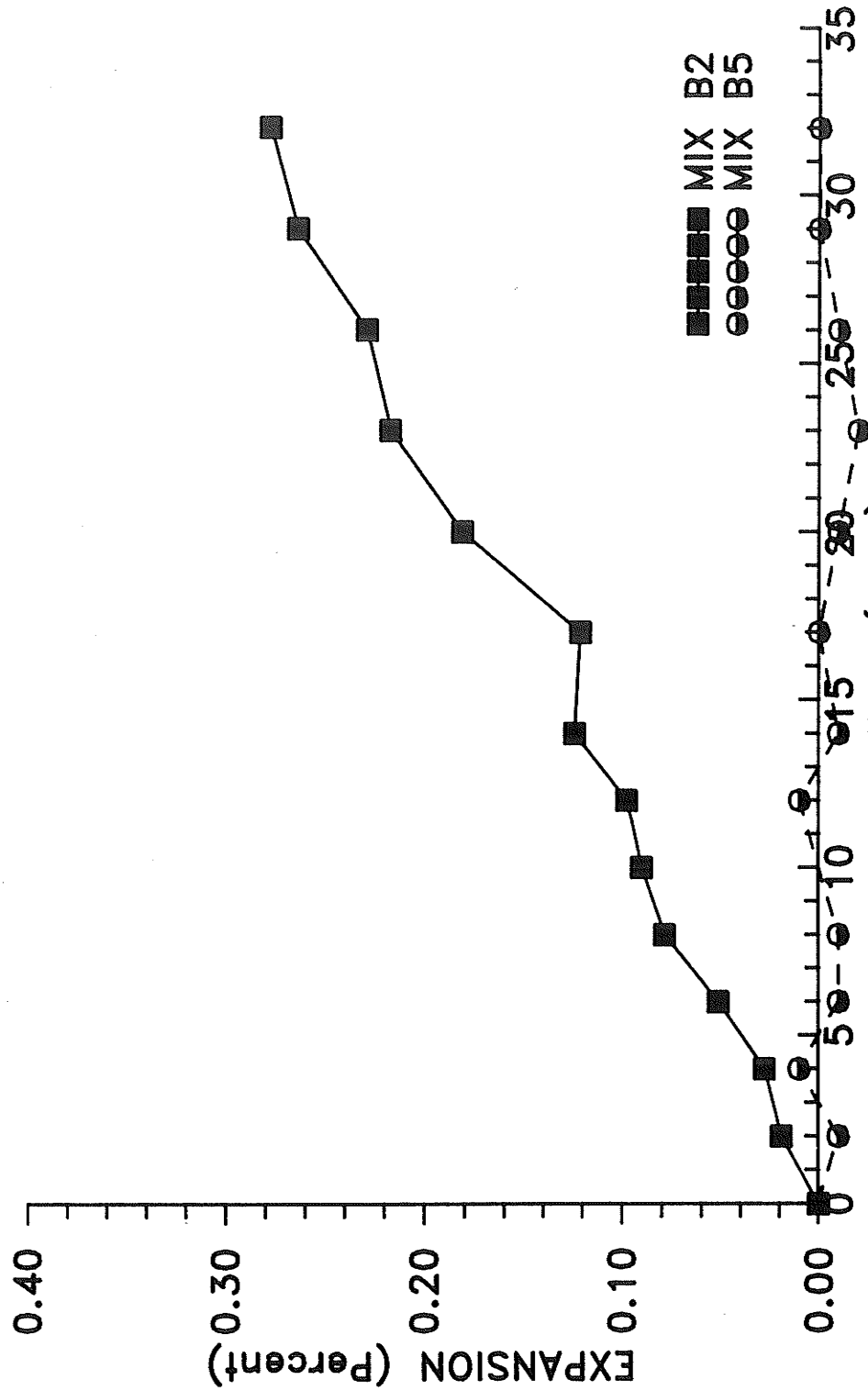

Figure 4.42 Comparison of expansion for test specimens made with alkali-silica (Aggregate 2) and alkali-silicate (Aggregate 5) reactive aggregates

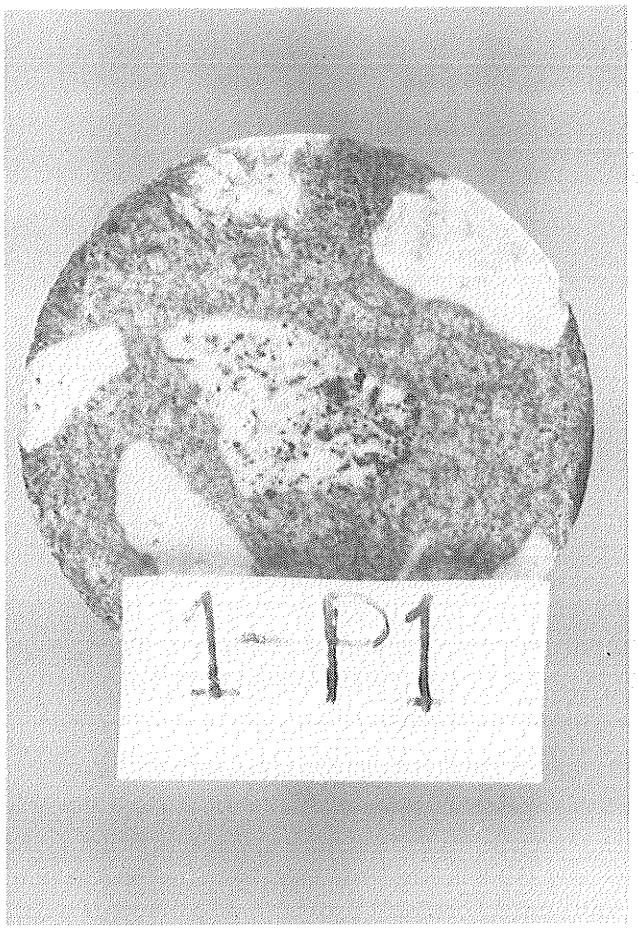

Figure 4.43 Cross-section of uncracked specimen for Aggregate 1 (non-reactive) at end of test

Figure 4.44 Cross-section of uncracked specimen for Aggregate 5 (alkali-silicate reactive) at end of test

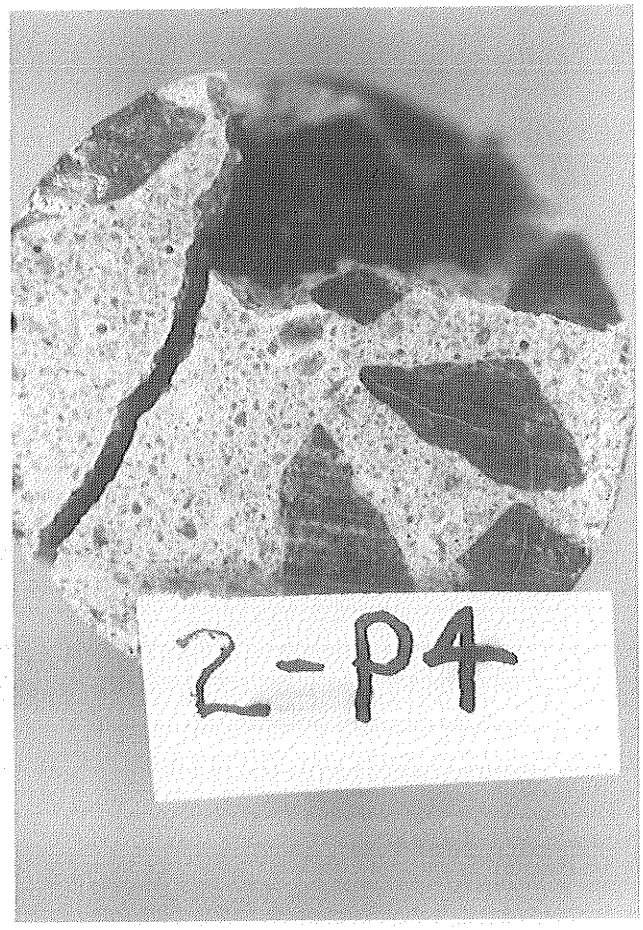

Figure 4.45 Cross-section of cracked specimen for Aggregate 2 (alkali-silica reactive) at end of test

Figure 4.46 Longitudinal view of cracked specimen for Aggregate 2 (alkali-silica reactive) at end of test

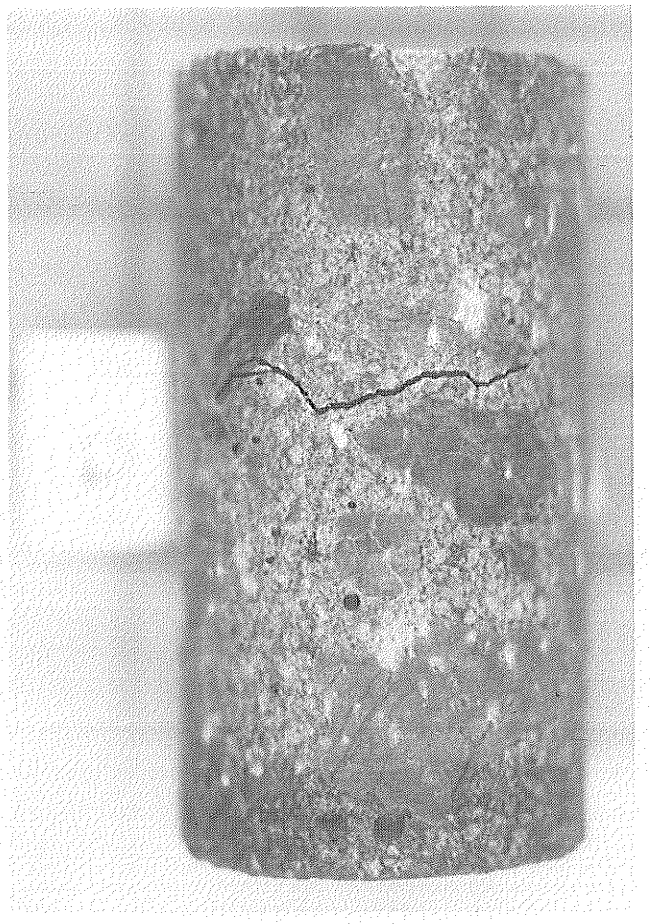

Figure 4.47 Longitudinal view of cracked specimen for Aggregate 3 (alkali-carbonate reactive) at end of test

Figure 4.48 · Cross-section of specimen for Aggregate 3 (alkali-carbonate reactive) with white spots of gel

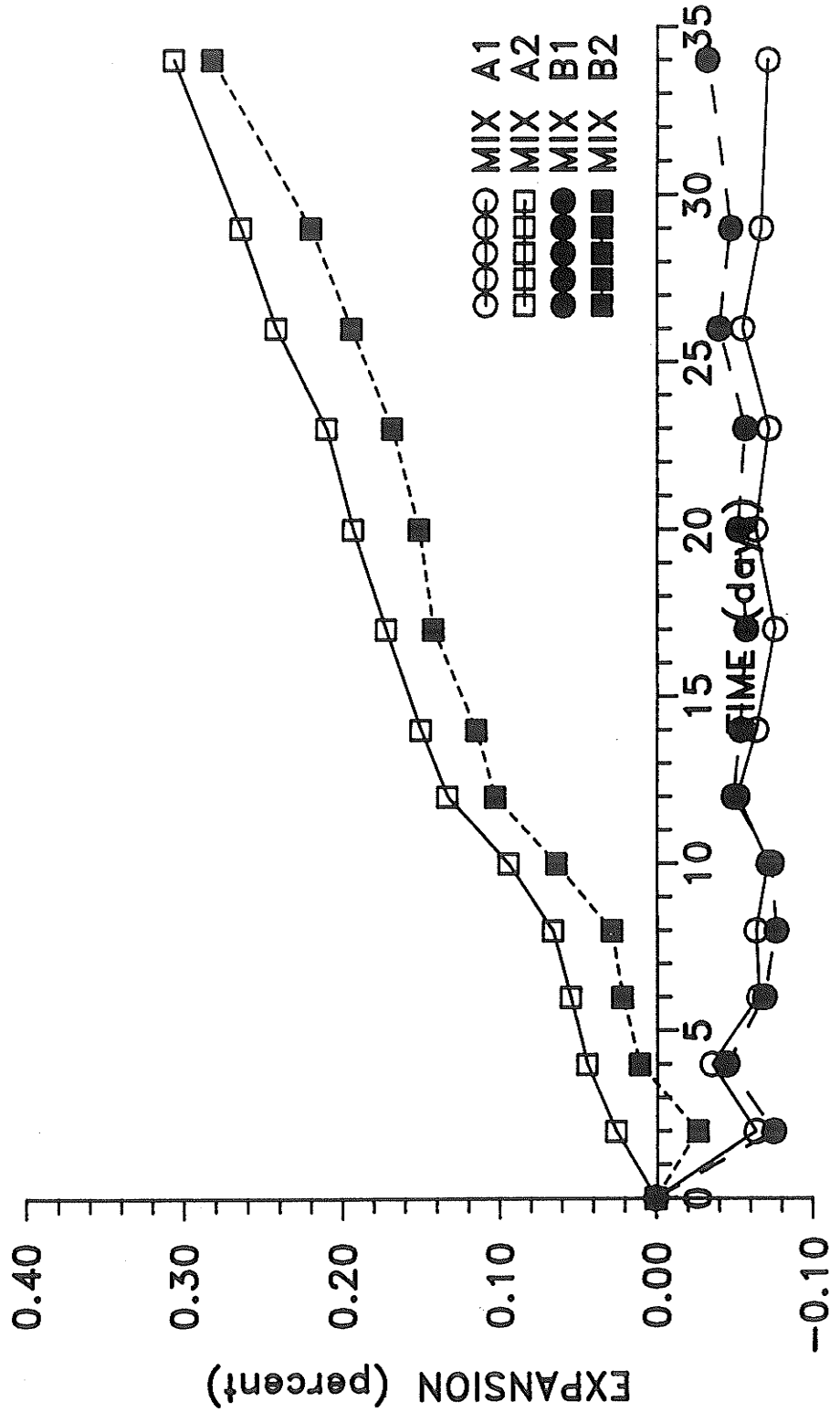

Figure 4.49 Expansion of pretreated specimens stored in NaOH solution at 80°C

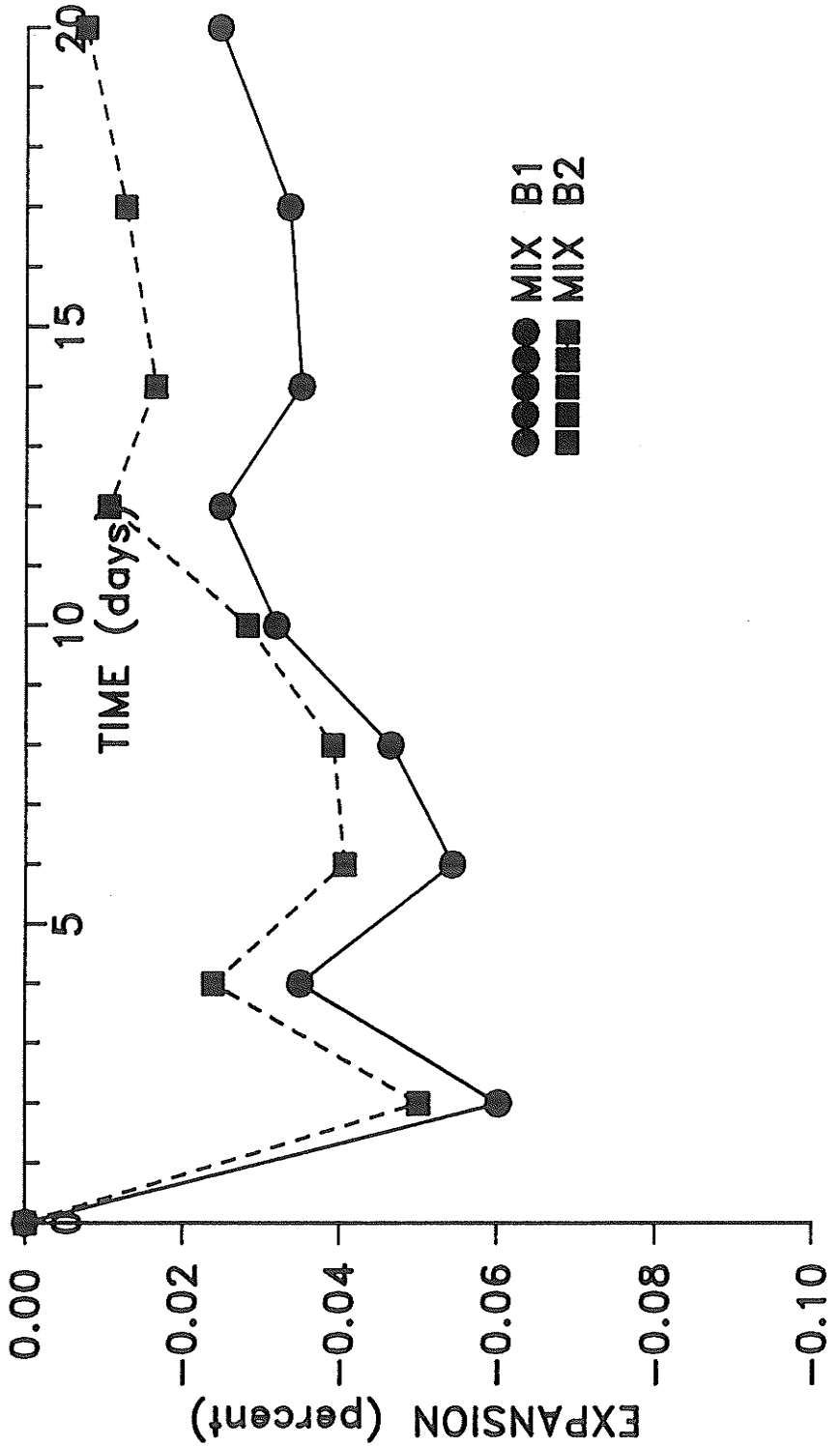

Figure 4.50 Contraction of pretreated specimens stored in water at 80°C

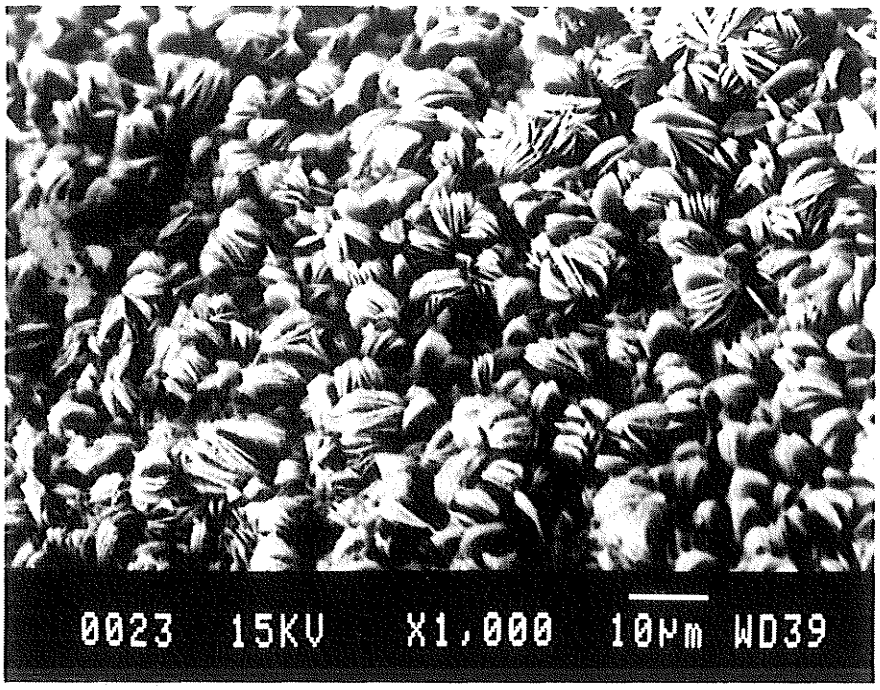

Figure 4.51 Rosette morphology of alkali-silica gel in specimen made with Aggregate 2

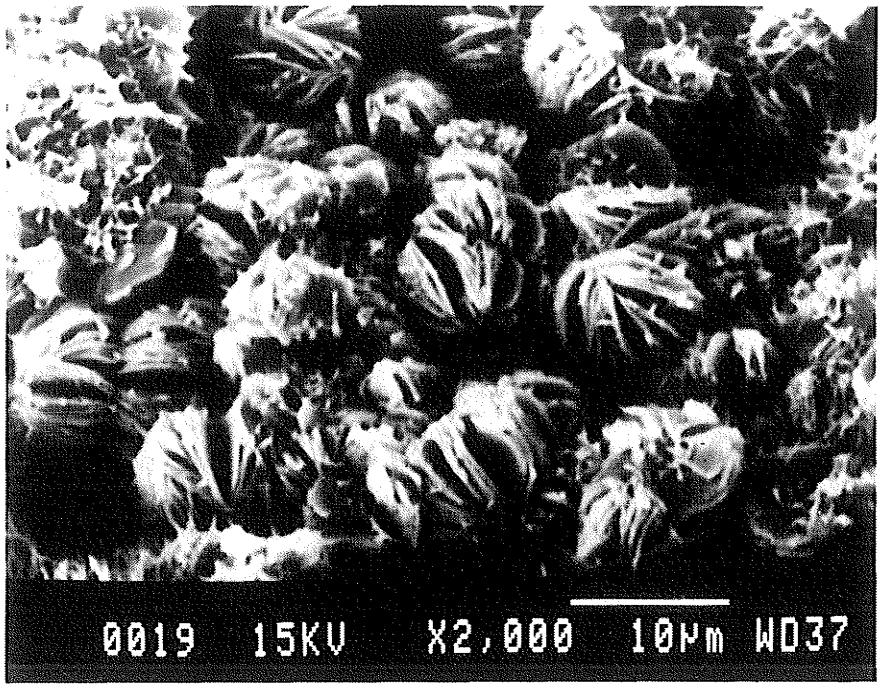

Figure 4.52 Rosette morphology of alkali-silica gel in specimen made with Aggregate 2 (higher magnification of Figure 4.51)

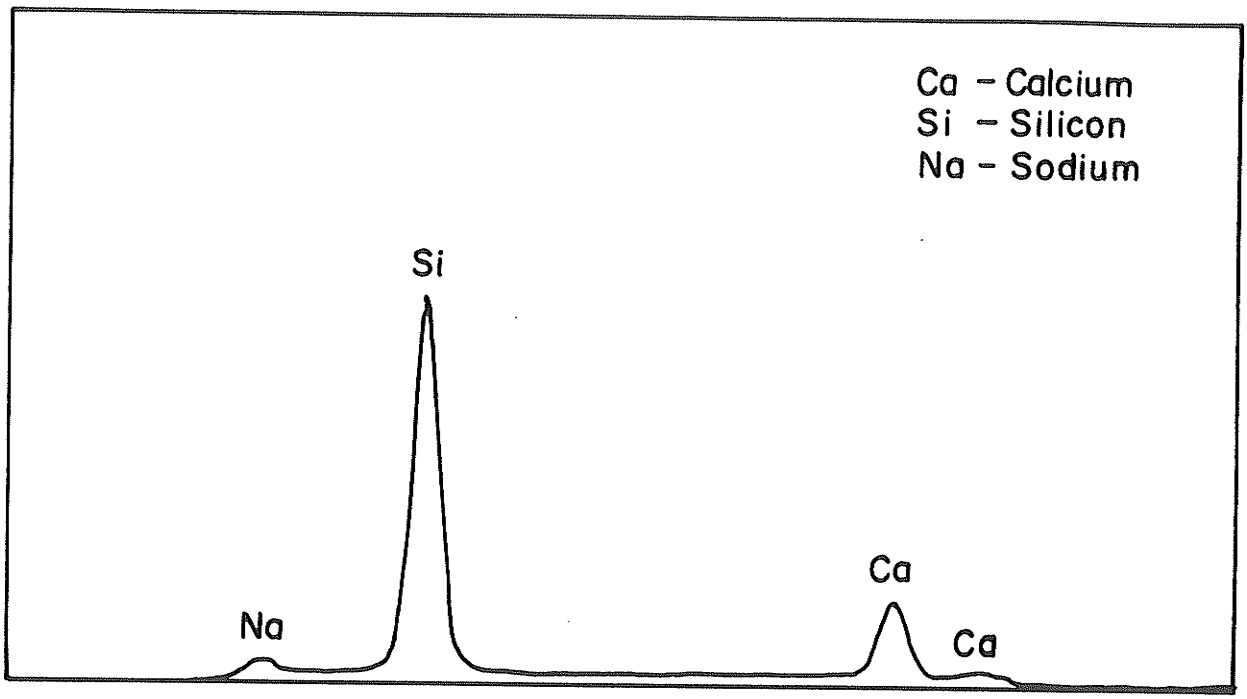

Figure 4.53 Elemental energy-dispersive spectrum for rosette morphology of gel in Figure 4.51 and 4.52

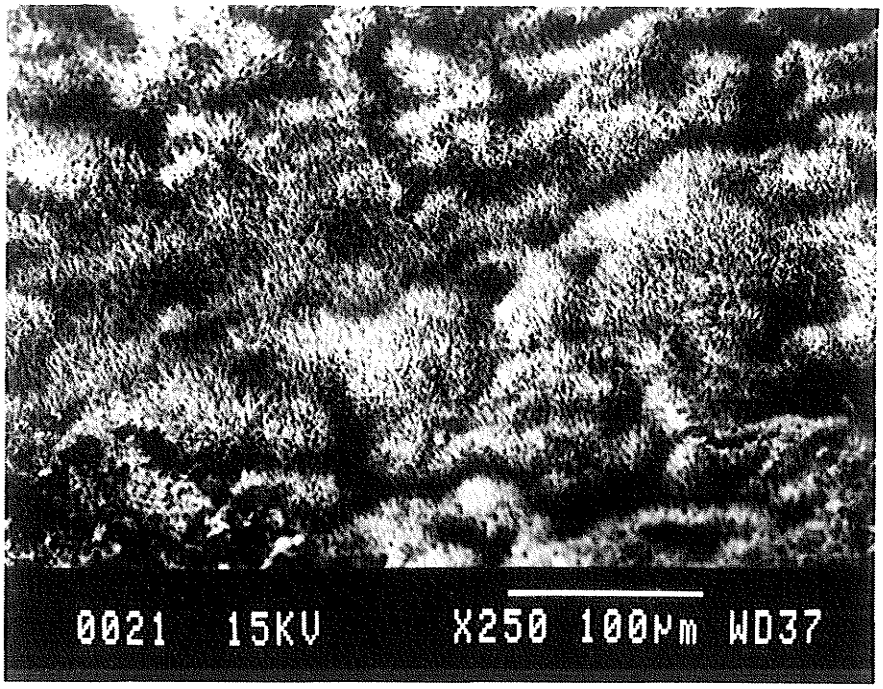

Figure 4.54 Fibrous morphology of alkali-silica gel in specimens made with Aggregate 2

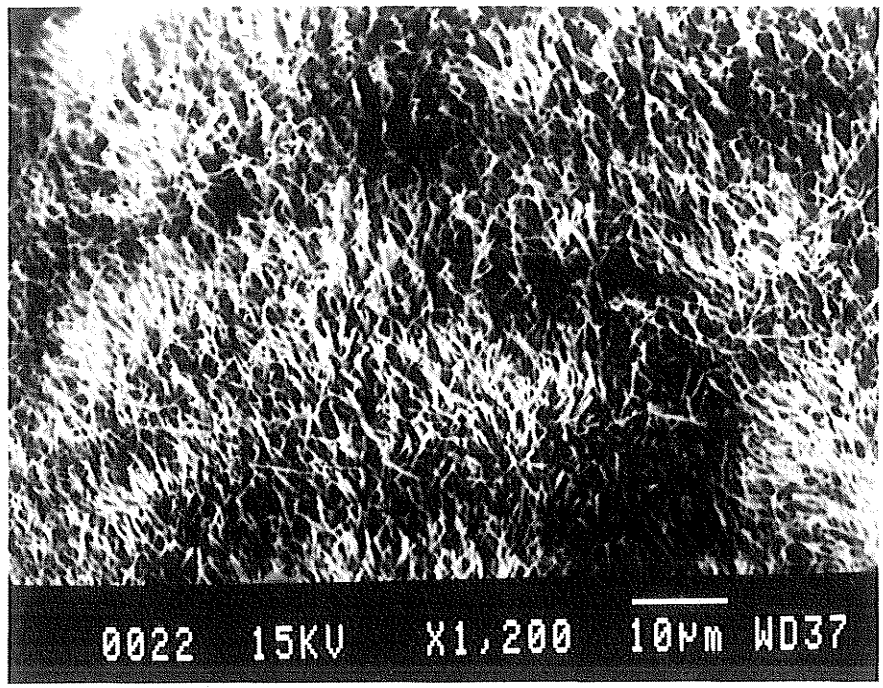

Figure 4.55 Fibrous morphology of alkali-silica gel in specimen made with Aggregate 2 (higher magnification of Figure 4.54)

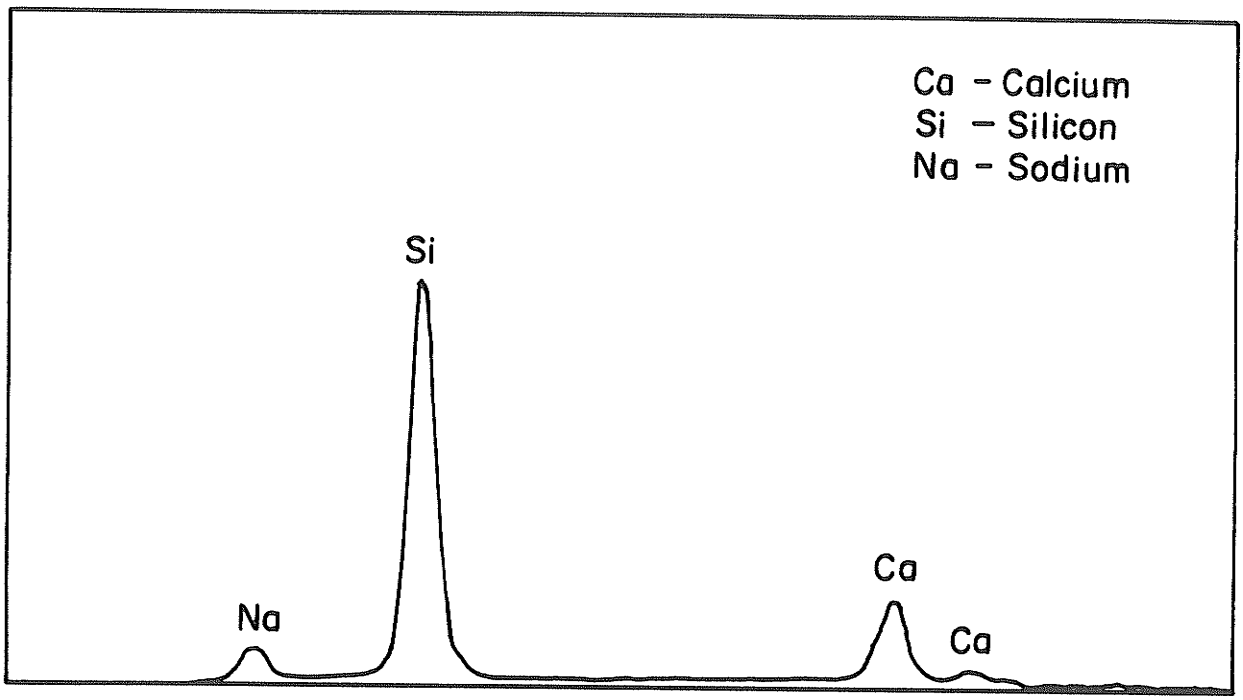

Figure 4.56 Elemental energy-dispersive spectrum for fibrous morphology of gel in Figures 4.54 and 4.55

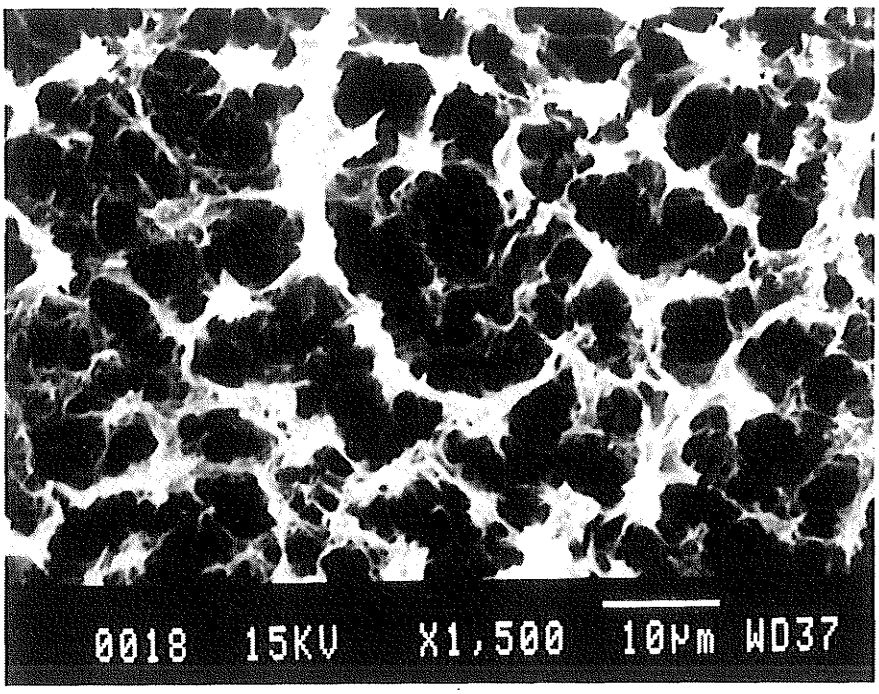

Figure 4.57 Sponge-like morphology of alkali-silica gel in specimen made with Aggregate 2

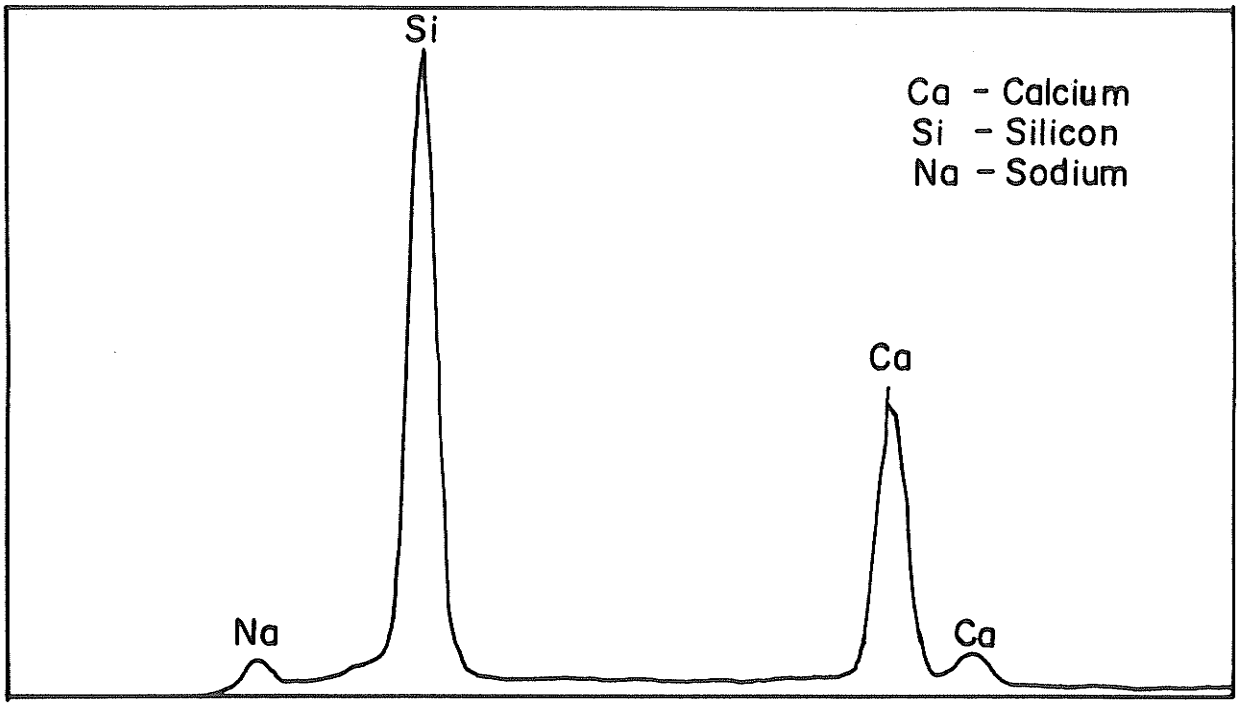

Figure 4.58 Elemental energy-dispersive spectrum for sponge-like morphology of gel in Figure 4.57

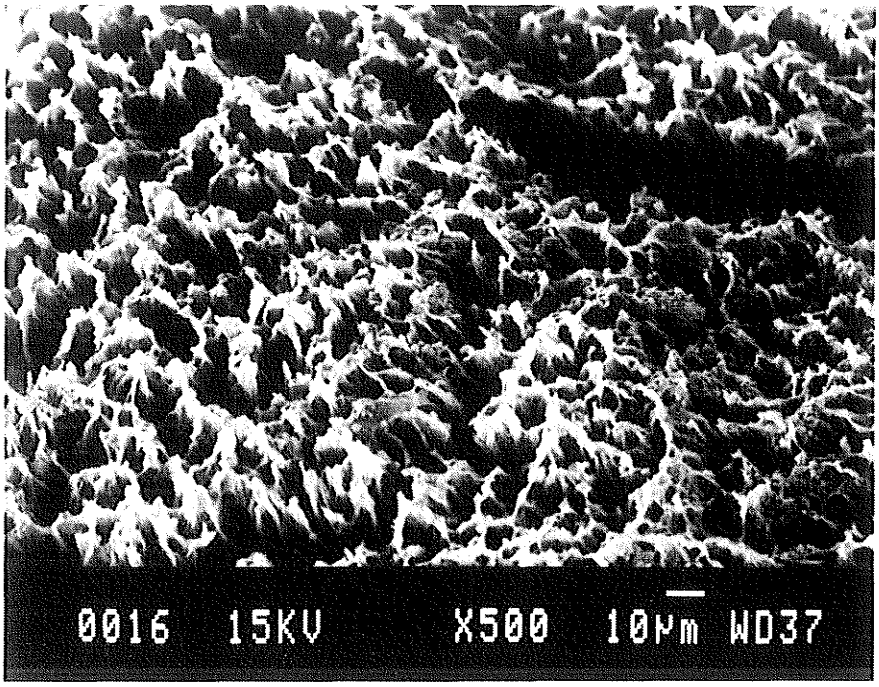

Figure 4.59 Alkali-silica gel with oriented morphology in specimen made with Aggregate 2

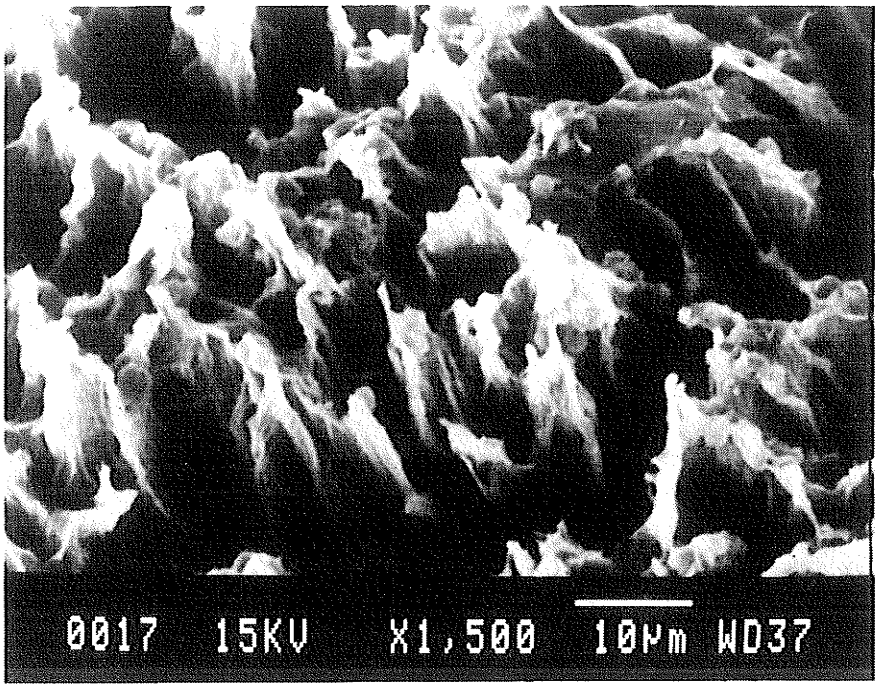

Figure 4.60 Alkali-silica gel with oriented morphology in specimen made with Aggregate 2 (higher magnification of Figure 4.59)

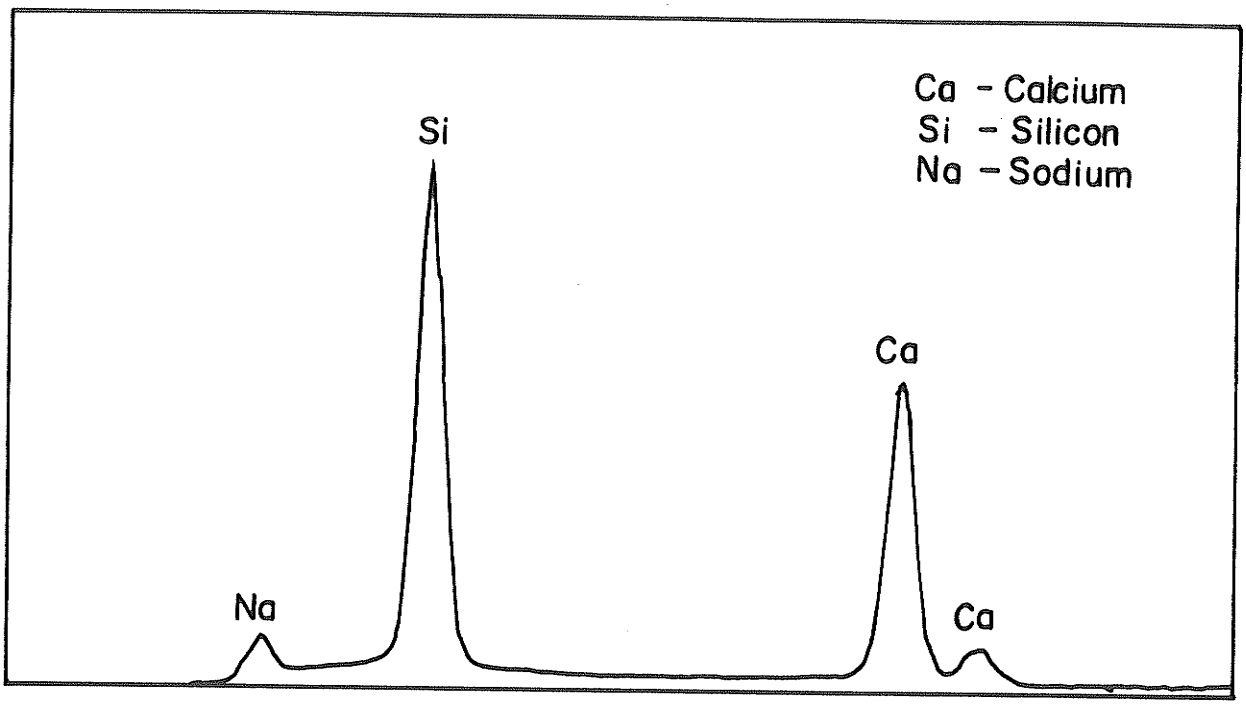

Figure 4.61 Elemental energy-dispersive spectrum for gel in Figures 4.59 and 4.60

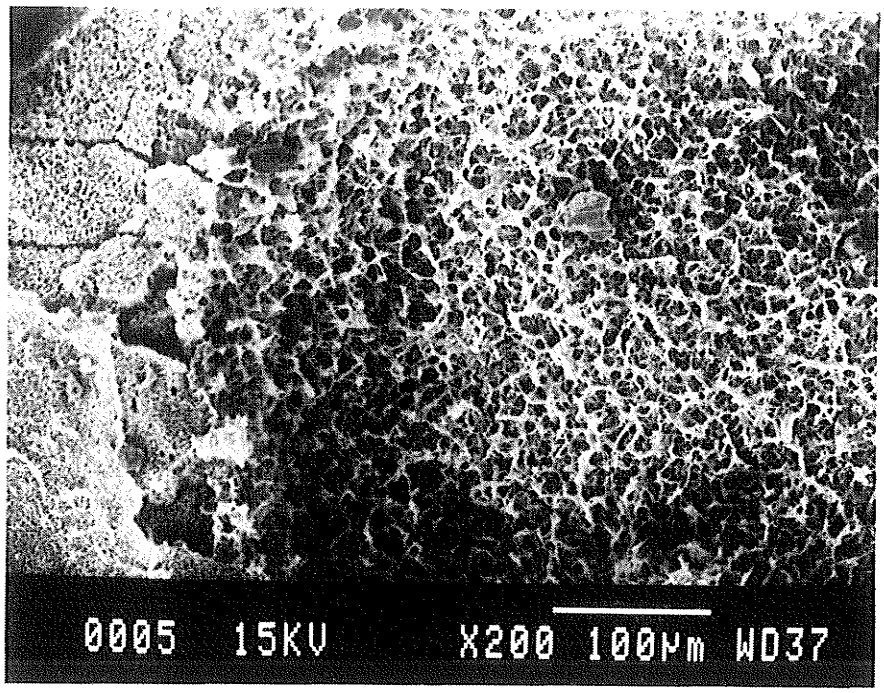

Figure 4.62 Sponge-like gel in void of a specimen made with Aggregate 3 (alkali-carbonate reactive aggregate)

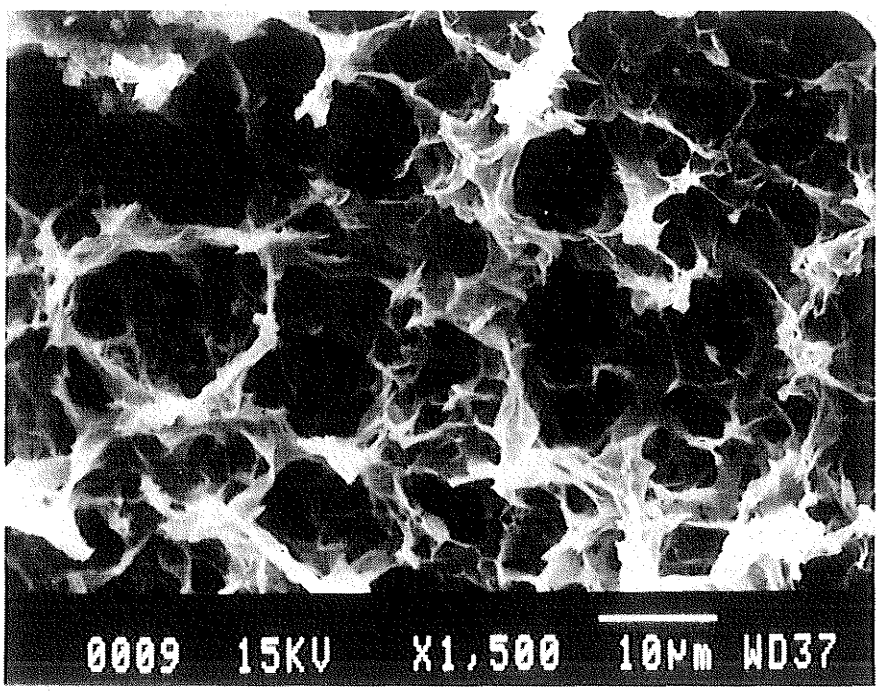

Figure 4.63 Sponge-like gel in specimen made with Aggregate 3 (higher magnification of Figure 4.62)

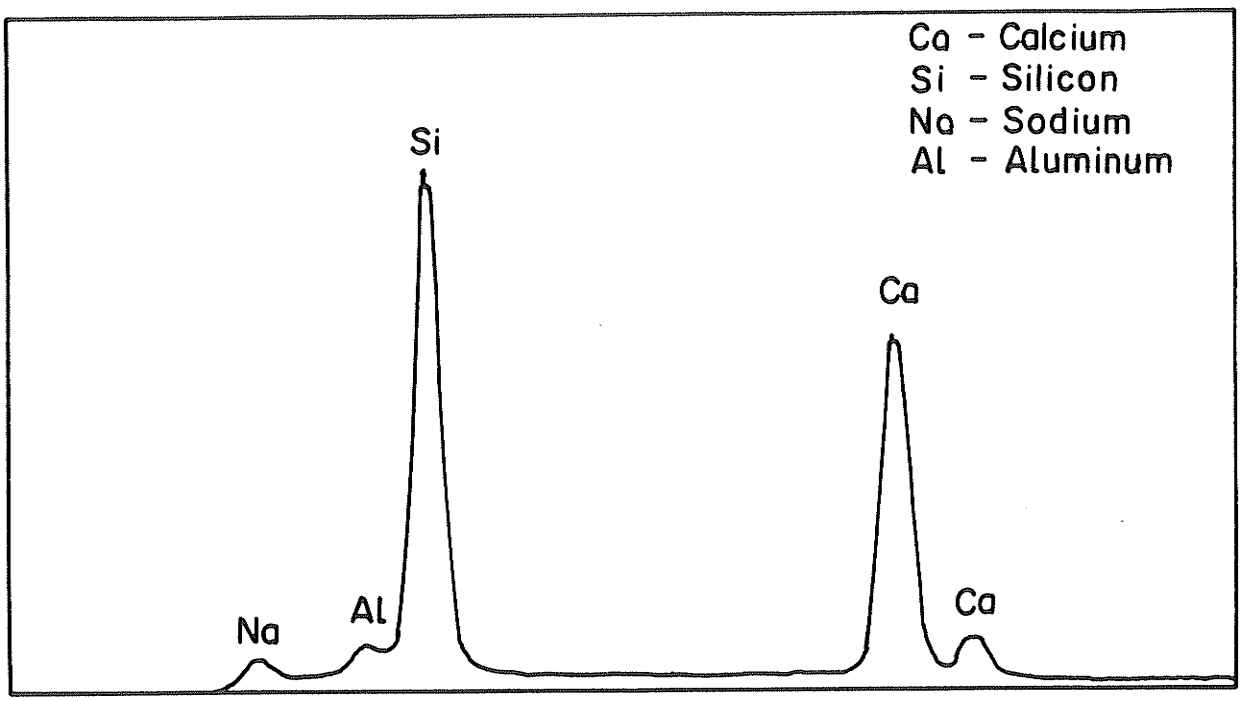

Figure 4.64 Elemental energy-dispersive spectrum for sponge-like gel in Figures 4.62 and 4.63

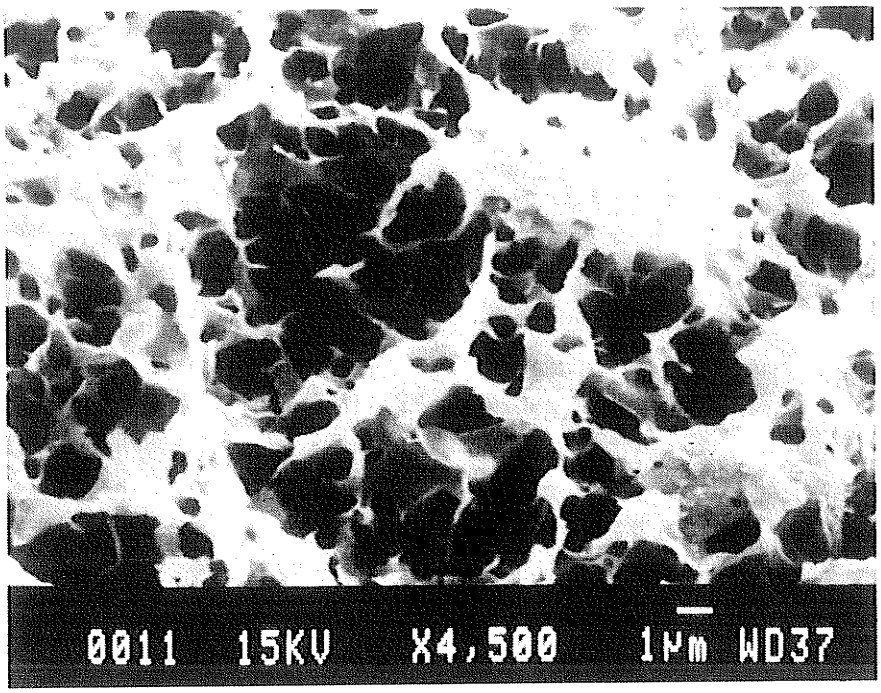

Figure 4.65 Sponge-like gel at paste-aggregate interface in specimen made with Aggregate 3

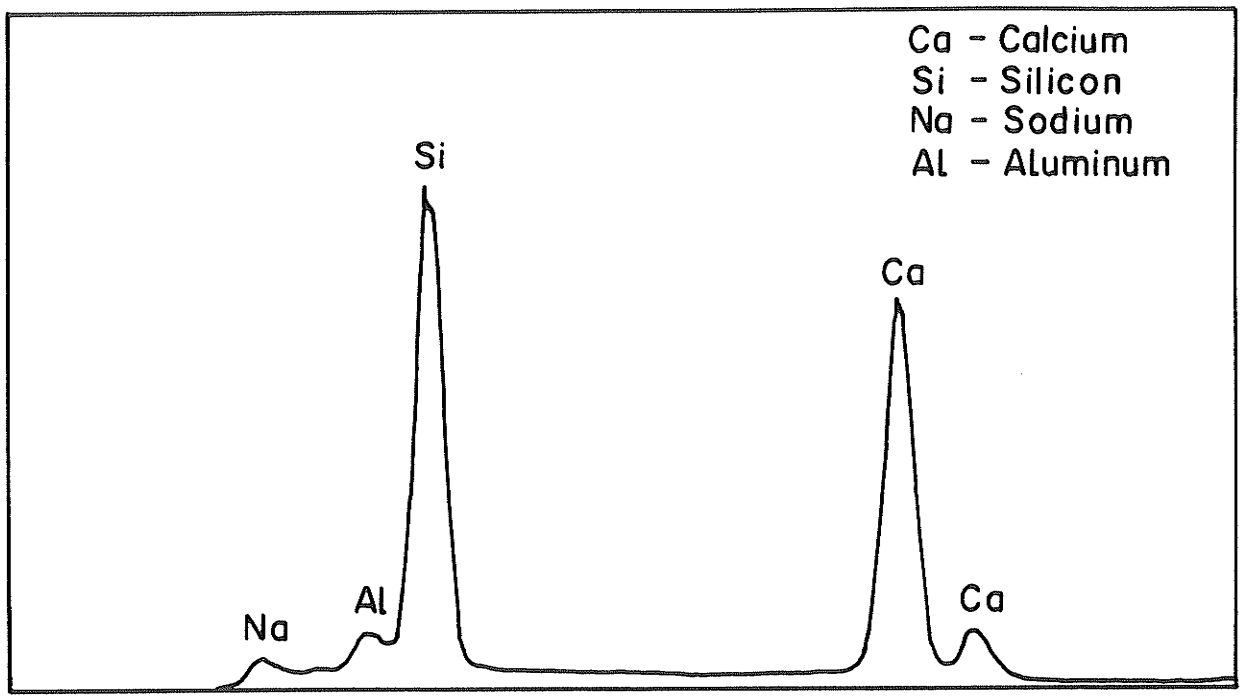

Figure 4.66 Elemental energy-dispersive spectrum for sponge-like gel in Figure 4.65

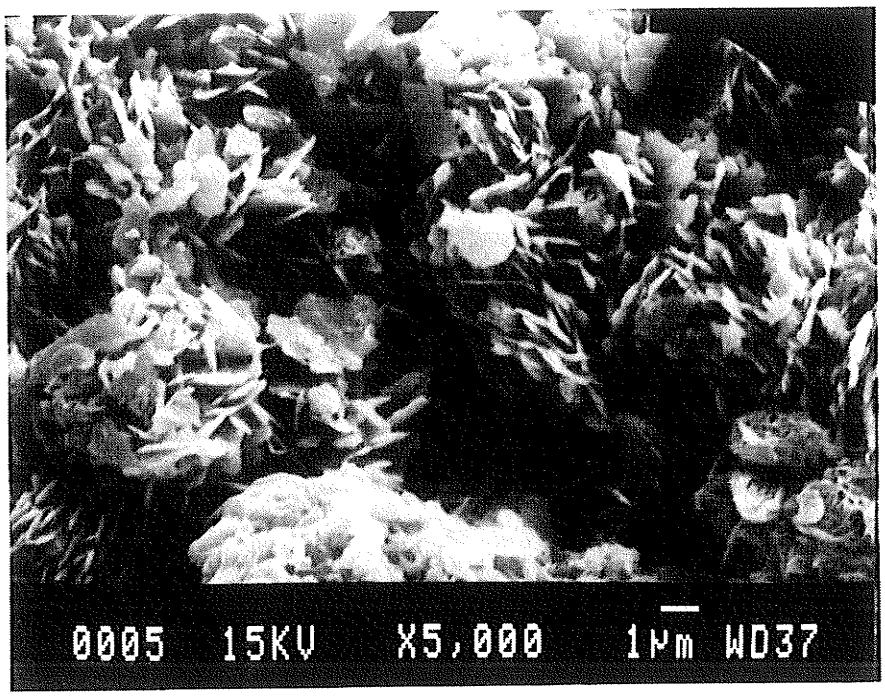

Figure 4.67 Gel on surface of a specimen made with Aggregate 3

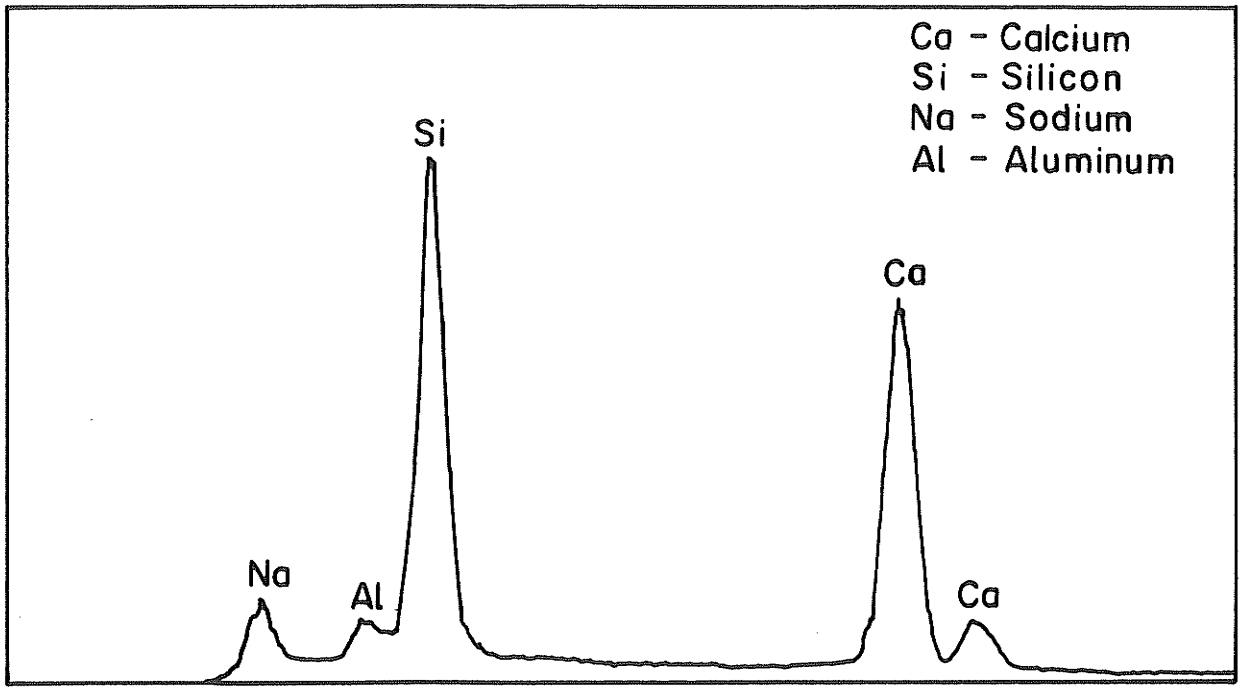

Figure 4.68 Elemental energy-dispersive spectrum for gel in Figure 4.67

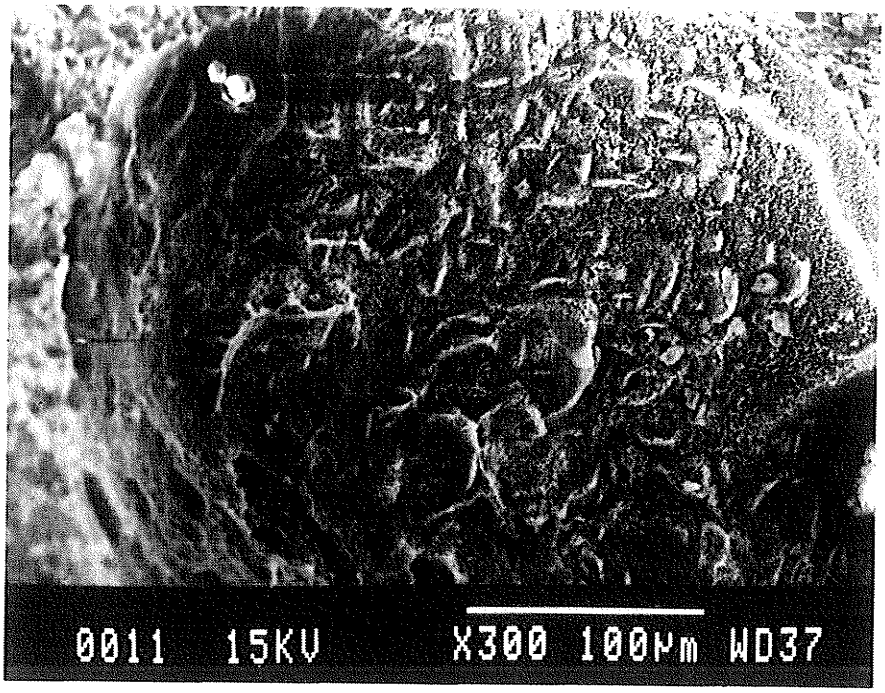

Figure 4.69 Gel at base of void in a specimen made with Aggregate 4 (alkali-silica reactive aggregate)

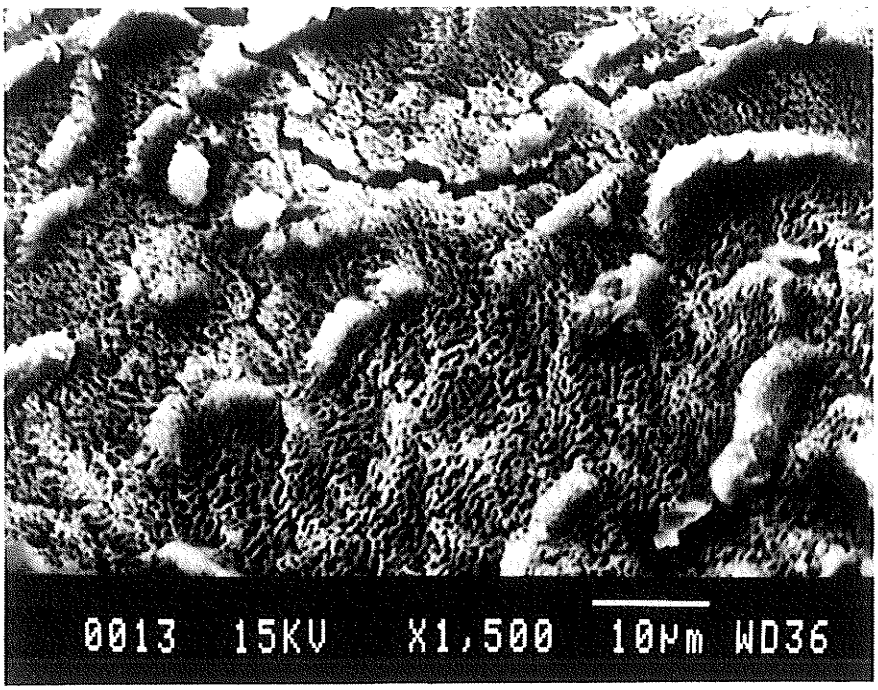

Figure 4.70 Gel at base of void in a specimen made with Aggregate 4 (higher magnification of Figure 4.69)

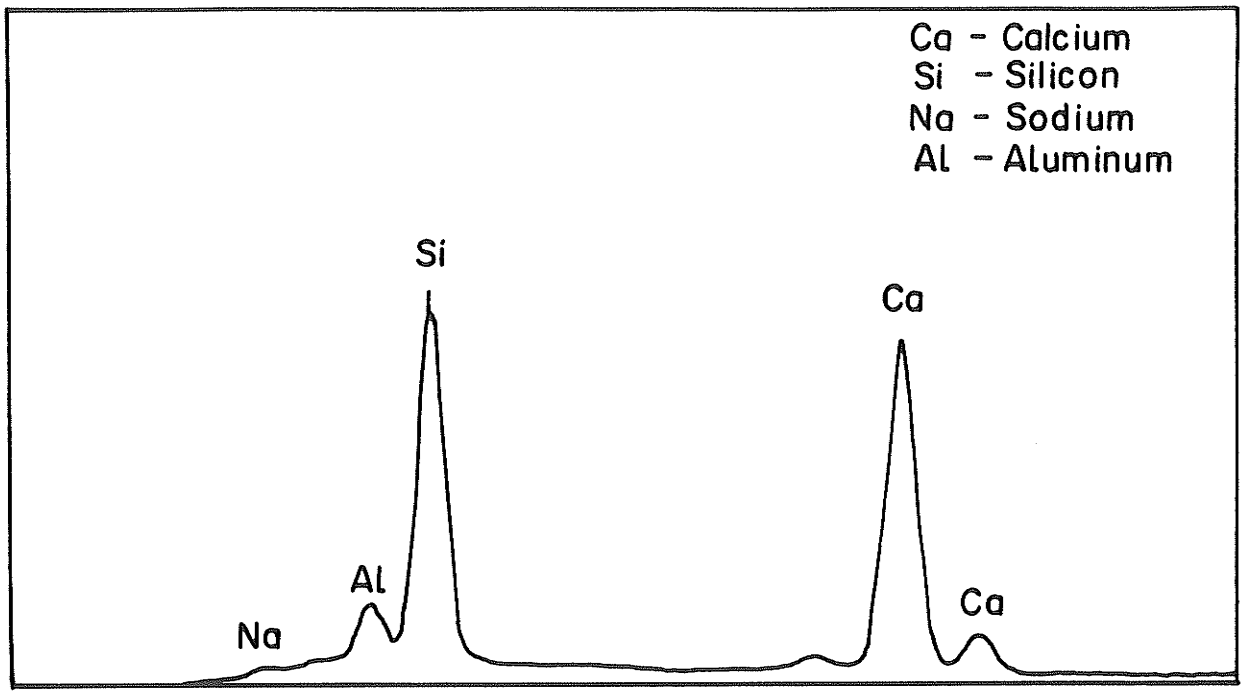

Figure 4.71 Elemental energy-dispersive spectrum for gel in Figures 4.69 and 4.70

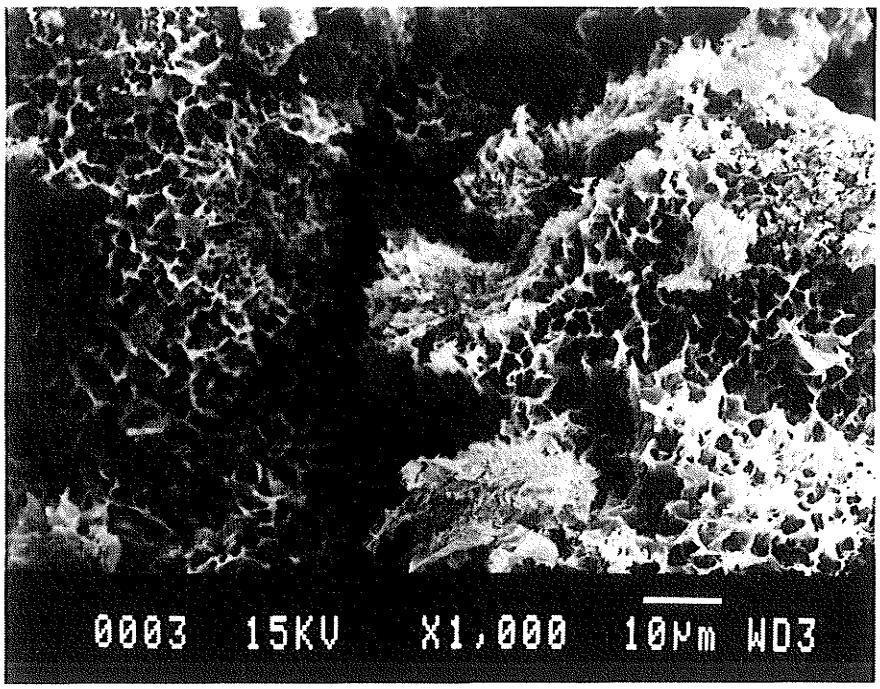

Figure 4.72 Sponge-like gel on surface of a specimen made with Aggregate 4

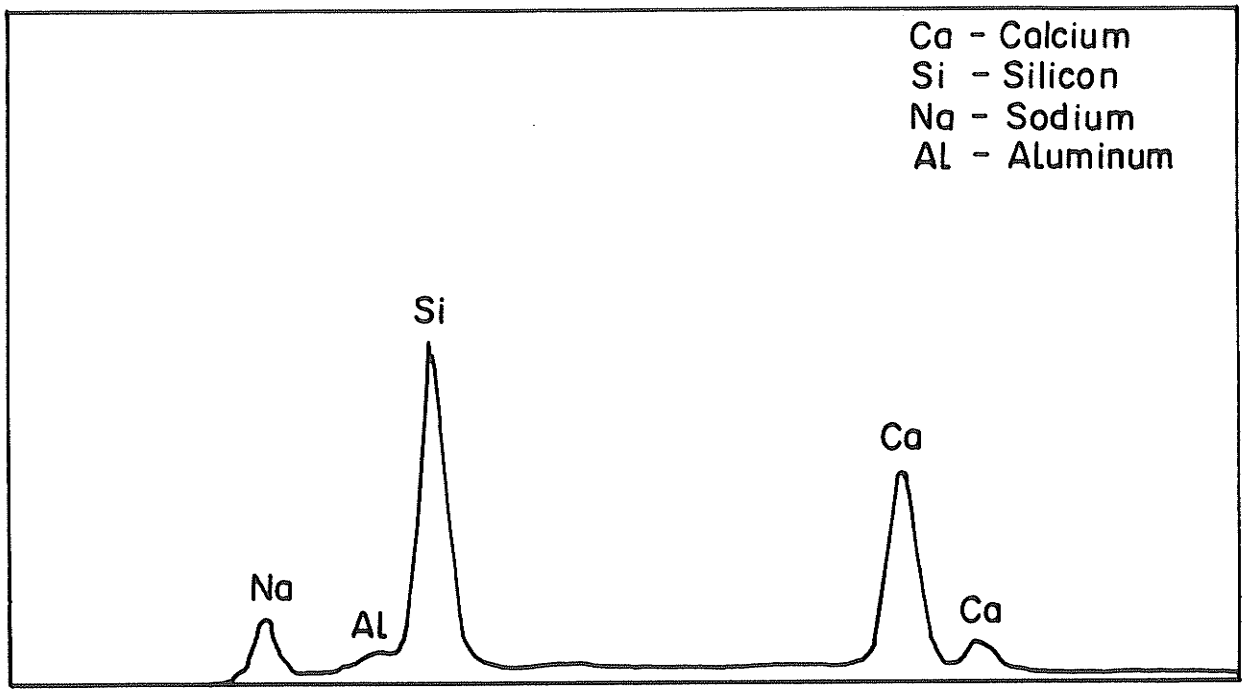

Figure 4.73 Elemental energy-dispersive spectrum for gel in Figure 4.72

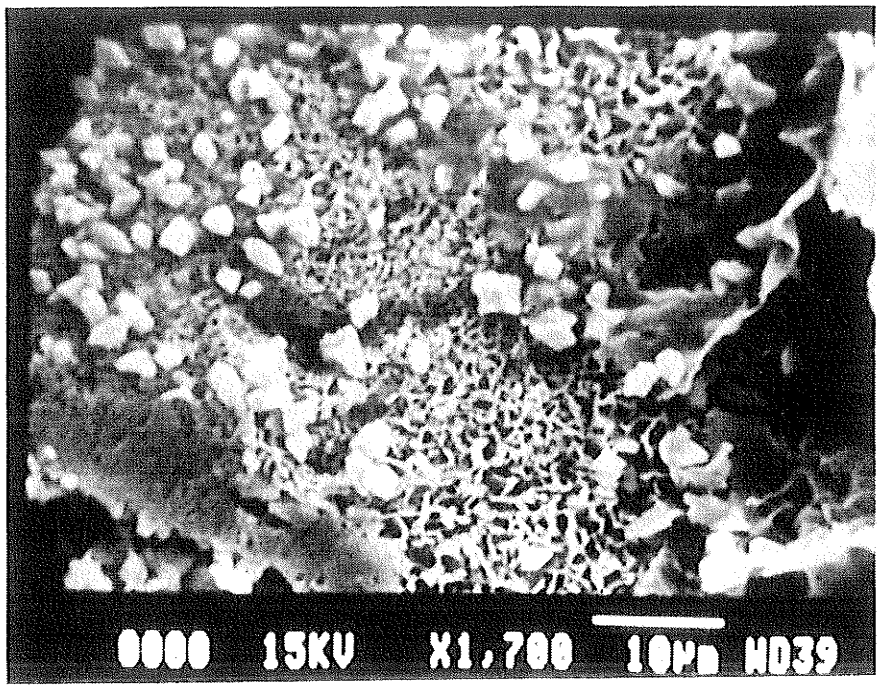

Figure 4.74 Gel on surface of a specimen made with Aggregate 5 (alkali-silicate reactive aggregate)

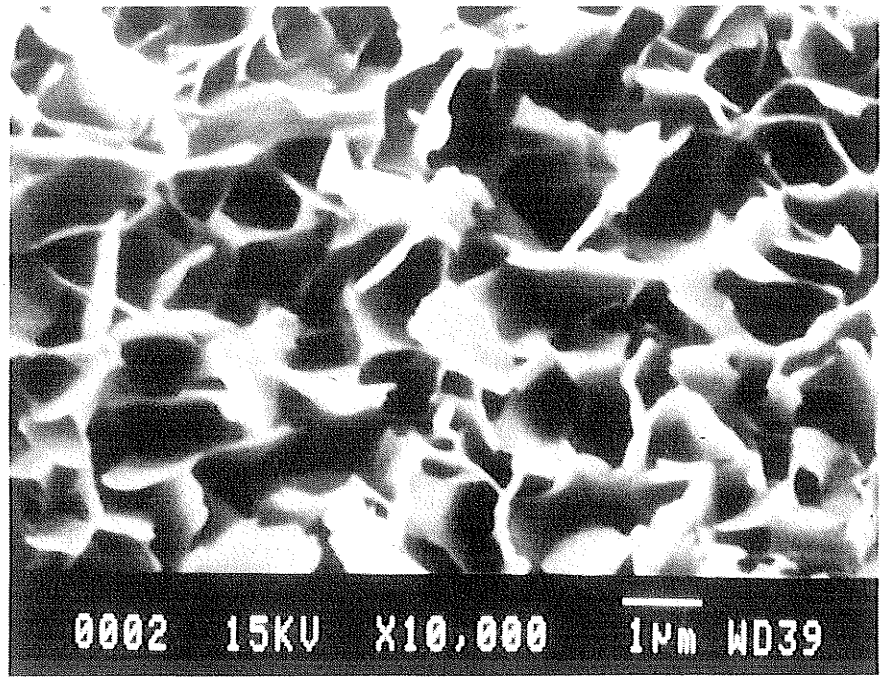

Figure 4.75 Gel on surface of a specimen made with Aggregate 5 (higher magnification of Figure 4.74)

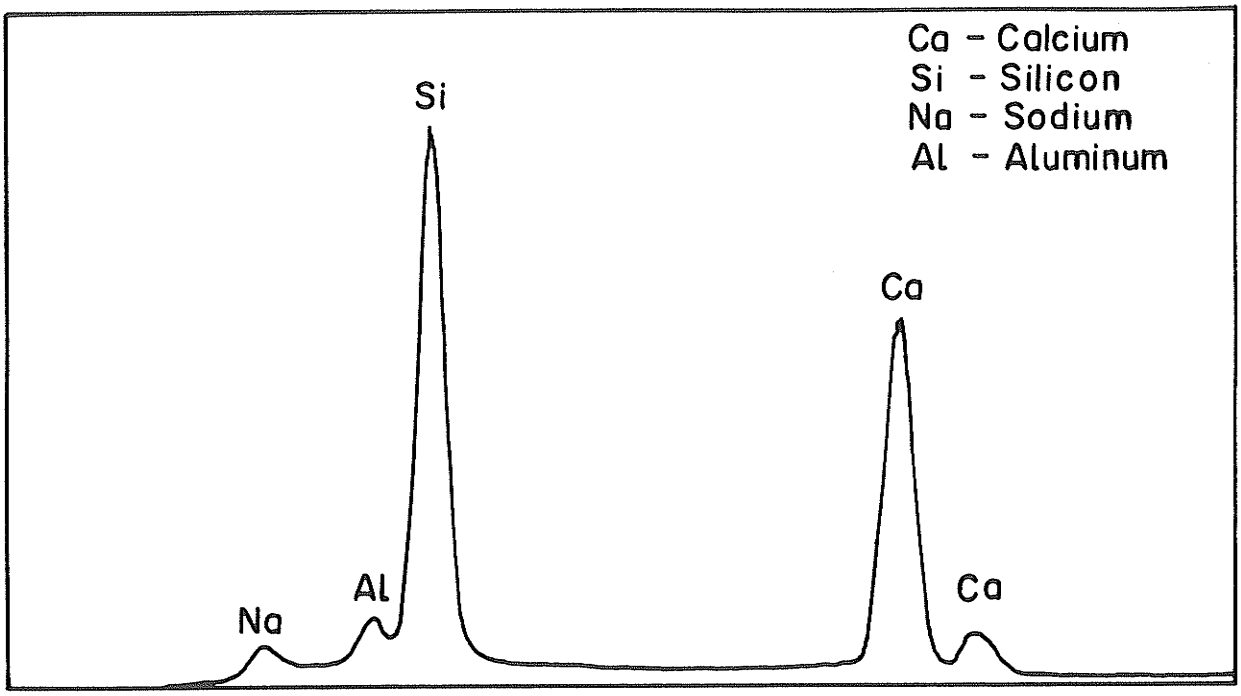

Figure 4.76 Elemental energy-dispersive spectrum for gel in Figure 4.74 and 4.75

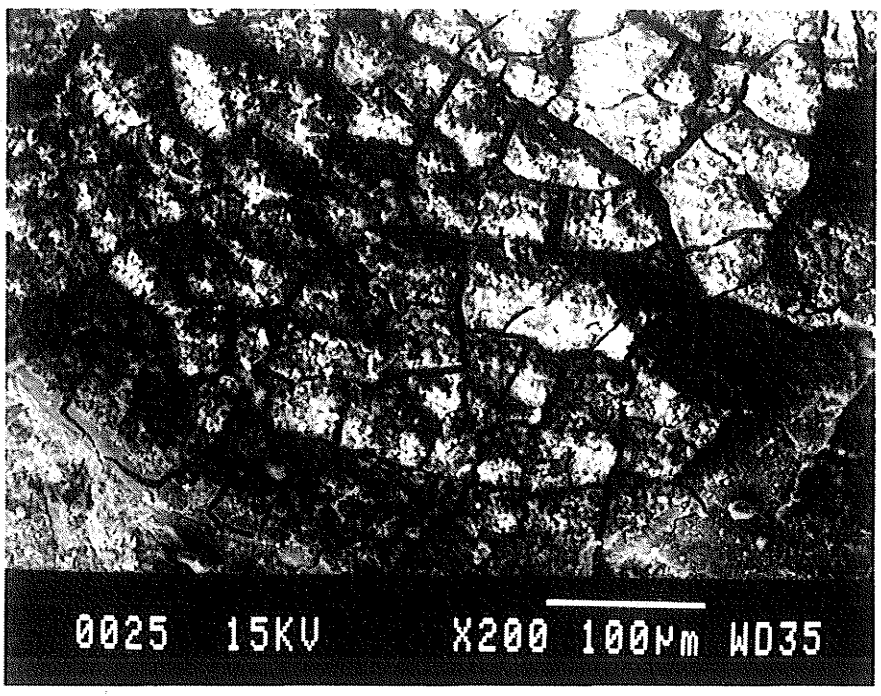

Figure 4.77 Mud-like morphology of gel in specimen made with Aggregate 6

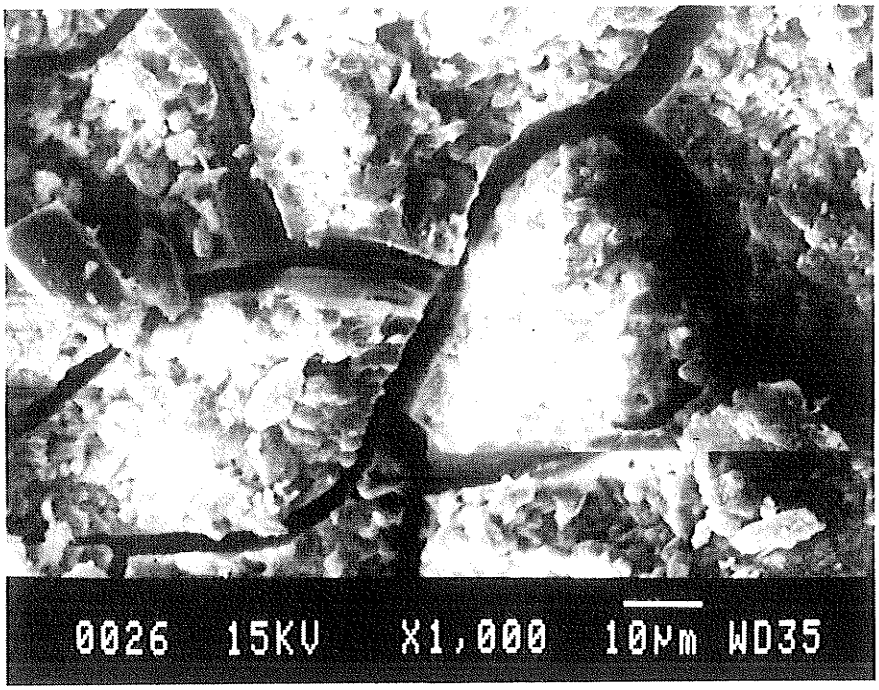

Figure 4.78 Mud-like morphology of gel in specimen made with Aggregate 6 (higher magnification of Figure 4.77)

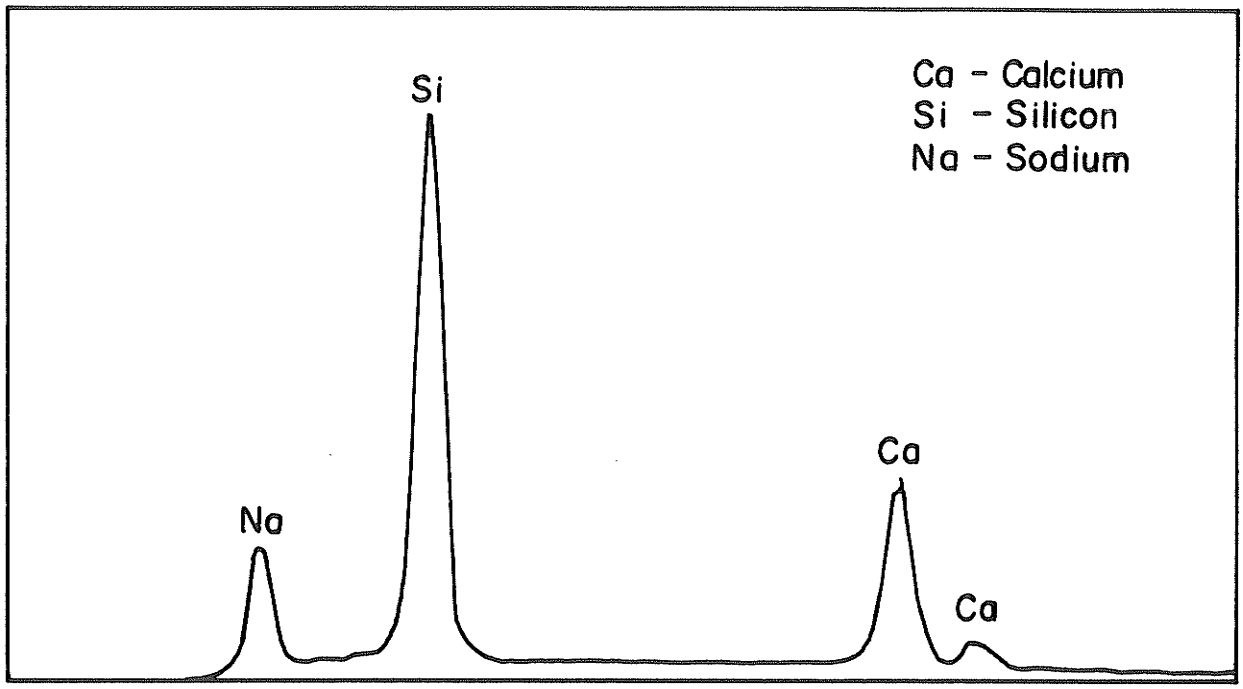

Figure 4.79 Elemental energy-dispersive spectrum for mud-like gel in Figures 4.77 and 4.78

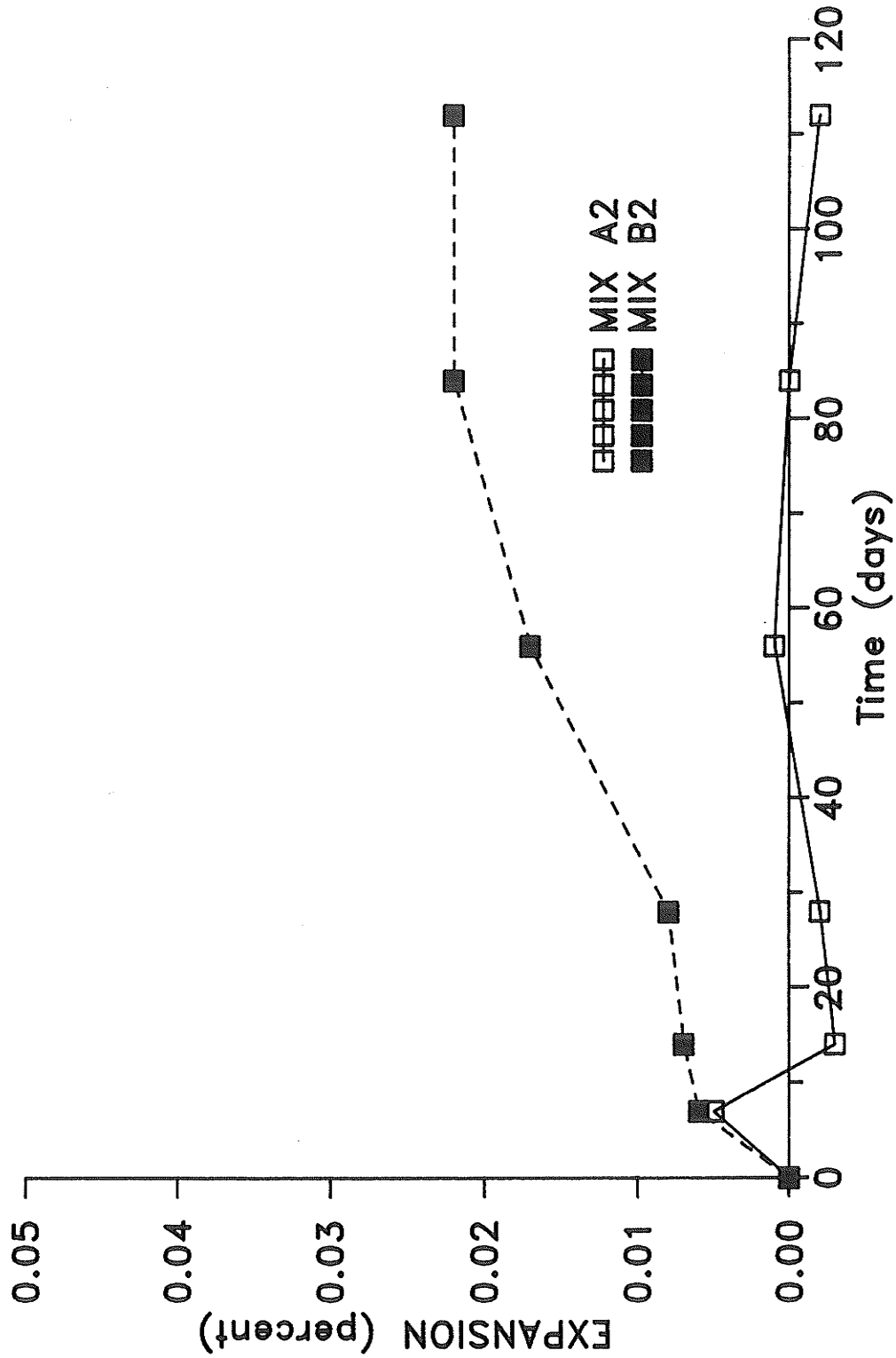

Figure 4.80 Expansion of specimens used in concrete prism test. Test specimens made with low alkali (A2) and high alkali (Mix B2) cements

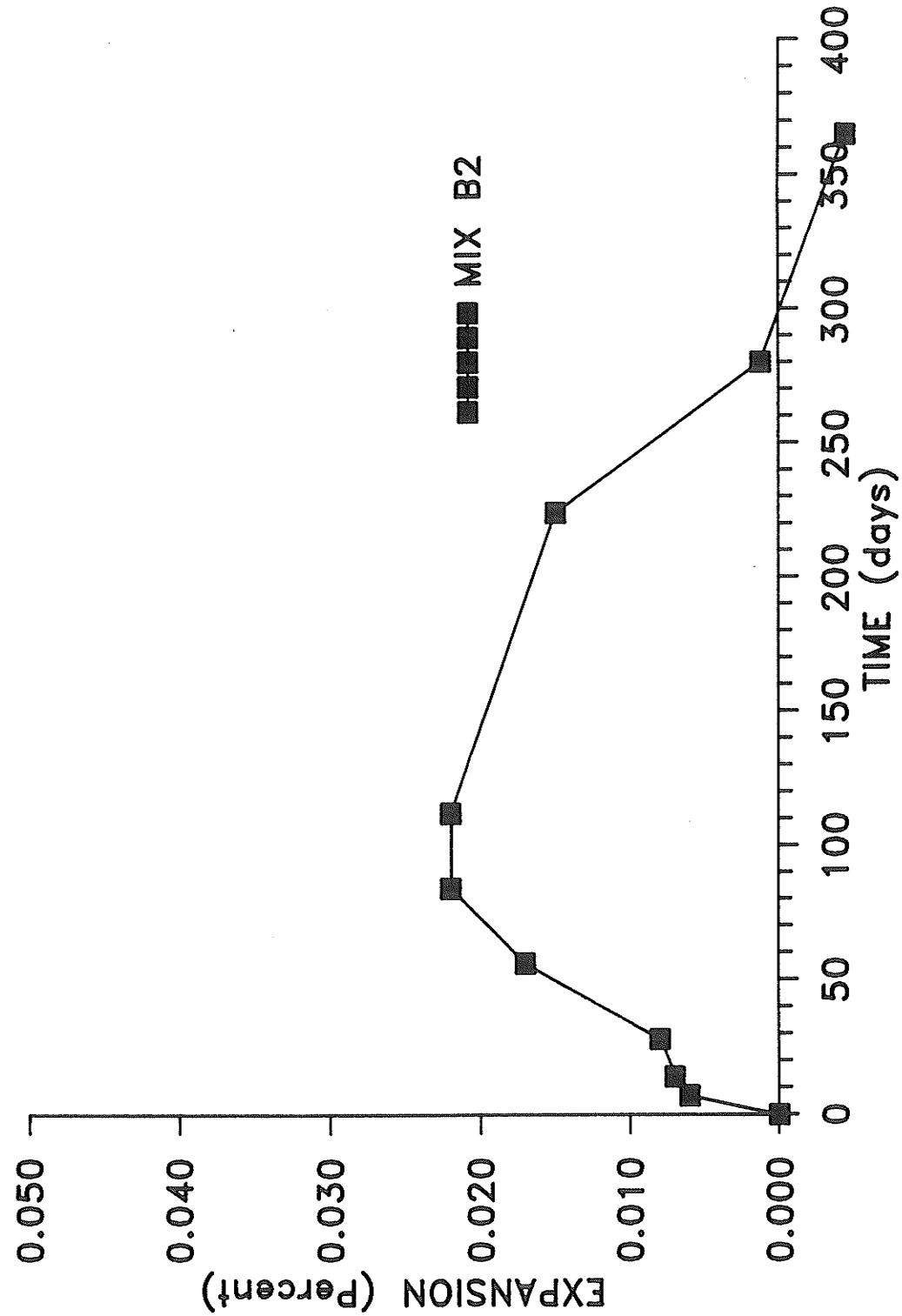

Figure 4.81 Typical expansion-time results in concrete prism test up to 1 year

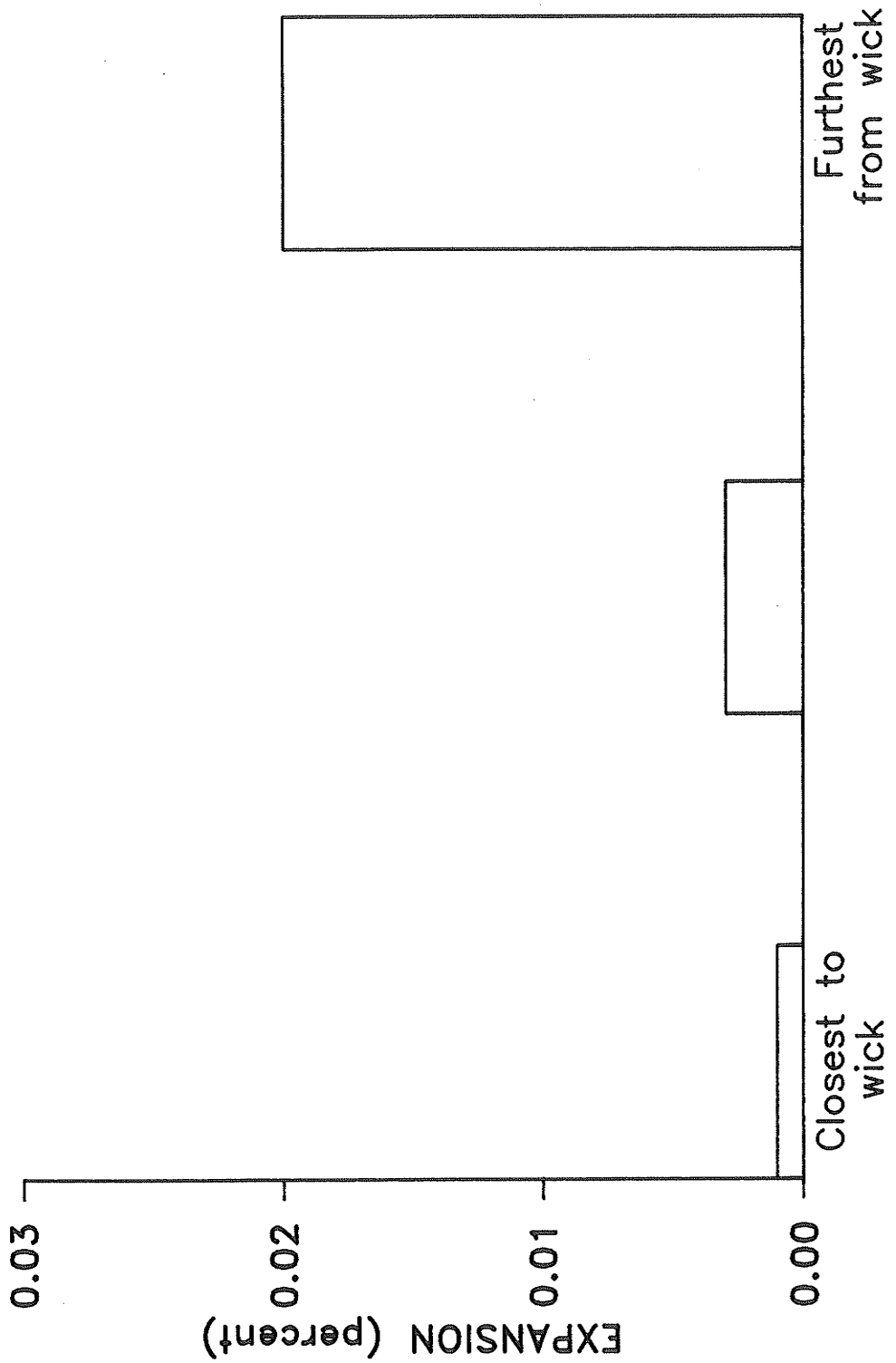

Figure 4.82 Expansion of prisms after 365 days with respect to location in tank (Mix C4)